University of Turin

Doctoral School in Life and Health Sciences

PhD Programme in Molecular Medicine

XXXIV cycle

PhD Thesis

Discovery and validation of synthetic lethal interactions with oncogenic KRAS dependency in colorectal cancer organoids

Tutor:
Andrea Bertotti

PhD Candidate:
Marika Pinnelli

Academic years 2018 - 2022

ABSTRACT

Colorectal cancer (CRC) is the third most commonly diagnosed malignancy and the second leading cause of cancer death worldwide. About 50% of CRCs acquire *KRAS* mutations (mainly in codons 12 and 13) during tumor progression from adenoma to carcinoma, subsequent to *APC*- or β-catenin-dependent mutational activation of Wnt signaling. Consistent with the idea that oncogenic RAS vigorously sustains the transformed phenotype, patients with *KRAS*-mutated CRC typically have a worse prognosis and remain refractory to available standard-of-care treatments. However, efforts to develop drugs that inhibit mutant RAS proteins have been largely unsuccessful (with the exception of covalent inhibitors of KRAS G12C, a variant with a relatively low prevalence in CRC). Moreover, emerging evidence suggests that not all *KRAS*-mutant tumors rely on RAS hyperactivation for their growth. Rather, RAS dependency may be modulated by context-specific survival signals that become essential in some KRAS-mutant tumors, but not in others.

We exploited our collection of patient-derived, KRAS-mutant CRC tumoroids to identify potential synthetic lethal druggable vulnerabilities in those models that show a dependency on the RAS pathway. First, we evaluated how and to what extent tumoroids recapitulated the mutational landscape and gene copy number architecture of parental PDXs. Then, we performed viability assays after CRISPR/Cas9-mediated KRAS knock-out in order to stratify tumoroids that are addicted to KRAS function for maintaining viability versus tumoroids in which KRAS inactivation is inconsequential. We found that KRAS ablation resulted in polarized outcomes: some models remained substantially unaffected, whilst others experienced dramatic decreases in viability (suggestive of RAS independency and RAS dependency, respectively). As complementary approach, we conducted drug screens with the MEK1/2 inhibitors (MEKi) selumetinib and trametinib, with the assumption that tumoroids categorized as RAS-dependent may be more reliant on the MAPK pathway than RAS-independent tumoroids. Pharmacologic screens confirmed the same distribution obtained with KRAS knock-out, indicating that KRAS-dependent CRCs predominantly rely the MAPK pathway signals for their growth. These results are consistent with our assumption that not all KRAS mutant tumors rely on aberrant RAS activity for their growth and survival. Moreover, when translated to an *in vivo* PDX setting, MEKi treatment of two RAS-dependent tumoroids did not produce the same therapeutic benefit as observed *in vitro*. This suggests that KRAS-addicted CRCs display MAPK co-dependencies that are not apparent *in vitro* and become implemented *in vivo*.

To extract functional differences that typify RAS-dependent versus RAS-independent CRC tumoroids, we compared the basal gene expression levels in these two groups. We found that KRAS-dependent and KRAS-independent tumors are functionally different: gene set enrichment analyses highlighted that RAS-dependent models showed a less differentiated epithelial phenotype than RAS-independent models.

In conclusion, the combination of computational, genetic and biological approaches has enabled the identification of functional traits specifically enriched in KRAS mutant, KRAS-dependent tumors as a prelude to the nomination of new synthetic lethal interactions in KRAS-mutant CRCs. This investigation is expected to establish phenotypic traits of 'RAS addiction' in clinically pertinent CRC models as a means to discovering pharmacologically tractable, synthetic lethal pathways for these aggressive and largely treatment-refractory cancers. By leveraging the power of CRISPR/Cas9 technology and the breadth of our tumoroid collection, we hope to gain a deeper understanding of the complex genetic and molecular mechanisms that drive cancer progression and therapy resistance in KRAS mutant mCRC and identify new avenues for the development of more effective treatments.

INTRODUCTION

Colorectal cancer: tumorigenesis and genomic landscape

Cancer cells, by definition, grow and proliferate by escaping normal controls. Tumors are thought to originate from a single cell that has undergone an initial mutation that produces a selective advantage over the non-mutated population [1]. However, a cell, to become cancerous, requires numerous additional mutations and genetic events. Cancer progression takes many years and is reminiscent of a Darwinian evolutionary process, in which somatic cells undergo mutations and epigenetic changes accompanied by natural selection. Through this progressive accumulation of alterations, cells acquire a multitude of characteristic properties, such as the ability to evade growth and cell death control mechanisms and the propensity to invade, induce angiogenesis, and alter energy metabolism [1].

Much of the information on the general mechanisms of oncogenesis has been provided by studies on colorectal carcinogenesis [2-4]. The combinations of molecular events that lead to colon adenocarcinoma formation can be very diverse and include both genetic and epigenetic abnormalities. The WNT-APC/β-catenin signaling is the best know pathway that accompanies the classic morphological progression from epithelial hyperplasia to adenoma and finally carcinoma. The classic adenoma-carcinoma sequence, which affects up to 80% of sporadic colon cancers, typically involves APC mutation at the beginning of the neoplastic process (Fig.1). For adenoma development, both copies of the APC gene must be functionally inactivated, either through mutation or epigenetic events such as promoter methylation. APC is an essential negative regulator of β-catenin, a component of the WNT signaling pathway. Normally, the APC protein binds to and promotes the degradation of β-catenin. Upon APC inactivation, β-catenin accumulates and translocates into the nucleus, where it activates transcription of genes including those encoding for MYC and cyclin D1, which promote proliferation and stem cell traits. This phase is followed by further mutations, including activating mutations in KRAS, which promote growth and prevent apoptosis. Neoplastic progression is also associated with mutations in other oncosuppressor genes, such as those encoding SMAD2 and SMAD4, effectors of TGFβ signaling. Since normally TGFβ

signaling inhibits the cell cycle and promotes epithelial differentation, loss of these genes may allow uncontrolled growth of neoplastic cells. Another event that commonly occurs late in colorectal cancer progression is loss of function of p53.

The sequence of molecular events described above is merely a simplification, often used for educational purposes, of one of the many pathways by which the process of tumor progression in the colon can occur. In reality, the range of alterations detectable in this pathology turns out to be much more complex and extremely varied.

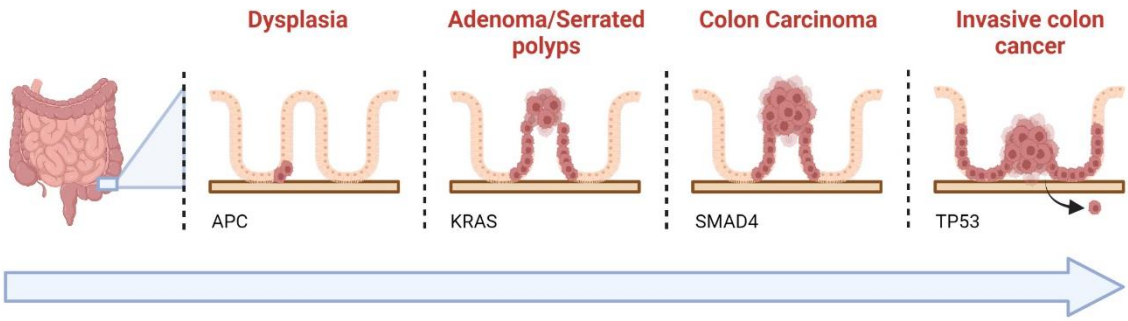

Figure 1. A step-wise model of colorectal tumorigenesis as proposed by Fearon and Vogelstein. Mutational alterations in genes such as *APC*, *KRAS* and p53 (*TP53*) advance the histopathological malignancy of CRC cells. Created in Biorender.com.

An important contribution to a comprehensive understanding of the genetic and genomic alterations characteristic of the process of colon tumorigenesis was made in 2012 by The Cancer Genome Atlas (TCGA) research network, which conducted genome-wide studies of 244 colorectal tumors and corresponding healthy tissue samples through six different platforms [5]. Based on their molecular features, two major CRC categories can be identified. 16% of the cases were defined as hypermutated (mutational burden >12 per 10^6 bases) due to alterations of mismatch repair genes (MSH) or polymerase ε (POLE), leading to microsatellite instability. The remaining cases (84%), classified as microsatellite stable (MSS), are characterized by chromosomal instability (CIN), which may be caused by defects in chromosome segregation or telomere stability or even alterations in DNA damage response.

Within the group of non-hypermutated tumors, 17 recurrent somatic mutations in expressed genes were identified. Among them, the most frequently involved were

found to be: *APC*, *TCF7L2* (belonging to the TCF/LEF class of transcription factors that are regualated by β-catenin, *TP53*, *KRAS*, *NRAS*, *PIK3CA*, *FBXW7* (a subunit of a ubiquitin-protein ligase complex), and SMAD4 (a downstream effector of TGFβ). Within this context, *KRAS* mutations are found in more than 40% of all MSS colorectal tumors, highlighting their prominent role in sustaining the progression of the disease.

Metastatic colorectal cancer: current treatment strategies

Colorectal cancer (CRC) is the third most commonly diagnosed malignancy and the second leading cause of cancer death worldwide, with a 5-year survival rate of less than 20% in the metastatic setting [6]. Metastatic disease accounts for 25% of patients at the time of diagnosis, and about 50% of patients will develop metastasis later [7]. Although 5-year survival rates of patients with metastatic colorectal cancer (mCRC) remain low (14%)[8], the development of new treatment options, such as improved surgical techniques and the application of more effective therapies, has prolonged median overall survival (OS) from 12 to 30 months in recent years [9]. Standard treatments for patients with mCRC include cytotoxic agents and targeted biological compounds.

Chemotherapy

Most patients with metastatic colorectal cancer (mCRC) are initially not eligible for potentially curative resection. In these cases, treatment is palliative rather than curative, with goals consisting in prolonging survival, attenuating tumor-related symptoms, and possibly reducing the tumor mass to allow resection and/or maintaining quality of life [10]. The therapeutic armamentarium available for the treatment of advanced and metastatic disease consists of fluoropyrimidines, irinotecan, oxaliplatin, and biologic agents. Combination chemotherapy regimens (e.g., FOLFOX, FOLFIRI, FOLFOXIRI, CapOX) have shown advantages in objective response rate and prolongation of progression-free survival (PFS) compared with single-agent treatment and now represent the standard-of-care treatment.

Immunotherapy

Over the past decade, immunotherapy emerged as an effective therapeutic strategy to achieve long-term durable response in different solid tumors, such as melanoma and lung cancer. A marker of sensitivity included the high tumor mutational burden, caused by a compromised DNA repair machinery. Thus, immune checkpoint inhibitors (ICIs) are recommended for mCRC patient with MSI-H or with mismatch-repair deficiency (dMMR) [11]. In 2017, pembrolizumab (the first anti-PD1 drug) and nivolumab (an anti-CTLA4 antibody) received FDA approval as a second-line treatment for mCRC patients with MSI-H, and their administration has been recently anticipated to the first-line setting. However, the vast majority of CRC patients are affected by MSS tumors, which respond poorly to checkpoint inhibitors.

Molecularly targeted therapies

The use of molecularly targeted therapies directed against angiogenic factors or the epidermal growth factor receptor (EGFR) have been shown to significantly improve the efficacy of chemotherapy [12, 13].

The prototypical anti-angiogenic therapy is bevacizumab, a humanized monoclonal antibody directed against vascular endothelial growth factor A (VEGFA), the use of which was approved by the FDA in 2004. By blocking the interaction between VEGF and its receptors, this drug causes inhibition of downstream transduction of the receptor and thus angiogenesis, on which solid tumors depend for their growth and metastatic ability [14, 15]. Currently, bevacizumab is approved in many countries for the first- and second-line treatment of metastatic disease in combination with 5FU-based chemotherapy with or without irinotecan or oxaliplatin. However, the benefit of adding bevacizumab to the standard chemotherapy backbone is very limited, leading to an increase in disease free survival of only 4.4 months (10.6 vs 6.2 months), and an improvement in overall survival of only 4.7 months (20.3 vs. 15.6 months) [12].

The two clinically approved anti-EGFR drugs that are part of the therapeutic schemes for the treatment of colon cancer are cetuximab and panitumumab. Cetuximab is a chimeric human/mouse IgG1 monoclonal antibody that acts against the extracellular domain of EGFR; antibody binding results in internalization of the receptor causing direct inhibition

of its tyrosine kinase activity, resulting in blockade of downstream signal transduction and inhibition of cell proliferation, angiogenesis and invasion [13, 16]. Panitumumab is a monoclonal antibody of the IgG2 class, the first fully humanized monoclonal antibody used in therapeutics: it acts, like cetuximab, by inhibiting EGFR activity and blocking binding to EGF and TGFα [17]. Both antibodies, according to the 2015 AIOM guidelines, provide a significant benefit (including major objective responses and, rarely, complete responses) in patients affected by KRAS and BRAF wild-type colorectal cancer, but are completely ineffective (and not indicated) in the treatment of KRAS (or BRAF) mutated tumors [18-20].

Treatment strategies for BRAF-mutated tumors include vemurafenib or encorafenib, two small molecules that are specific to the ATP-binding domain of $BRAF^{V600E}$ [21]. Although BRAF inhibitors showed a great activity in patients with metastatic melanoma, in the mCRC context, vemurafenib showed poor efficacy when used in monotherapy [22, 23]. This difference is due to feedback reactivation of EGFR induced by mutant BRAF blockade. Indeed, EGFR is highly expressed in colon cancer cells and, when adaptively activated by BRAF inhibition, triggers a RAS-dependent bypass pathway that substitutes for BRAF inactivation [24]. Consistently, trials using the combination of BRAF inhibitor, cetuximab and irinotecan reported promising survival outcomes and response rates in patients with BRAF-mutant CRC [25, 26]. Moreover, new evidence suggested that vertical MAPK blockade through the addition of a MEK1/2 inhibitor such as binimetinib to encorafenib and cetuximab provided a significantly further improved the survival benefit for BRAF-mutant mCRC patients [27].

While drug design efforts against critical prolifertive signaling molecules such as EGFR and BRAF has been successful, RAS targeting has proved to be exceedingly difficult. Thus the subset of MSS *KRAS*-mutated CRCs represents a therapeutical unmet need, as no therapeutic options other than standard chemotherapy and (with modest effects) anti-angiogenic agents seem to be effective against these tumors.

An overview of RAS signaling and function

Since its discovery more than half a century ago, *KRAS* has been considered an undruggable target. Indeed, unlike most protooncogenes, its enzymatic activity is necessary to inhibit (and not to activate) its signaling function, thus rendering the design of specific inhibitors extremely difficult. However, gigantic steps forward have been done in clinical research and the recent development of covalent inhibitors that target specific KRAS mutants (G12C and, very recently, G12D) proves that the way towards KRAS direct inhibition is now paved [28-30]. However, a significant improvement in our knowledge of liabilities in KRAS-mutant tumors is needed, before these findings can be translated into a widely effective therapeutic approach. Indeed, mechanisms of resistance inevitably take place also when KRAS G12C and G12D are blocked pharmacologically, due to the fact that KRAS interacts with a plethora of upstream regulators and downstream mediators [31, 32].

Discovery of RAS: the first human oncogene

The concept that tumors arise from somatic gene alterations originated from the study of cancer-inducing retroviruses isolated from animals, such as the Harvey and Kirsten murine sarcoma viruses [33]. In 1964 Harvey and Kirsten independently observed that a preparation of a murine leukemia virus, taken from a leukemic rat, induced sarcomas in new-born rodents and isolated the p21ras transforming protein. In 1982, the laboratories of Robert Weinberg, Michael Wigler and Mariano Barbacid independently discovered and successfully cloned the first human oncogenes from T24 and EJ human bladder carcinoma cell lines by serial transfection and transformation of NIH-3T3 mouse fibroblasts [34-36]. The isolated transforming genes were found to be the human counterparts of the ras genes previously identified in the Harvey and Kirsten sarcoma viruses, and were accordingly named *HRAS* and *KRAS*. It was concluded that the Harvey and Kirsten retroviruses were replication-defective and contained exogenous genetic information transduced from a previous host genome that encodes proteins required for tumor transformation. Subsequently, a new human transforming gene, the third member of the RAS gene family, was identified and designated NRAS for its identification from neuroblastoma cells [37, 38]. In later years, further work led to the discovery that

RAS human oncogenes, unlike their retroviral counterparts, were unable to transform primary cells in culture. Indeed, the transforming allele differed from the wild-type RAS oncogene by a single amino acid modification: G12V, a glycine to valine mutation at position 12. The isolation and characterization of RAS oncogenes not only corroborated the cellular oncogene hypothesis, but also laid the groundwork for rigorous research into how various genetic lesions contribute to cancer initiation and progression.

RAS: a GTPase family

The RAS family consists of three RAS proto-oncogenes (*HRAS*, *KRAS*, and *NRAS*) that encode four distinct but highly homologous RAS proteins of ~21 kDa: HRAS, NRAS, KRAS4A and KRAS4B. In general, KRAS refers to the KRAS4B isoform, due to its wide and high expression in human cancers cells [39]. These three members are closely related, having 85% amino acid sequence identity and, although they function very similarly, some indications of subtle differences between them have recently emerged. For example, although HRAS, KRAS and NRAS proteins are widely expressed, only KRAS results to be expressed in almost all cell types [40].

The crystal structure shows two major domains: a catalytic domain, the G domain, and a C-terminal domain [41]. The G domain consists of three regions: switch I, switch II, and the P loop, which binds guanine nucleotides and activates signaling by interacting with effectors. The C-terminal domain includes a hypervariable region (HVR), comprising the CAAX motif, which is important in the membrane localization of the protein [42].

Being a small GTPase, RAS cycles from an activated guanosine triphosphate (GTP)-loaded state to an inactive guanosine diphosphate (GDP)-loaded state. When the intracellular level of GTP is higher than that of GDP, GTP preferentially enters the guanine nucleotide binding site and this binding converts RAS to an active conformation. Hydrolysis of this GTP molecule into GDP, in turn, returns RAS to the inactive state. In unstimulated cells, most RAS is inactive and bound to GDP, suggesting that the rate of GTPase is faster than the rate of guanine nucleotide exchange. Wild-type isoforms of RAS possess intrinsic, albeit weak, hydrolytic (GTPase) activity and can therefore self-inactivate; however, two classes of regulatory proteins facilitated these switching processes. The guanine nucleotide exchange factors [GEFs, such as son of sevenless (SOS) factor] catalyse the release of bound GDP to promote its replacement by GTP [43,

44]. Conversely, GTPase-activating proteins [GAPs, such as neurofibromin 1 (NF1)] speed up GTP hydrolysis [43, 45].

Under physiological conditions, when cells receive relevant stimuli, such as the interaction between a growth factor ligand and its tyrosine kinase receptor, the GEFs activity facilitates the exchange of GDP for GTP, which has higher affinity and higher cellular concentration (approximately 10-fold) than GDP [46]. Structural studies of GDP-bound RAS and GTP-bound RAS complexes have revealed GTP-induced changes in two specific regions of the RAS protein, namely region switch I and region switch II. This results in drastic conformational changes of the whole protein, which results in a rewiring of the interactions with upstream regulators and downstream effectors [47,

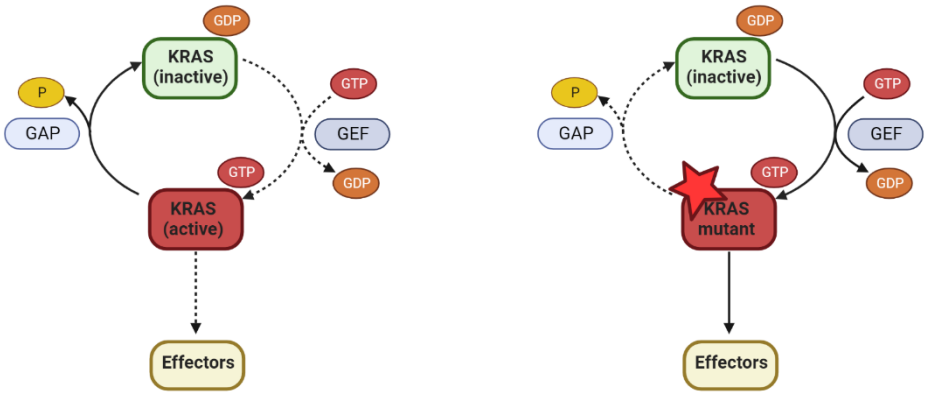

Figure 2. Regulation of the Ras GDP-GTP cycle in normal and neoplastic cells. The left panel illustrates the regulation in normal cells, where GDP-bound Ras in the "OFF" state is activated by a GEF, which facilitates the conversion of GDP to GTP (yielding the "ON" state of Ras). The hydrolysis of GTP to GDP and P_i converts the active form of Ras to the inactive form. In the right panel, the Ras mutant form typical of cancer cells is continuously in a GTP-bound, active state. Adapted from "Drugging the undruggable RAS: Mission Possible?". Cox et al, 2019. Created by BioRender.com

48]. In particular, in its GTP-bound form, KRAS binds a set downstream transducers to trigger a series of signaling cascades. In cancer, oncogenic RAS mutations result in a constitutively activated state whereby RAS proteins are no longer self-inhibited by their standard GTPase activity [43, 49] (Fig. 2).

RAS main pathways: regulators and effectors

RAS proteins can be activated by extracellular signals, such as growth factors, chemokines and receptor tyrosine kinases (RTKs) and, in turn, activate a large repertoire of signaling pathways.

Many growth factors can activate RTKs and then KRAS, such as epidermal growth factor (EGF), platelet-derived derived growth factor (PDGF) and fibroblast growth factors (FGFs). One of the major pathways implicated in KRAS activation is characterized by the initial stimulation of EGFR by its ligand, EGF. Signal transduction between EGFR and RAS is mediated by cytosolic adaptor proteins such as growth receptor-binding protein 2 (GRB2). These adaptor proteins contain one Src homology 2 (SH2) domain that recognizes tyrosine phosphorylated sites on RTKs, and two SH3 domains that bind C-terminal proline- rich motifs of GEFs [50]. Three main classes of RAS-GEFs are currently known: SOS, RAS-GRF and RAS-GRP. Among these, the most characterized are SOS proteins (SOS1 and SOS2), which accelerate the release of GDP from RAS, enabling GTP to take its place.

In addition to SOS proteins, another key factor of KRAS activation is Src homology phosphatase 2 (SHP2), a protein tyrosine phosphatase (PTP). Several studies have shown that SHP2 is implicated in the activation of different signaling pathways, in particular those mediating signals through the KRAS signaling cascade [51]. In fact, some phosphorylation sites of SHP2, such as tyrosine 542 and 580, have been identified as the main binding sites for GRB2 [52]. Therefore, SHP2 may promote recruitment of the GRB2-SOS1 complex to the receptor and the subsequent KRAS activation.

The GTP-bound form of RAS can engage a significant roster of effectors, which regulate different pathways important for cell growth and survival. The canonical downstream pathway of KRAS is the RAF-MEK-ERK axis (Fig. 3). RAS enables the activation of rapidly accelerating fibrosarcoma (RAF) kinase family, composed of ARAF, BRAF and CRAF. These serine-threonine kinases work as homodimers or heterodimers and their task is to phosphorylate mitogen-activated protein kinase 1 and 2 (MEK1 and MEK2). MEKs mediate the phosphorylation of extracellular signal-regulated kinases 1 and 2 (ERK1 and ERK2); activated ERK phosphorylates ribosomal S6 kinase (RSK), serum response factor (SRF), E26 transformation-specific transcription factors (ETS) and ETS like-1 protein to

affect the transcription and translation of target genes, thus regulating cell proliferation, differentiation, migration and other fundamental cellular activities [53]. The MAP kinase pathway can, eventually, stimulate cell replication thanks to the MYC-regulated expression of proteins such as cyclin D, piloting the cell cycle into G1 phase [54].

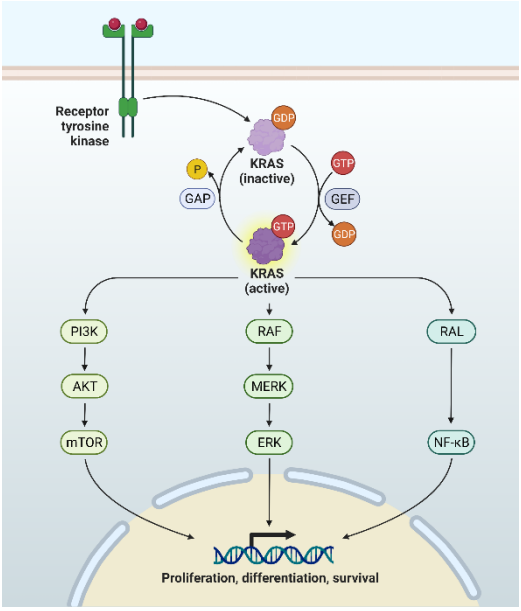

Figure 3. **The RAS signaling pathway.** KRAS signaling is involved in various cellular processes such as cell proliferation, differentiation and survival. RAS manifold activities rely on the stimulation of different downstream pathways, including the MAPK cascade, the PI3K-AKT axis, and the REL-NFkB system. All these pathways convey mitogenic, pro-migratory and anti-apoptotic signals that collectively define the malignant phenotype of cancer cells. Created in Biorender.com.

Mechanisms of negative feedback have been highlighted within this pathway [55], involving Sprouty/Spred family and dual-specificity phosphatases (DUSPs); Spreds inhibit ERK activation by binding RAS and the NF1 GAP, thus blocking RAF activation [56]. DUSPs expression is stimulated by ERK itself, which can also directly inhibit BRAF and CRAF phosphorylation [57, 58].

KRAS was also found to be involved in the PI3K-AKT-mTOR pathway [43] (Fig.3), which is considered to play an important role in cell proliferation, differentiation, apoptosis and glucose transport. RAS activates type I phosphatidylinositol 3-kinase (PI3K), allowing its translocation to the membrane and conformational changes that activate the kinase. Executing its duty, PI3K phosphorylates phosphatidylinositol-4,5-bisphosphate (PIP2) in order to convert it into phosphatidylinositol-3,4,5-trisphosphate (PIP3). Thanks to its pleckstrin-homology and other domains, PIP3 binds various downstream effectors including 3-phosphoinositide-dependent protein kinase-1 (PDK1) and AKT (also termed PKB). AKT is a serine-threonine kinase that phosphorylates substrates relevant for cell-cycle progression, metabolism, migration, and survival, such as mammalian target of rapamycin (mTOR), forkhead box O (FOXO), nuclear factor NF-kB, MDM2, and BAD [59].

Many other effectors have been characterised throughout the years, even though less studied, like RAL guanine nucleotide dissociation stimulator (RALGDS), which promotes

GDP/GTP conversion in RAS-like protein (RAL) (Fig.3). The RALGDS pathway is involved in the inhibition of transcription factors of the FoxO family, capable of favouring cell cycle arrest through p27 and apoptosis through BIM and FAS ligand [60, 61]. Moreover, RAL downstream signals are associated with cell migration, through downstream signals mediated by Rac/cell division cycle 42 (Cdc42) [62], viral immunity (with TANK binding kinase1 – TBK1) [63, 64] and endocytosis [65]. In addition, KRAS regulates PKC and TIAM1. The latter activates the RAC1 pathway, relevant for motility, membrane trafficking and migration [66].

Oncogenic RAS mutations in human cancers

Ras is the most commonly mutated oncogene in human cancers, occurring in approximately 30% of human tumors [49]. Among RAS genes, the KRAS isoform is the leading cause of 85% of RAS-driven cancers, followed by NRAS (found in 11% of RaAS-driven cancers) and HRAS (in 4% of RAS- driven cancers) [49, 67]. KRAS mutations occur most frequently in solid tumors such as non-small cell lung cancer (NSCLC), CRC and pancreatic ductal carcinoma (PDAC), at rates of 30%, 42% and 80%, respectively [5, 68-70] (Fig. 4).

NRAS mutations are common in hematopoietic malignancies and melanoma, whereas HRAS mutations are frequently associated with tumors of the bladder, thyroid and head and neck [71, 72]. The involvement of RAS signaling in cancer is evident not only by the high incidence of RAS mutations, but also by the high frequency of mutations in RAS regulators (such as RTKs and NF1) and effectors (such as members of the MAPK and PI3K pathways) [73, 74]. KRAS mutations prevent GAP interaction with KRAS and subsequent hydrolysis of KRAS-bound GTP, leaving the protein in a constitutively active form. KRAS mutations generally occur (in 98% of cases) at codon 12, 13 or 61, with a relative distribution that is variable across different cancer types. Indeed, KRAS G12C is mainly represented in lung adenocarcinoma (41%), whereas KRAS G12D variants are the two most common mutations present in CRC and PDAC, with a distribution of 29% and 43%, respectively [75].

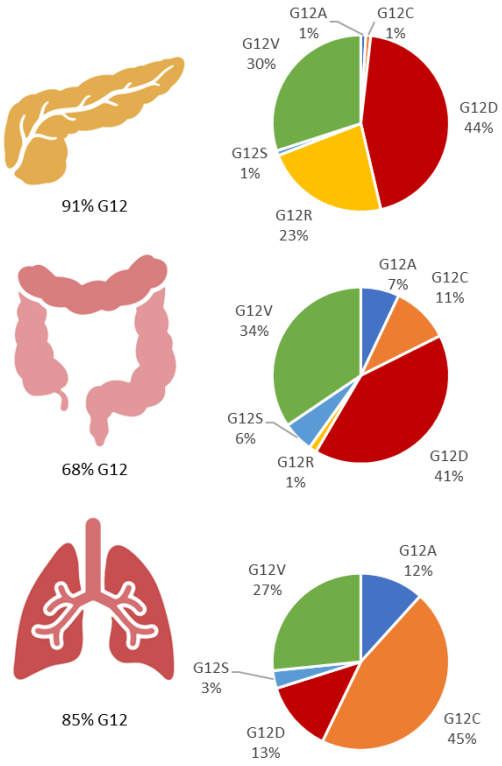

Figure 4. RAS isoform in different human cancers. Percentages of codon 12 KRAS mutations in pancreatic, colorectal and lung adenocarcinoma. The distribution of amino acid substitutions at the mutated codon 12 for each tissue type is shown in pie charts. Data acquired from The Cancer Genome Atlas (pan-Cancer), cBioPortal and Project GENIE269 (GENIE v7.0 public). Adapted from Moore, A.R., Rosenberg, S.C., McCormick, F. et al. RAS-targeted therapies: is the undruggable drugged?. Nat Rev Drug Discov 19, 533–552 (2020). Created by BioRender.com

Each variant has a specific and unique impact on KRAS GTPase activity. For example, G12C mutants show GTPase activity similar to wild-type, while G13 and Q61 mutants show increased intrinsic, GEF-mediated nucleotide exchange [76]. On the opposite, KRAS codon 13 mutations maintain residual sensitivity to NF1 GAP-mediated hydrolysis, as opposed to KRAS isoforms mutated in codon 12 or 61. Interestingly, concurrent mutations of KRAS G13 and NF1 are frequently found in cancer cells, emphasizing the fitness advantage provided by blunting the residual inhibitory activity of NF1 GAP [77]. At the same time, different mutations confer to KRAS a different propensity to bind downstream effectors. For example, when compared to other mutations or to the wild-type KRAS isoform, G12C and G12V mutations preferentially activate Ral signaling, which results in reduced phosphorylation levels of PI3K pathway [78]. In contrast, KRAS G12D-mutated cells have slow affinity for RAF1 (around five-fold less than wild-type protein) and increased levels of phosphorylated AKT [79].

Role of oncogenic KRAS in tumorigenesis

RAS-activating mutations are genetic events that typically occur early in tumor development, suggesting that they play a critical role in initiating neoplastic transformation and promoting cancer progression [47]. Several pieces of evidence in

tumor cell lines and mouse models have shown that *KRAS* mutations exert important cancer-inducing activity in RAS-driven tumors. However, activation of RAS together with loss of tumor suppressor genes, such as *TP53*, *LKB1*, or *APC*, in several cancer types led to further enhancement and acceleration of KRAS-driven tumor progression [80-82]. These observations suggest that additional genetic lesions that cooperate with the oncogenic activity of KRAS are required to unleash complete malignant transformation. Accordingly, studies in *in vivo* models have documented that restricted expression of KRAS G12V in mouse lungs led to tumor formation, but inactivated or mutant forms of P53 further promoted progression to more advanced lung tumors and metastasis [83, 84]. In mouse colonic epithelium, expression of KRAS G12D was sufficient to initiate hyperplastic growth [82]. However, it is believed that oncogenic KRAS may play a greater role in accelerating tumor progression in the colon, since inactivation of APC typically precedes KRAS activation in human colon cancer.

KRAS oncogene addiction

Not only do RAS mutations occur early in cancer onset, but there is abundant experimental evidence suggesting that continued expression of mutant RAS is necessary for tumor maintenance [59, 85]. The phenomenon whereby cancer cells with mutant oncogenes often depend on continuous signaling of a single gene product is termed "oncogene addiction" [86]. This knowledge has led to the discovery of drugs that specifically target these oncogenes and in some cases to the development of FDA-approved drugs, such as in chronic myeloid leukemia with *BCR-ABL* oncogene fusion treated with ABL kinase inhibitors (Imatinib/Gleeevec) [87], *BRAF*-mutant melanoma treated with MEK and BRAF inhibitors [88], anaplastic lymphoma kinase (ALK) translocated NSCLCs treated with crizonitinib [89, 90] and EGFR inhibitors for *EGFR*-mutant NSCLC [91]. Despite these successes, clinical validation of oncogene addiction of different oncogenic drivers, such as *MYC* mutations and amplifications or RAS mutant forms, has not been possible because pharmacological approaches to directly inhibit these targets have been particularly difficult to develop or poorly explored. Further, even when possible, targeting oncogene dependence with single agents often results in

primary or acquired drug resistance. The difficulty in targeting individual cancer genes can be attributed to the inter- and intra-tumor genomic heterogeneity that characterizes most cancers [92].

In the case of *KRAS*, some reports have shown that KRAS dependency is variable across tumors and that not all *KRAS*-mutant tumors rely on RAS hyperactivation for their growth. In two studies from Settleman and collegues [93, 94], *KRAS* dependency was determined by performing short hairpin RNA (shRNA)-mediated *KRAS* knock-down in different cancer cells types. The results of these screens showed that KRAS depletion has a variable effect on cell viability, which led to the classification of some cancer cell lines as KRAS-dependent and others as KRAS-independent. KRAS-dependent cells displayed a decreased viability and induction of apoptosis after KRAS knock-down, whereas KRAS-independent cells did not. In addition, a gene signature [93] identifying the KRAS-dependent group was established through a differential gene expression analysis to discriminate up-regulated genes. In particular, KRAS dependency was related to an epithelial phenotype due to E-cadherin expression, while KRAS independency was associated to a mesenchymal-like phenotype involving vimentin expression, suggesting a possible mechanism of resistance to KRAS inhibition. Interestingly, the correlation between KRAS dependence and an epithelial phenotype has been reported only in lung and pancreatic adenocarcinoma cell lines, but not in *KRAS*-mutant colorectal cancer cells, suggesting that lineage-specific KRAS-dependency might exist in various tumor contexts. In the following years, several other groups, together with Settleman's group, have observed heterogeneous dependence for sustained KRAS expression in *KRAS*-mutant cancer cell lines [93, 95-98]. In particular, a large-scale RNAi screening known as Project DRIVE [99] reports KRAS independence following shRNA-mediated KRAS knock-down in several commonly used *KRAS* mutant models. These findings have important clinical implications, as they suggest that a further stratification of KRAS-mutant tumors may be required to deploy effective KRAS-directed therapies, as the mere presence of the mutation is likely not sufficient to predict addiction.

Therapeutic targeting of KRAS in cancer

For more than 30 years after its discovery, RAS has been considered an undruggable target because of its small size and the absence of deep pockets to which small molecule inhibitors can bind [100]. The picomolar affinity of RAS to GTP and the high intracellular concentration of GTP have made the development of KRAS inhibitors even more difficult. However, even if drugs able to fully abrogate the function of all *KRAS*-mutant isoforms in cancer cell are still to be identified, in recent years a notable effort has led to the development of molecules capable of inhibiting specific *KRAS* mutations.

Direct inhibition of KRAS: the case of G12C and G12D

Given the major role of KRAS post-translational modifications for its membrane-association, farnesyltransferase inhibitors (FTI) were tested in clinical trials (the hypervariable region and CAAX motifs are easier to target). Unfortunately, FTIs lack efficacy in *KRAS*-mutant cancer, as the abrogation of farnesyltransferase activity is balanced by alternative prenylation of *KRAS* through geranyltransferase type 1 [43, 101]. The option of co-inhibiting both enzymes to overcome redundancy remains relatively unexplored at the clinical level, due to the high risk of toxicity in normal tissues [49]. Nonetheless, new therapeutic approaches are being developed in this field, as well [102]: for instance, an inhibitor of isoprenylcysteine carboxylmethyltransferase has recently led to promising result *in vitro* [103].

The breakthrough in the identification of new drugs targeting directly KRAS came in 2013, when Shokat's group first detected, through crystallographic studies, a new allosteric pocket – named switch-II pocket - beneath the effector binding switch-II. They exploited the properties of the cysteine located in this pocket to create new molecules capable of covalently binding and specifically inhibiting only the G12C-mutant protein [104].

The idea to selectively target mutated forms of KRAS has a great translational potential, because wild-type isoforms, present in normal tissues, should be preserved [105], limiting toxicity. Therefore, following the initial studies mentioned above, multiple small molecules have been developed against KRAS G12C, including ARS-1620, sotorasib (AMG 510), and adagrasib (MRTX849). By binding the acquired cysteine within the

switch-II pocket, these compounds reduce the activity of KRAS by two mechanisms. On the one hand, they promote the maintenance of GDP binding, thus trapping KRAS in its inactive conformation. On the other hand, these small molecules reduce the affinity of KRAS for its downstream effectors, with an inhibitory effect on the pathway.

Although ARS-1620, the first specific inhibitor of KRAS G12C, has shown little clinical activity [106], it paved the way for the development of the other two drugs, AMG 510 and MRTX849, which entered clinical trials in August 2018 and January 2019 respectively (CodeBreaK100 ClinicalTrials.gov identifier: NCT03600883 and KRYSTAL-1 ClinicalTrials.gov identifier: NCT03785249). Other compounds [LY3499446 from Eli Lilly (NCT04165031); JNJ-74699157 from Johnson & Johnson (NCT04006301); GDC-6036 from Roche (NCT04449874); and D-1553 from InventisBio (NCT04585035)] are currently under evaluation in phase 1 clinical trials. However, trials with LY3499446 and JNJ-74699157 have been suspended due to the development of unexpected toxicities and for still-undisclosed reasons, respectively.

A recent work has shown that AMG510 cures CRC tumor models in immune-competent mice. Results indicated that the drug can increase the infiltration of T cells, mainly CD8+ T cells, macrophages and dendritic cells into the tumor mass, creating in this way a pro-inflammatory microenvironment with the collaboration of interferon and chemokine signaling [107] that contributes to cancer eradication. However, although a phase I clinical trial conducted in 129 patients with solid tumors [80] showed promising efficacy results for AMG510, responses were suboptimal in individuals with CRC, suggesting that anti-KRAS G12C monotherapy is insufficient to achieve meaningful and durable responses in these patients. This suggests that in the clinical setting the scenario is more complex than in preclinical model systems. As explained before, KRAS is at the centre of a dense range of both upstream regulators and downstream mediators able to activate feedback loops [106]. In the case of CRC, functional adaptation to KRAS G12C blockade appears to be sustained by intrinsically high EGFR signaling [108]. In lung cancer, single-cell RNA sequencing approaches have shown that tumor cells adapt to KRAS G12C inhibition by synthetizing new KRAS G12C protein, which becomes activated by EGFR and the SHP2 phosphatase; the activation of upstream components of the EGFR-RAS pathway favors a switch towards a GTP-bound active form of KRAS that is insensitive to the drug. This reactivation was observed only in a subpopulation of KRAS-mutant lung

cancer cells, reinforcing the idea that resistance may be driven by genetic or functional heterogeneity of cancer cells [106]. Following these observations, a combined targeting of both EGFR and KRAS G12C was exploited to achieve a more effective treatment, thanks to the reversion of the resistance mechanism [109]. Since it has also emerged that SHP2 is essential in transducing the mitogen-activated stimulus of multiple RTKs to KRAS [51, 110], clinical trials studying a combinatorial treatment using both SHP2 and KRAS G12C inhibitors are being planned, based on promising results *in vitro* and *in vivo* [58, 111, 112].

In addition to those described above, other resistance mechanisms have been reported that render KRAS inhibition ineffective in KRAS-mutant tumors: amplification of the transcriptional co-activator YAP1 gene has been hinted as a way for cancer cells to survive KRAS function depletion in KRAS dependent tumors [113] and it is largely documented that mutations in downstream proteins of the pathway such as BRAF or MEK can occur as mechanisms of acquired resistance to KRAS G12C blockade [43]. Other examples include the observation that KRAS G12C mutant lung cancer cells express higher levels of ERK1/2 phosphorylation than KRAS G12D and, because of this, might display peculiar susceptibility to treatment with MEK inhibitors [114]. Further, a positive effect on tumor regression has been demonstrated by combining KRAS G12C blockade and PI3K pathway inhibition both *in vitro* and *in vivo* [115]. Whether PI3K hyperactivation, following mutant KRAS inhibition, is due to an adaptive reaction to MEK/ERK inhibition and or to parallel and independent signals remains to be determined [115]. Theoretically, inhibiting multiple vertical and orthogonal effectors is expected to render distinct subgroups of cancers more sensitive to target therapies compared to single-agent inhibition [116, 117].

The success achieved with the development of KRAS G12C specific inhibitors has led to the search for new strategies to block other mutations that may occur in the context of KRAS-mutated tumors. In particular, new approaches took advantage of the lower intrinsic GTPase activity of other KRAS mutations compared with G12C, with the idea to target the active GTP-bound form of KRAS (Ras-ON inhibitors) [118]. Altogether, KRAS G12C inhibitors paved the way for the development of more efficient drugs and for new options to directly target also the other mutant variants of KRAS. Indeed, thanks to a better understanding of the dynamics of the nucleotide cycle and key structural

elements of the KRAS switch II pocket, MRTX1133 was recently identified as a potent inhibitor of KRAS G12D protein [30]. The identification of MTRX1133 provides the opportunity to target oncogenic KRAS G12D mutations, which are most prevalent in PDAC [69] and CRC [70], and to investigate how oncogenic KRAS G12D mutations contribute to the development and progression of these types of cancer. Exposure of both cell-line-derived and patient-derived tumor xenograft models to MRTX1133's resulted in significant tumor regression in eight out of eleven PDAC models and two out of eight CRC models [32]. These findings suggest that KRAS G12D consistently acts as a potent oncogenic driver in PDAC, but its role may vary in CRC. This may be due to the fact that KRAS mutations are a genetic event that occurs early on and is the main driving force in PDAC. In contrast, KRAS mutations in CRC may occur later on or in combination with other mutations that affect CRC dependence on KRAS [119], leading to a less uniform effect. Even though significant shrinkage of tumors was seen in several models, a better understanding of the anti-tumor activity of MRTX1133 is needed to determine its effectiveness in treating different types of cancer and to develop strategies to overcome potential limitations such as the recovery of KRAS-dependent signaling. As seen with most targeted therapies, preliminary evidence suggests that several mechanisms of resistance will limit the efficacy of these mutation-specific KRAS inhibitors when used as single agents, raising the need to develop more effective rational combinations.

Indirect targeting of KRAS-mutant tumors

In the past, several groups have shown that inhibition of different effectors of KRAS and the related RTK-mediated signaling pathways may be a potential vulnerability in the KRAS-mutant context. Large-scale drug screens have been conducted in cancer cell lines, with different lineages and genotypes, to compare the sensitivity of compounds in the RAS-mutant or RAS-WT context. The results of these studies repeatedly reported that treatment with inhibitors of the MAPK pathway, such as MEK1/2 and RAF kinases, although leading to a cytostatic rather than a cytotoxic response, was significantly more effective against KRAS-mutant cells compared to their RAS wild-type counterparts [120-122]. These studies have also demonstrated functional dependencies on RTK signaling pathways, such as those emanated by IGF1R, FGFR1 and MET, in a subset of KRAS-

mutant lines [121, 123, 124][124]. Co-dependence of KRAS mutants to RTK activity could be justified by the fact that RAS-mutant cancer cells are able to produce autocrine growth factors, such as EGF [125]. Accordingly, an *in vivo* study reported the importance of EGFR autocrine signals in the tumorigenesis driven by SOS-dependent skin tumors [126]. Although there is preclinical evidence suggesting that EGFR inhibition can increase the efficacy of MEK inhibitors against KRAS-mutated tumors [127], RTK blockade *per se* does not exert significant effects [18, 20]. Indeed, in clinical trials EGFR-targeted therapies proved to be ineffective in tumors carrying RAS mutations, which resulted in exclusion patients with KRAS-mutant tumors (including CRC and NSCLC) from treatment with EGFR inhibitors [128-130].

As we mentioned above, oncogenic KRAS signaling operates through a wide range of downstream signals that regulate key cellular functions in normal cells. Several efforts have been conducted over the years to develop effective drugs targeting the critical effectors that mediate these signals. However, downstream indirect inhibition of KRAS signals has proven particularly difficult, mainly due to the multiple feedback mechanisms that make the identification of a single target to block KRAS activity extremely challenging.

The canonical pathway that acts downstream to KRAS is the MAPK pathway. Indeed, numerous inhibitors targeting the critical RAF-MEK-ERK signaling cascade have been implemented and tested in different RAS-mutant context. BRAF is the best characterized isoform of the RAF family, and several approaches have been explored to inhibit it and its mutated form V600E. Among BRAF inhibitors, vemurafenib and dabrafenib, two first-generation ATP-competitive inhibitors, have been approved for the treatment of BRAF-mutant melanoma [131, 132]. However, when tested in RAS-mutant cancer cell lines, drug binding to one RAF homodimer paradoxically produces reactivation of ERK, due to trans-activation of the other drug-free RAF [133-136]. Notably, reactivation of C-RAF has been observed in wild type BRAF cells but not in BRAF-mutant cells [134]. More recently, novel pan-RAF inhibitors, such as LY3009120, have been developed to mitigate this paradoxical effect. However, despite promising preclinical data in several cancers [137, 138], monotherapy with LY3009120 has failed to produce the same efficacy in clinical trials. Currently, there are no active clinical trials using single-agent B-RAF inhibitors in K-RAS mutant solid tumors. Similarly, MEK inhibitors used as monotherapy

have shown disappointing results in KRAS-mutant tumors [139], due to compensatory feedback-mediated activation of the RTK-RAS-MAPK pathway, which leads to increased phosphorylation of MEK [140]. To date, no MEK inhibitors are clinically approved for the treatment of KRAS-mutant tumors. In preclinical models of KRAS-mutant cell lines the combination of MEK and RAF inhibitors has shown synergy [97, 141]. Currently, a phase I clinical trial studying the combination of belvarafenib (HM95573, RAF inhibitor) and cobimetinib (MEK inhibitor) is enrolling patients with advanced solid tumors (NCT03284502).

In addition to the MAPK pathway, KRAS can also activate PI3K-AKT-mTOR signaling. In contrast to the mutual exclusivity of BRAF and KRAS mutations, PIK3CA and KRAS mutations are often present in human tumors, suggesting that KRAS is not the major activator of the PI3K pathway. In fact, monotherapies targeting the PI3K/AKT pathway have failed to achieve effective results in KRAS-driven tumors both *in vitro* and *in vivo* [142]. On the contrary, a combination of MEK and AKT inhibitors showed encouraging results in pancreatic cancer cellular and animal models [143]. Accordingly, several combinatorial regimens have entered clinical trials, such as the combination of PI3K inhibitors with ERK inhibitors [95], MEK inhibitors (NCT01363232, NCT01337765, NCT01392521, NCT01390818) or RAF inhibitors. However, these promising results have not been further pursued clinically either because of lack of clinical benefit, such as in the case of CRC [144, 145], or because of high toxicity [146].

In recent years, growing interest has been placed on the protein tyrosine phosphatase SHP2. As stated above, SHP2 acts as a convergent node downstream of many RTKs, regulating the signaling strength of the RAS/MAP kinase pathway. Co-inhibition of SHP2 and MEK1/2 provided prolonged tumor growth control in preclinical models, suggesting dependency on SHP2 activity in KRAS-driven cancers [84]. Based on such findings, several SHP2 inhibitors (such as RMC-4630 and TNO155) are currently in clinical trials for the treatment of KRAS-mutant tumors, alone or in combination with MAPK inhibitors (LY3214996 - NCT04916236) [109, 110]. RTKs also activate RAS signaling through the GRB2-SOS complex, so another approach relies on SOS1 inhibitors, such as BI-3406. These compounds block KRAS upstream activation by preventing reloading of KRAS with GTP and limit cellular proliferation in KRAS-driven cancers [111, 112].

In conclusion, although emerging opportunities may change the current scenario, consolidated evidence suggests that inhibitors targeting single effectors along KRAS downstream signaling pathways will have limited efficacy due to compensatory feedback mechanisms. Therefore, although inhibition of KRAS effectors is a potential strategy to target KRAS-driven tumors, it remains a significant challenge, and successful targeting of KRAS-mutated tumors will likely require simultaneous targeting of multiple effector pathways [124].

Synthetic lethal interactions with KRAS: different approaches with RNAi and CRISPR/Cas9 screens

We have seen in previous sections how direct inhibition of KRAS and co-inhibition of multiple effectors can be difficult and has a narrow therapeutic window. To overcome this problem, it has been proposed that cancer treatment should focus not only on directly counteracting the signals triggered by oncogenic mutations, but also on looking for co-dependencies of cancer cells from non-mutated genes [147]. Indeed, following acquisition of an oncogenic mutation, cancer cells may develop secondary dependencies on other survival signals, the disruption of which can result in oncogene-specific 'synthetic lethal' interactions likely to provide novel therapeutic options [148, 149].

Sensu stricto, synthetic lethality occurs when cells with a given genetic alteration, such as a cancer-associated mutation, die upon inactivation of another specific non-lethal gene. In a broader sense, synthetic lethal codependencies can involve multigenic functional patterns at various levels, including signals within the same pathway regulated by the mutant oncogene, or within parallel pathways that cooperate with respect to an essential function, or even along distant pathways that become functionally connected because of the cellular responses to a particular perturbation. In last decade, increasing interest in the identification of novel oncogene-specific synthetic lethal interactions has been fostered by intensifying technological advances in genetic tools, first using RNA interference (RNAi) and more recently by applying CRISPR/Cas9 (clustered regularly-interspaced short palindromic repeats and CRISPR-associated proteins) technology [63, 150].

RNAi consists of introducing exogenous RNA molecules in a cell, which suppress endogenous gene expression at the transcriptional and/or translational level by binding

to mRNA transcripts through sequence complementarity [151]. RNA is targeted by double-strand small interfering RNAs (siRNAs) or ectopically expressed short hairpin RNAs (shRNAs). Differently, CRISPR technology involves the introduction in cancer cells of the CRISPR-associated endonuclease Cas9, able to edit the targeted DNA sequence and to induce double-strand breaks. A guide RNA (gRNA) transfected into the cell through different ways is complementary to the sequence in the genome and pilots Cas9 at the precise point where the cut is operated. To fulfil genome editing, Cas9 needs the presence of a specific sequence of three nucleotides located downstream of the site of cut, called protospacer-adjacent motif (PAM). After Cas9-dependent formation of DNA double-strand breaks, DNA damage is repaired by homologous end joining (NHEJ), which leads to a high rate of indel mutations because of an error-prone DNA repair system. Hence, the complete loss-of-function in the protein is obtained because DNA double-strand breaks lead to frameshift insertion or deletion mutations. The identification of this enzymatic system, phylogenetically used by bacteria and archaea to break and make inoffensive the genomic sequence introduced by phages, allows direct gene knock-out rather than RNAi-induced knock-down in gene expression. PAM sequence explains also the reason why only viral DNA is cut, since the bacterial genome does not include this motif and so Cas9 is not able to act as a nuclease towards it [152].

In recent years, several studies have applied RNAi technology in human cancer cell lines, employing a variety of siRNA or shRNA libraries to identify genes that exhibited lethal synthetic interactions with mutant KRAS. Results from these screens led to the identification of a wide range of candidate genes as synthetic lethal interactors with oncogenic KRAS, including PLK1, TBK1, STK33, and YAP1 [63, 150, 153, 154]. However, despite the large amount of information obtained by these screens (which further confirmed the critical role of KRAS in many cellular mechanisms), there are several limitations, including the off-target activity of RNAi libraries and an insufficient concordance in results of different screens [154]. Importantly, none of the targets identified is superior to KRAS itself in discriminating KRAS-mutant and KRAS-wild-type cells [49].

Growing evidence indicates a better reproducibility for CRISPR-based screening than RNAi-based screening, probably due to the lower frequency of gRNA off-targets and the higher specificity resulting from the production of more penetrant phenotypes due to

the null alleles generated by gene knock-out [155-157]. Therefore, genome-wide CRISPR/Cas9 screens have proven to be an efficacious tool to identify synthetic lethal interactions in tumors harboring oncogenic mutations such as KRAS [158]. However, now that results from a number of CRISPR/Cas9 screening approaches have been gathered, it is becoming increasingly clear that not all synthetic lethal interactions are applicable to all RAS-driven tumors. Stated differently, there are idiosyncratic differences and specificities among research groups, cellular models and analytical interpretations that make it difficult to distil generalizable conclusions. This lack of significant overlap may be due to both differences in oncogenic and secondary mutations and differences in the types of cells selected for individual screenings. Indeed, the vast majority of synthetic lethality screens have been performed on isogenic cell lines, which are amenable to experimental manipulation, but introduction of mutant KRAS into wild-type cells does not necessarily confer KRAS oncogene addiction, and loss of mutant KRAS may force KRAS-dependent cells to upregulate compensatory pathways [49]. Moreover, cultured cell lines hardly recapitulate the overall biological texture of the original tumor due to extensive adaptation and selection.

Recently developed 3D culture technologies have led to the development of novel and more physiological human cancer models, which rely on self-organization of tumor tissues into organotypic cultures following embedment into a 3D matrix. In particular, patient-derived tumoroids have been shown to maintain the genetic characteristics and drug response of the corresponding patient donors [159]. Thus, patient-derived tumoroids more faithfully reflect the functional consequences of KRAS mutant alleles and more comprehensively incorporate the repertoire of driver and passenger mutational events and the signaling networks that spontaneously evolve during the tumor natural history. We envision that the deployment of more valuable preclinical models that more thoroughly take into account tumor heterogeneity and evolution, coupled with the use of more precise technological tools, such as CRISPR/Cas9, could provide further insights into the biology of KRAS in oncogenic KRAS-driven cancers to facilitate the development of KRAS-directed therapeutic strategies.

AIM OF THE WORK

To date, pharmacologic targeting of activated RAS has failed. With the exception of KRAS G12C inhibitors, mutationally activated RAS proteins are not susceptible to compounds that inhibit GTPase function, and therapies that interfere with RAS post-translational modifications have not been clinically efficacious. More recently, several genome-wide RNAi-based screens revealed synthetic lethal relationships in which silencing of a candidate gene was found to affect proliferation of KRAS mutant cancer cell lines in different tumor settings. However, these findings have not translated into the development of effective inhibitors to treat KRAS mutant tumors, likely due to the difficulty in generalizing synthetic lethal discoveries across a broad range of tumor-specific backgrounds and the relative inadequacy of the cell models tested in terms of population representativeness and biological fidelity.

On these premises, the aims of this thesis work are to:

- Evaluate the reliability of CRC patient-derived organoids as a relevant model to investigate KRAS function.
- Optimize the CRISPR/Cas9 technology in organoids, to achieve efficient and reproducible KRAS knock-out.
- Exploit organoid models to evaluate the requirement for sustained RAS function in maintaining viability (KRAS dependency).
- Combine computational, genetic and biological approaches to identify functional traits specifically related to RAS dependency.
- Identify new synthetic lethal interactions in KRAS-mutant CRCs and design new, clinically applicable biomarkers for better patient stratification.

RESULTS

Establishment and characterization of a large mCRC PDX-derived tumoroid biobank

In the last 10 years our laboratory has collected, implanted sub-cutaneouslly in immunocompromised mice, and propagated approximately 600 mCRC samples. The structure of the platform and the reliability of PDX models for molecular and therapeutic stratification of CRC biology are discussed in previous works [160, 161]. Starting from this platform of mCRC PDXs, we embarked on the production of a parallel collection of matched tumoroids. We christened this resource of paired xenografts and tumoroids XENTURION (XENografts and TUmoroids for Research In ONcology).

We processed 264 samples from fresh surgical resections or explanted PDXs (for three cases, two liver metastases from the same patient were available). To minimize alterations in the biology of tumors and avoid biased selection of specific growth dependencies, we standardized culture conditions that sustained long-term growth of tumoroids in a medium with minimal composition, in line with the notion that CRC tumoroids become gradually independent from niche signals during cancer progression [162]. For preliminary inclusion into the biobank, each PDX-tumoroid pair had to show correct identity by genetic fingerprinting, negativity for human and mouse pathogens, and a histology congruent with CRC phenotypes (Fig 1A). This approach left us with 243 models; 19 cases were excluded because of wrong fingerprinting; four were diagnosed as lymphomas by histopathological evaluation; and one was excluded for technical reasons (deterioration of archived material) (Table 1 https://doi.org/10.6084/m9.figshare.23500194.v1).

We defined tumoroids as 'established' when they could be propagated for at least three passages or expanded enough to be cryopreserved. The vast majority of PDX-derived tumoroids (PDXTs) (211/243, 87%) were processed using freshly explanted PDX tumors as only source, with an 80% establishment success rate (169/211) (Fig. 1B). In the few cases where PDXT derivation was attempted starting from frozen PDX tumors, the success rate was lower (5/10, 50%) (Fig. 1B). Differences in the production of established PDXTs were also observed when tumoroids were derived in parallel from fresh and

frozen material from the same PDX; in particular, starting from eight PDXs for which both fresh and frozen tumor fragments were available, the establishment rate was 75% for fresh tissues (6/8), and 25% for frozen material (2/8) (Fig. 1B). Although the number of PDXTs established from frozen PDX tumors is small, these figures suggest that freshly explanted tumors may be more suitable to PDXT establishment than frozen material. XENTURION also includes 13 tumoroids derived directly from fresh human specimens after surgery; in this subgroup, the success rate in the production of established tumoroids was markedly lower (5/13, 38%). Finally, for one case, tumoroids were successfully established from both fresh PDX explants and the original patient sample (Fig. 1B). Overall, XENTURION comprises 186 established mCRC tumoroids, with a success rate of 77% (186/243); the collection is almost completely represented by PDXT lines (181/186, 97%) for which paired PDXs are available (Fig. 1B). For tumoroid establishment, a single derivation procedure was sufficient in most models, with a success rate of 60% (147/243) (Fig. 1C). When establishment failed after the first attempt, two or more additional rounds were performed if PDXs were in line. The success rate of tumoroid establishment decreased proportionally with attempt repetition, dropping down to 44% after the second attempt, 36% after the third attempt, and 29% after the fourth or subsequent attempts (Fig. 1C). Hence, mCRC tumoroids that do not grow in culture after the first derivation round are unlikely to become established models.

Established tumoroids were credentialed as bona fide immortalized models, capable of long-term recovery and expansion, through a stringent validation protocol that included periodic identity checks, microbiologic tests and – critically – various freeze-thaw cycles. One hundred and forty-five established tumoroids underwent at least three freeze-thaw cycles, and 121 (83%) passed validation (Fig. 1D). Of practical utility, lack of recovery after the first freeze-thaw cycle was sufficient to identify 92% (22/24) of cases that would not survive additional 'rescue' cycles; at the same time, 100% of tumoroids that were recovered after the first freeze-thaw cycle successfully completed validation in subsequent cycles (Fig. 1D). For this reason, we relaxed the credentialing criteria and admitted in the final collection seven additional models that had survived two cycles and five models that had survived one cycle. Ultimately, XENTURION encompasses a

total of 133 validated tumoroids: 129 PDXTs (with paired PDXs) and four tumoroids directly derived from donor patients (Fig. 1A-D).

Fig. 1E summarizes the main clinical and molecular features of the samples that fed into XENTURION, including primary tumor sidedness and stage, patients' sex, age and exposure to therapy before sample donation, DNA microsatellite status, and the presence of clinically relevant driver mutations. To explore whether tumoroid derivation favored over- or under-representation of such features in XENTURION with respect to the starting population, we assessed their relative distribution in validated versus non-validated models. Enrichment analysis revealed that metastatic samples whose primary tumor was located in the right colon failed validation more often than expected by chance (Fig. 2A). This could be due to the fact that left-sided mCRC tumors are usually more dependent on EGFR signaling [163], thus more stimulated to grow by the EGF ligand present in the culture medium, than right-sided tumors. A similar enrichment among samples that failed validation was observed for tumors harboring KRAS mutations (Fig. 2A). This was quite unexpected, as KRAS mutant mCRC tumors are notoriously more aggressive than KRAS wild-type tumors [164, 165] and ectopic introduction of mutant KRAS promotes – rather than contrasts – the expansion of CRC tumoroids [166]. We suspected that the higher representation of KRAS mutant cases among tumoroids that did not pass validation could be due to a procedural bias related to the time when tumoroids were generated. PDXTs from KRAS wild-type tumors were more often derived from late-passage (more than three) PDXs, typically from large cohorts that had been propagated *in vivo* several times to obtain an adequate number of replicas for testing with the anti-EGFR antibody cetuximab. Since mutant KRAS is known to confer resistance to cetuximab [167], PDXs with KRAS mutations were not repeatedly expanded for cetuximab treatment, and tumoroids were generated from smaller cohorts at earlier passages. Confirming the hypothesis that PDX passaging rather than KRAS mutations impacts on PDXT stability, we found that late-passage PDXs were more likely to give rise to validated tumoroids than early-passage PDXs (Fig. 2B). This is in line with our observation that fresh samples from patients (never passaged in mice) were less prone to grow in culture (Fig. 1B) and suggests that serial mouse engraftment eases adaptation of cancer cells to long-term propagation *ex vivo*.

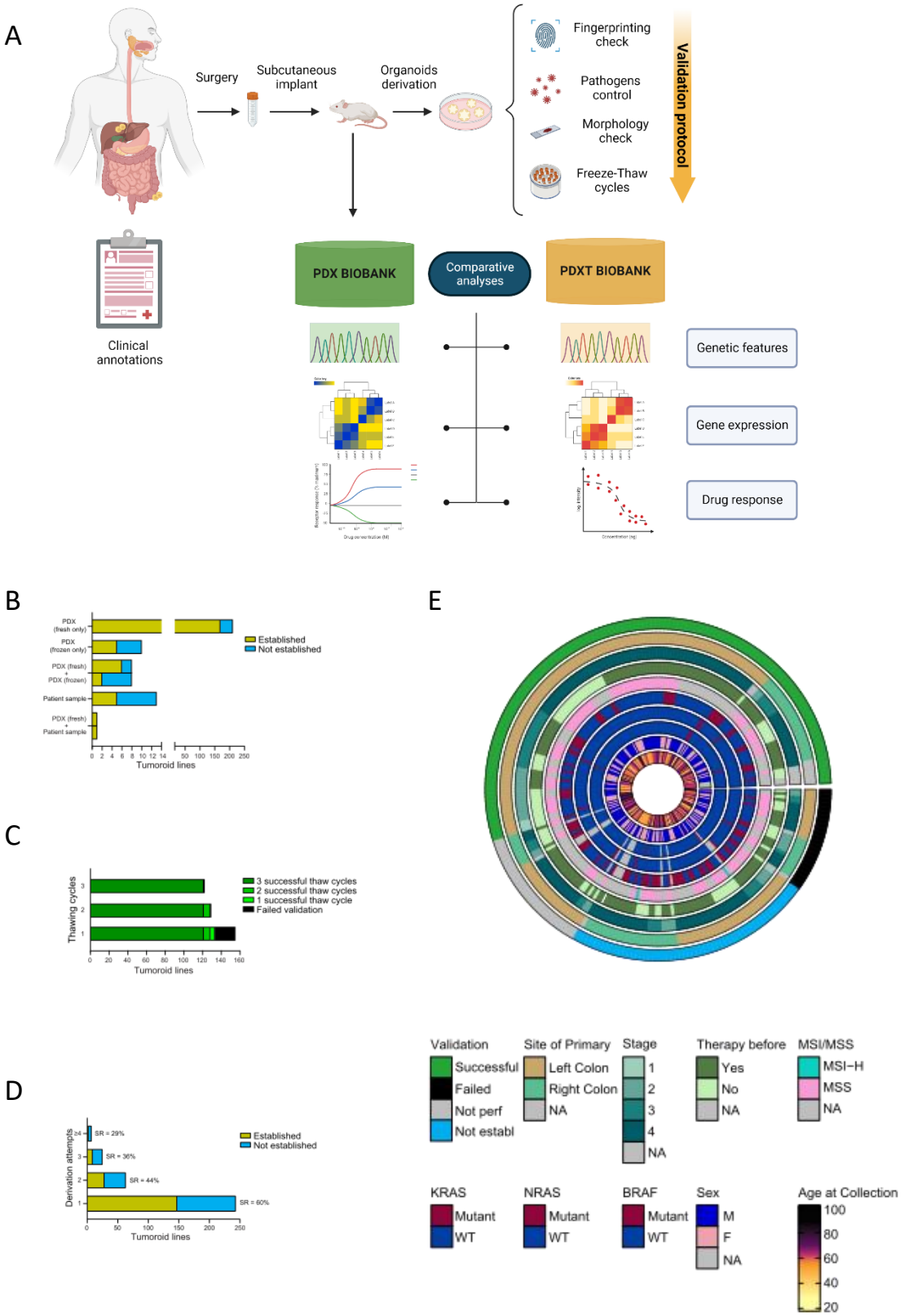

Figure 1. Metastatic colorectal cancer tumoroid derivation and patient characteristics. A) Schematic overview of XENTURION experimental design: matched patient-derived xenografts and tumoroids were compared for their genomic and transcriptomic profiles and for their response to clinically approved drugs. **B**, **C**) Success rate in the establishment of tumoroid lines according to the nature of the sample of origin **B**) or the number of derivation attempts **C**). When

tumoroids were established from different originating samples (e.g., fresh and frozen PDX explants), success rates were computed for models derived from freshly explanted tumors. SR, success rate. **D**) Number of validated tumoroids according to the number of freeze-thaw cycles. **E**) Main clinical and molecular features of the starting population from which tumoroid derivation was attempted. The circus plot includes all cases with successful validation (N = 133), those that failed validation (N = 24), established cases for which validation was not performed (Not perf, N = 29), and those that failed initial establishment (Not establ, N = 57). F, female; M, male; MSI-H, microsatellite instability high; MSS, microsatellite stability; NA, not available; WT, wild-type.

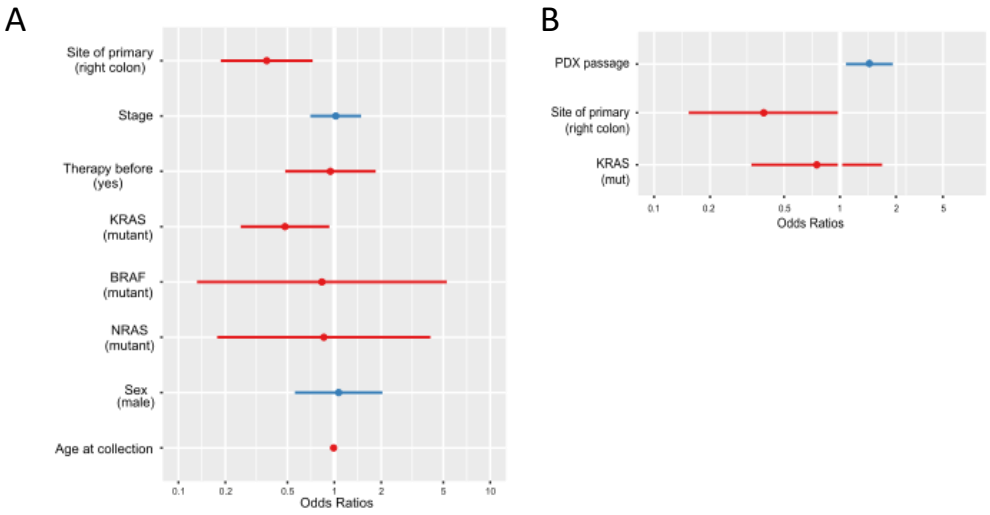

Figure 2. Impact of PDX passage on PDXT validation rates. A) Odds ratios of a multivariate logistic regression with PDXT validation success status (1, successful, N = 129; 0, failed, N = 73) as dependent variable and several clinical and molecular annotations as independent variables. **B**) Forest plot showing the odds ratios of a multivariate logistic regression with the establishment/validation status (1: successful - total: 64, 0: failed, total: 49) of tumoroids as dependent variable and the two significant terms (KRAS and site of primary) found in Fig.1E as independent ones, alongside the PDX passage at which the tumoroids were derived. KRAS mutated PDXTs are often derived from earlier xenografts passages, which are more prone to fail the validation procedure. Red color indicates that the independent variable has a negative effect on the validation rate; blue color indicates the opposite. The only continuous variables are stage and age at collection; all other variables are binary.

Mutational and gene copy number analysis of paired PDXTs and PDXs reveals substantial model concordance

We performed targeted next-generation sequencing of 116 relevant CRC genes [5] to detect small somatic alterations [single nucleotide variants (SNVs) and indels] in a set of 144 PDXTs and their matched PDXs. The overall distribution of allele frequencies and the number of identified variants were consistent between PDXTs and PDXs. Mutational profiles were analyzed more in depth for a subset of 125 sibling pairs, in which only validated PDXTs were included. At the level of individual genes, the vast majority of mutations were conserved, with no preferential occurrence in PDXTs or PDXs (Fig. 3A). This consistency was also maintained at the level of specific mutations; the Jaccard similarity coefficient was several logs higher for matched models than for unmatched models (average matched, 0.828; average unmatched, 0.006) (Fig. 3B). Specifically, KRAS mutations found in PDXs were confirmed in matched PDXTs in 36/37 models (97,2%). Importantly, the extent of mutational concordance between PDXTs and PDXs was superimposable to that of a recent comparison of 536 original patient tumors and matched PDXs across 25 cancer types [168], indicating negligible divergence between pre-derivation samples, PDXs and PDXTs when considering the general mutational repertoire.

Next, we compared the frequency of gene alterations in our collection with that of two large datasets of human samples from CRC patients: TCGA, which mainly includes primary tumors, and MSK-IMPACT, which is predominantly composed of metastatic samples [5, 70]. We found significant correlations between PDXTs and the two clinical datasets (Pearson coefficient, 0.93 for TCGA and 0.96 for MSK-IMPACT) (Fig. 3C) as well as between PDXs and the clinical datasets (Pearson coefficient, 0.92 for TCGA and 0.95 for MSK-IMPACT) (Fig. 3D). This comparison indicates that XENTURION reflects the mutational landscape of patient cohorts and points to a substantial similarity of mutational frequencies in primary and metastatic CRC tumors. We then investigated whether PDXT establishment and stabilization may result in the enrichment or depletion of defined variants. When testing genes mutated in at least five tumoroids, only mutations in the CTNBB1 gene (encoding β-catenin) were significantly over-represented in PDXTs that failed validation (odds ratio, 0.067) (Fig. 4). Both CTNBB1 and APC

mutations result in constitutive activation of the Wnt pathway (which sustains CRC proliferation), but mutant β-catenin is known to be more modulatable by exogenous Wnt stimulation than mutant APC [169]. Since PDXTs were cultured in the absence of Wnt agonists, it could be argued that CTNBB1 mutant samples are less fit to grow in a nutrient-poor medium than APC mutant samples.

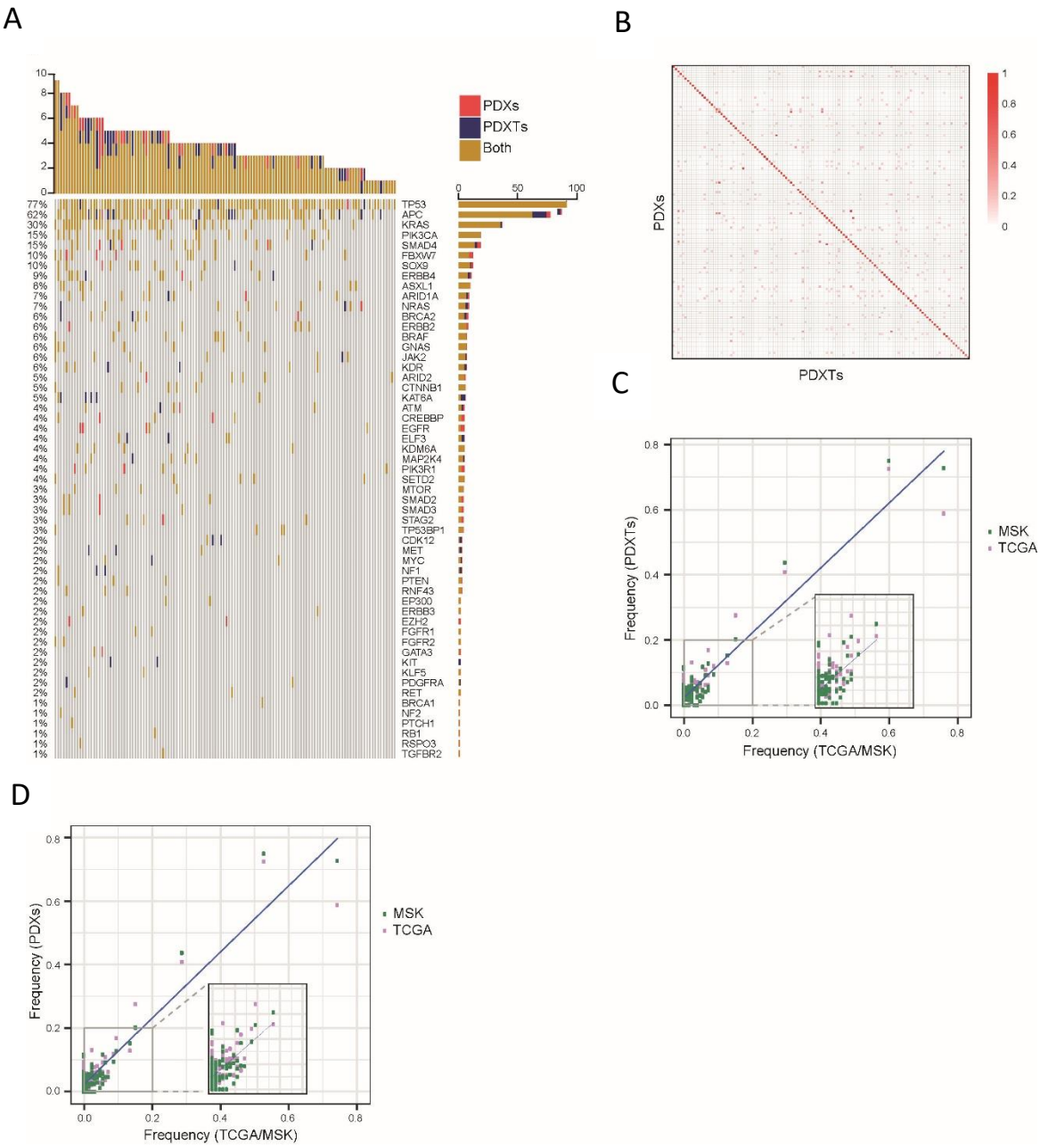

Figure 3. Comparative landscape of somatic single nucleotide variations and indels in paired PDXTs and PDXs. **A**) Common and private alterations for in 124 pairs of matched PDXTs and PDXs. One pair for which mutational data were available was excluded because no alterations with allele frequencies > 0.05 were detected. Genes without any alteration in the whole cohort were removed. The top barchart shows the total number of mutations for each sample. The barchart on the right shows the percentage of mutations for each gene in the cohort. **B**) Jaccard similarity indexes of somatic alterations between 124 matched PDXs and PDXTs. P < 2.2e-308 by two tailed Mann-Whitney test. **C**) Gene-level population frequencies of mutational alterations

in PDXTs versus those detected in the TCGA dataset or the MSK-IMPACT dataset; the inset shows that the correlation is not driven solely by genes with high mutational frequencies. **D**) Frequencies of altered genes in PDXs versus public datasets. Specular to Figure 2C. Scatterplot showing gene level frequencies of alterations in xenografts (y axis) and TCGA/MSK (x axis) - the inset is a magnification to show that the correlation is not driven solely by the higher frequencies driver genes. Pearson coefficient, 0.93 (P = 1.46e-51) for TCGA; Pearson coefficient, 0.96 (P = 2.37e-64) for MSK-IMPACT.

Most colorectal tumors display chromosomal instability, which could be exacerbated by evolutionary bottlenecks such as those imposed by tissue culture propagation. To examine whether copy number changes materialized in our models following ex vivo culturing, we surveyed PDXTs versus their matched PDXs using DNA shallow sequencing in the same 125 pairs used for mutational profiling. We found a high consistency between PDXTs and the corresponding PDXs compared with unmatched samples, as shown by Pearson correlations between the segmented log ratios (average matched, 0.88; average unmatched, 0.39) (Fig. 5A). In PDXTs, the overall landscape of chromosomal alterations was in line with that observed in patients [5] (Fig. 5B). Accordingly, the population frequencies of copy number alterations at the gene level, obtained with GISTIC, were positively correlated between PDXTs and the TCGA or MSK-IMPACT patient cohorts [Pearson coefficient, 0.93 (gains) and 0.87 (losses) for TCGA; 0.80 (gains) and 0.88 (losses) for MSK-IMPACT] (Fig. 5C) and between PDXs and the patient cohorts [Pearson coefficient, 0.92 (gains) and 0.90 (losses) for TCGA; 0.84 (gains) and 0.89 (losses) for MSK-IMPACT] (Fig. 5D). In summary, our data suggest that PDXTs generally retain the mutational and genomic structure of parental PDXs. Moreover, the distribution of major mutational drivers and copy number alterations observed in XENTURION PDXTs and PDXs is largely superimposable to that of human CRC samples.

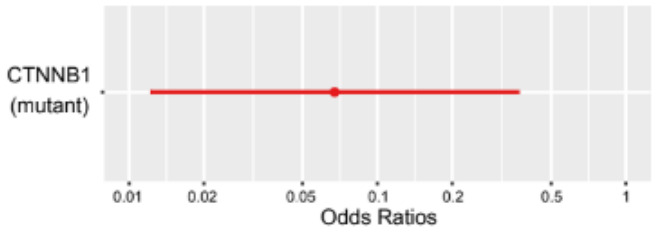

Figure 4. **Role of BCAT mutational status on the PDXTs validation rates**. Forest plot showing the odds ratios of a univariate logistic regression with the establishment/validation status (1: successful - total: 125, 0: failed, total: 7) of tumoroids as dependent variable and BCAT mutational status as independent one.

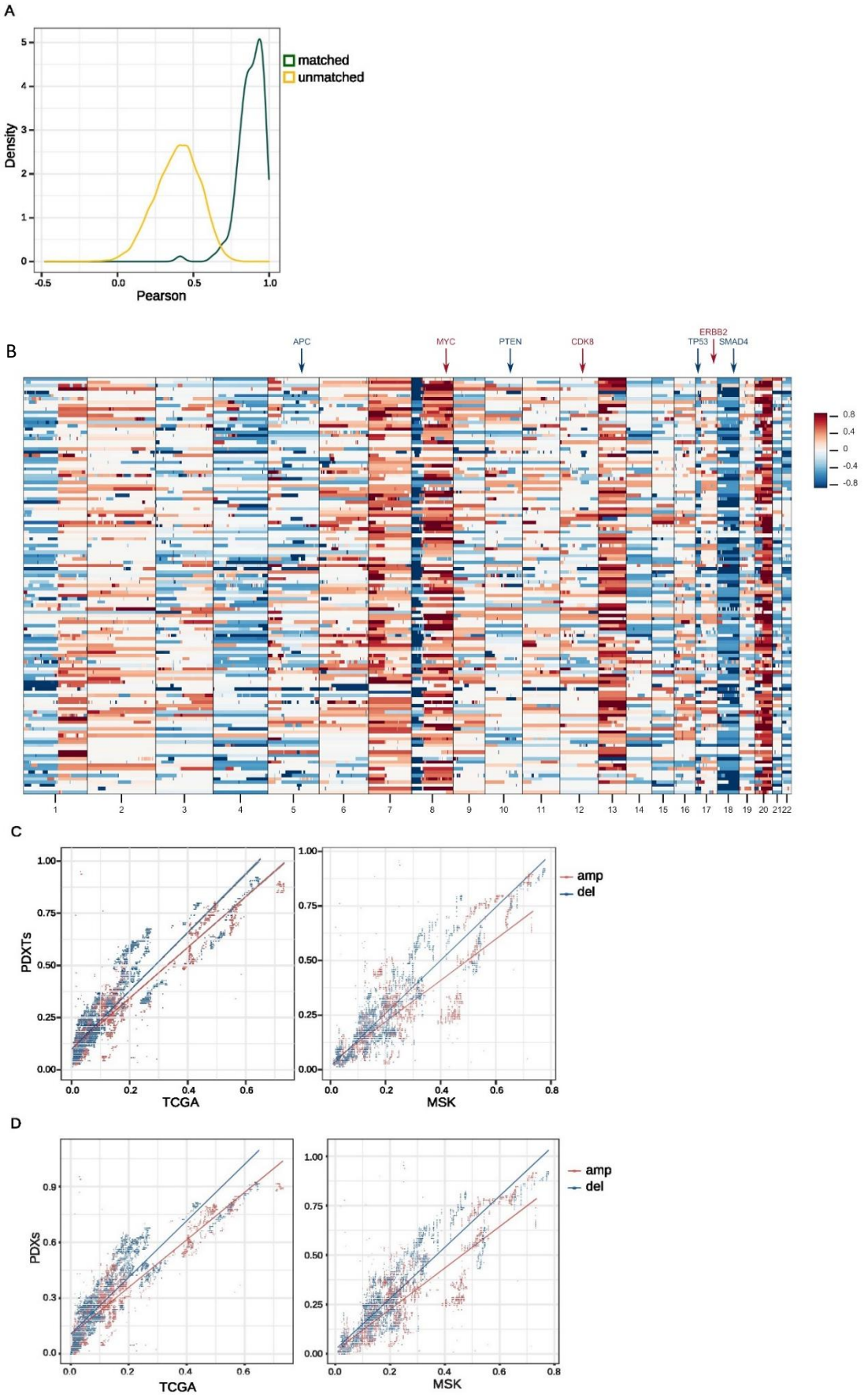
A
matched
unmatched
Density
Pearson
B
APC
MYC
PTEN
CDK8
ERBB2
TP53
SMAD4
C
PDXTs
TCGA
MSK
amp
del
D
PDXs
TCGA
MSK
amp
del

Figure 5. Comparative copy number architecture in paired PDXTs and PDXs. A) Distribution of Pearson correlations between copy number profiles of matched (N = 125) and unmatched (N = 15,500) pairs of PDXTs and PDXs. Matched pairs, average Pearson coefficient, 0.88; unmatched pairs, average Pearson coefficient 0.39; matched versus unmatched pairs, P = 1.92e-81 by two-tailed Mann-Whitney test. **B**) Autosomal copy number profiles of PDXTs (N = 125), expressed in segmented log2 ratio of the normalized read depth. Red and blue colors indicate gain and loss events, respectively. The chromosomal localization of frequently altered genes in CRC is shown. **C**) Gene-level population frequencies of gain or loss events, as identified by GISTIC, in PDXTs versus those detected in the TCGA or the MSK-IMPACT datasets. **D**) Frequencies of genes involved in copy number events in PDXs versus public dataset. Comparison of the population frequencies of gain (red) or loss (blue) events, identified by Gistic at the gene level, between TCGA/MSK and xenografts. Pearson coefficient, 0.93 (gains) and 0.87 (losses) for TCGA; 0.80 (gains) and 0.88 (losses) for MSK-IMPACT (P < 1e-230 for both comparisons). Amp, amplification; del, deletion.

CRISPR/Cas9 gene editing optimization for tumoroid manipulation

The goal of this project is to use CRISPR/Cas9 technology to stratify a panel of KRAS mutant CRC tumoroids on the basis of their requirement for sustained RAS function in maintaining viability and to illuminate characteristics of such tumoroids that relate to their RAS dependency. Therefore, a crucial aspect for successful execution of the project was tailoring CRISPR/Cas9 genome editing technology to achieve effective manipulation of CRC tumoroids.

Firstly, we leveraged literature data [94] to verify that sgRNAs targeting KRAS (sgKRAS) produced the same effect as RNAi-based KRAS silencing in cell lines reported to be RAS-dependent or independent. To this aim, we decided to employ an all-in-one plasmid transfection [170], where both the Cas9 cassette and the sgRNA were present in each construct. We transfected two plasmid constructs, each containing a different sgRNA targeting KRAS, into GP5d and HCT116 CRC cells, which, based on RNAi depletion approaches, do or do not require KRAS for their growth, respectively. Of note, given the lack of unique protospacer adhesion motifs (PAM) encompassing mutant codon 12, our sgRNAs did not discriminate between wild-type and mutant forms of KRAS, modeling a non-selective KRAS inhibitor, and produce double-strand breaks affecting exon 4 (sgKRAS1) or exon 3 (sgKRAS2). Congruent with the RNAi results, the consequence of short-term (one week) CRISPR/Cas9-mediated KRAS knock-out mimicked the effect of shRNA-mediated KRAS knock-down on cell viability. Indeed, sgRNA:Cas9 transfection of

the bulk cell population strongly affected viability in GP5d, previously defined as RAS-addicted cells, but it was inconsequential in HCT116, defined as RAS-independent cells (Fig. 6A). Supporting efficient DNA editing, KRAS protein levels were reduced in both cell lines (Fig. 6B).

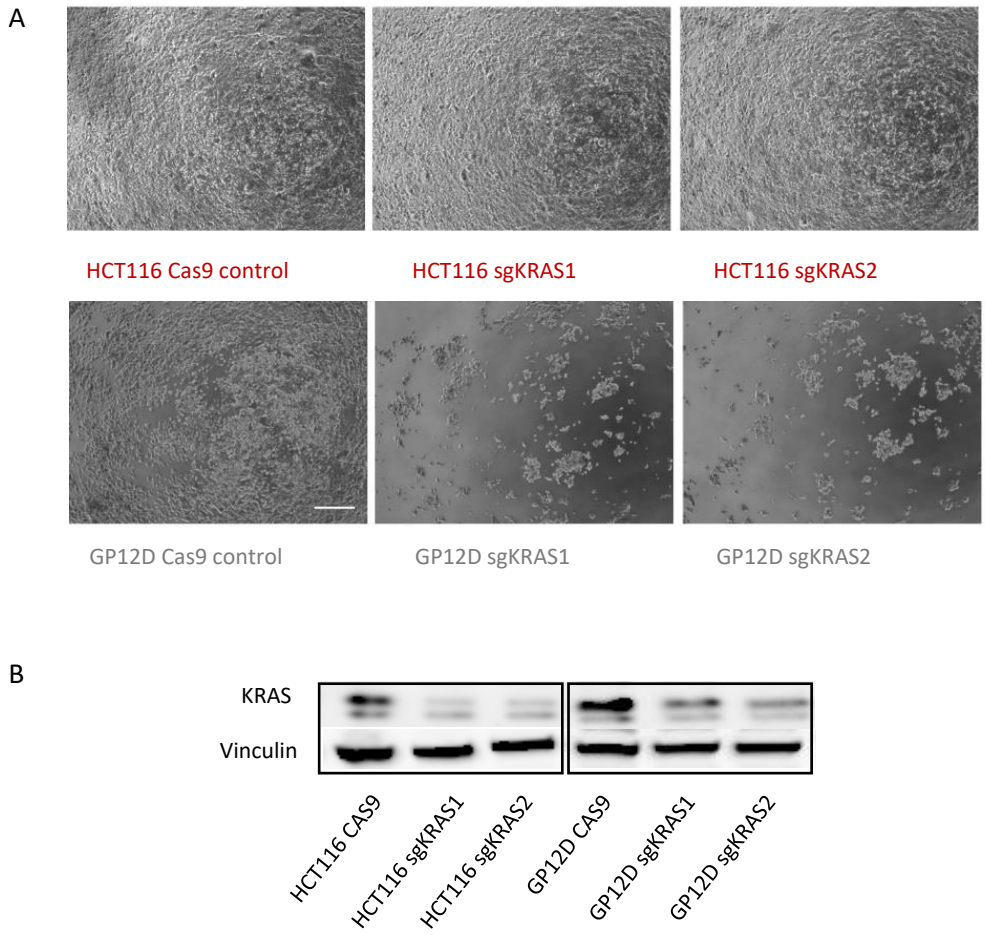

Figure 6. RAS dependency after CRISPR/Cas9 *KRAS* editing in CRC cell lines.
A) HCT116 cells (red, classified as KRAS-independent on the basis of RNAi experiments) and GP5d cells (green, classified as KRAS-dependent) were bulk-transfected with two expression plasmids containing a Cas9 cassette and two different sgRNAs against KRAS. **B**) Western blot analysis of KRAS protein in short-term CRISPR/Cas9 assay. Vinculin was used as a loading control. Total proteins were collected 96 hours after infection. Micrographs were taken one week after transfection. Bar, 300 μm.

When moving from cell lines to CRC tumoroids, we found that plasmid-based transfection – assessed using GFP fluorescence as a readout of transfection efficiency – resulted in weak and uneven protein expression (data not shown), a limitation that might hamper efficient gene editing. To overcome this hurdle, we decided to apply a

two-step protocol using a high-efficiency gene delivery method. Tumoroids were firstly transduced with a lentiviral vector containing the Cas9 cassette and a blasticidin selection marker, in order to obtain engineered lines stably expressing the Cas9 protein. Then, the bulk Cas9-expressing population was superinfected with lentiviral constructs containing the sgRNAs, a fluorescent protein and a puromycin selection marker. In our hands, lentiviral transduction was more efficacious in delivering exogenous plasmids in tumoroids with respect to plasmid-based transfection. Indeed, with this approach we obtained a higher percentage of infected tumoroids, resulting in higher genome editing activity.

CRC KRAS mutant tumoroids can be stratified on the basis of their RAS dependency

With the aim to investigate Ras dependency in our collection of KRAS-mutant PDXTs, we adapted the experimental design used in previous collaborative work with the Sanger Institute, UK [171], optimizing the procedures for tumoroid-based oncogenic dependency testing. In particular, we performed a dependency assay, in which each Cas9-expressing KRAS mutant tumoroid was transduced in parallel with ZsGreen-expressing lentiviral vectors containing a sgRNA targeting a neutral/non-essential gene (sgNESS: CYP2A13, encoding cytochrome P450 family 2 subfamily A member 13) or a lethal/essential gene (sgESS: PLK1, encoding Polo-like kinase 1), and the two different sgRNAs targeting KRAS. Seven days after infection, transduced tumoroids were processed for detection of ATP content as a proxy of cell viability (Fig.7). We exploited the viability scores following transduction of sgRNAs targeting the essential and non-essential genes as a reference to determine KRAS dependency. The reasoning was that if a tumoroid is KRAS-independent, its viability after KRAS knock-out is expected to be comparable to that of the same tumoroid infected with the sgRNA against the non-essential gene. In contrast, KRAS-dependent tumoroids should respond to KRAS depletion with a reduction in viability comparable with that of the tumoroids infected with the sgRNA against the essential gene. Moreover, by using sgESS and sgNESS targeting we were able to normalize the results with respect to the variable

susceptibility to viral transduction of the different tumoroids. For each experiment, KRAS gene knock-out was confirmed at the protein level by Western blot analysis and the genomic scar consequent to CAS9 activity was assessed by Sanger sequencing. In some cases, Sanger sequencing analysis was unsuccessful. In such instances we hypothesize that the NHEJ repair mechanism activated as following Cas9-mediated cleavage resulted in larger scars that that prevented proper annealing of the amplification primers to the DNA. Figure 8 depicts an example of two paradigmatic PDXTs that resulted KRAS-independent (CRC1139) or KRAS-dependent (CRC0568) based on the approach outlined above.

To perform systematic dependency assays, we selected 36 models (Table 2 https://doi.org/10.6084/m9.figshare.23500191.v1). For this assay, we exploited the sgESS/sgNESS viability ratio as a means to quantitatively gauge the extent of Cas9 activity in various tumoroid models and thus to determine whether the experiment could be considered informative. Based on this, only experiments with a sgESS/sgNESS ratio lower than 0.6 were considered reliable. Notably, our findings indicated that there was no discernible variation in the efficacy of CRISPR/Cas9 editing and repair among the

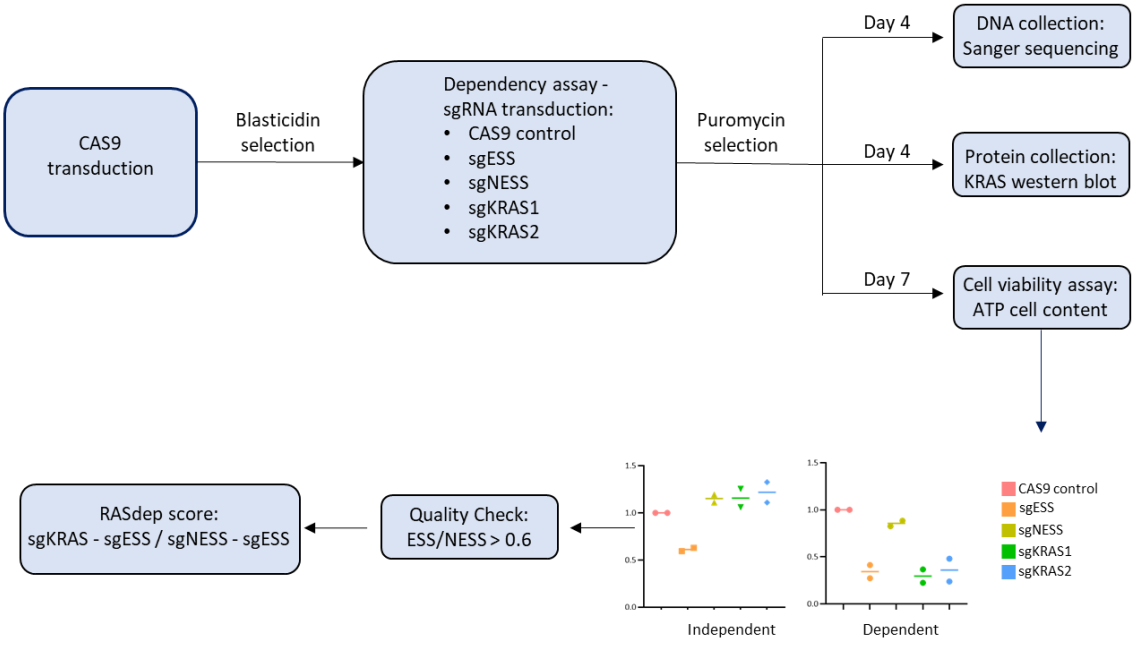

Figure 7. Dependency assay pipeline. CRISPR–Cas9 dependency assay workflow, including timeline and quality checks.

different models (Fig. 9A).

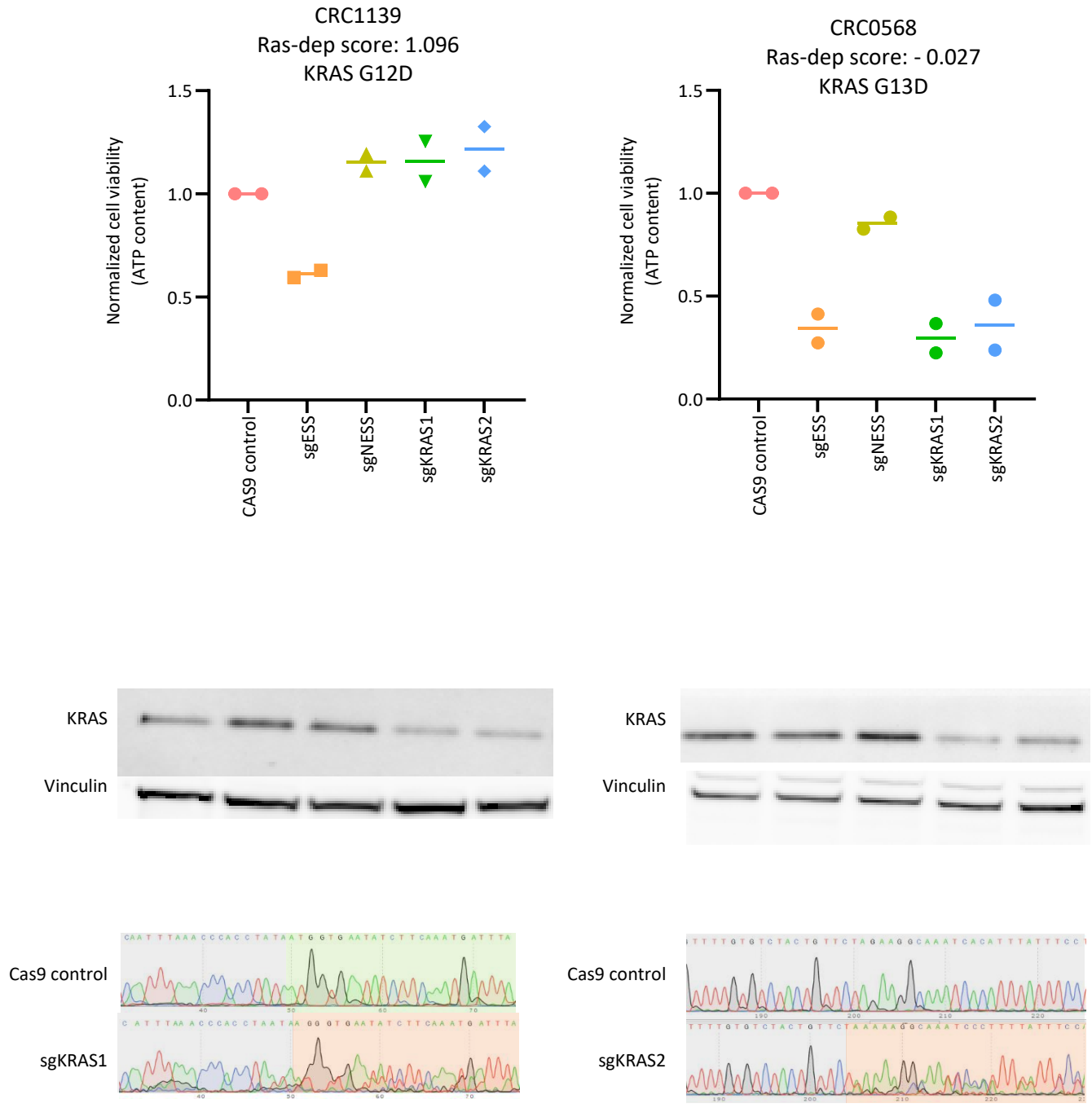

Figure 8. CRISPR/Cas9 assay to determine Ras dependency in representative PDXTs. A) Cas9-expressing tumoroids were superinfected with sgRNAs that target essential (sgEss – PLK1) and non-essential (sgNess - CYP2A13) genes, used as controls, and two different sgRNAs targeting KRAS exon 4 (sgRNA1) and exon 3 (sgRNA2). Viable cells were measured 7 days after infection using ATP content as a proxy of cell numbers. Data were plotted relative to Cas9 non-infected controls. Results are the mean of one experiment, performed in three biological replicates. **B**) Reduction in KRAS protein levels with all KRAS sgRNAs was confirmed by Western blot. Vinculin was used as a loading control. Total proteins were collected 96 hours after infection. **C)**

Electropherograms to assess genetic knock-out of KRAS. The electropherograms show the DNA region adjacent to KRAS sgRNAs. DNA was collected 96 hours after infection.

30 out of 36 models included in our panel of KRAS-mutant PDXTs were profiled for KRAS dependency and passed all the quality control criteria (Fig. 7). For all these, we computed a RAS dependency score calculated as the fraction of viable cells following KRAS knock-out, normalized against the number of viable cells surviving the knock-out of essential and non-essential control genes, as defined by Behan and colleagues in 2019 [170] (RAS dependency score= sgKRAS - sgESS / sgNESS – sgESS). We found that KRAS ablation resulted in polarized outcomes: some models remained substantially unaffected, whilst others experienced massive cell sufferance (suggestive of RAS independency and RAS dependency, respectively) (Fig. 9B). This is consistent with our assumption that not all KRAS mutant tumors rely on aberrant RAS activity for their growth and survival and bodes well for distilling biological and molecular enrichments in dependent versus independent models. In this assay, we assessed the RAS dependency score of a KRAS wild-type organoid. Interestingly, we found that knocking out KRAS did not impact the viability of cells in this particular model (Fig. 9C).

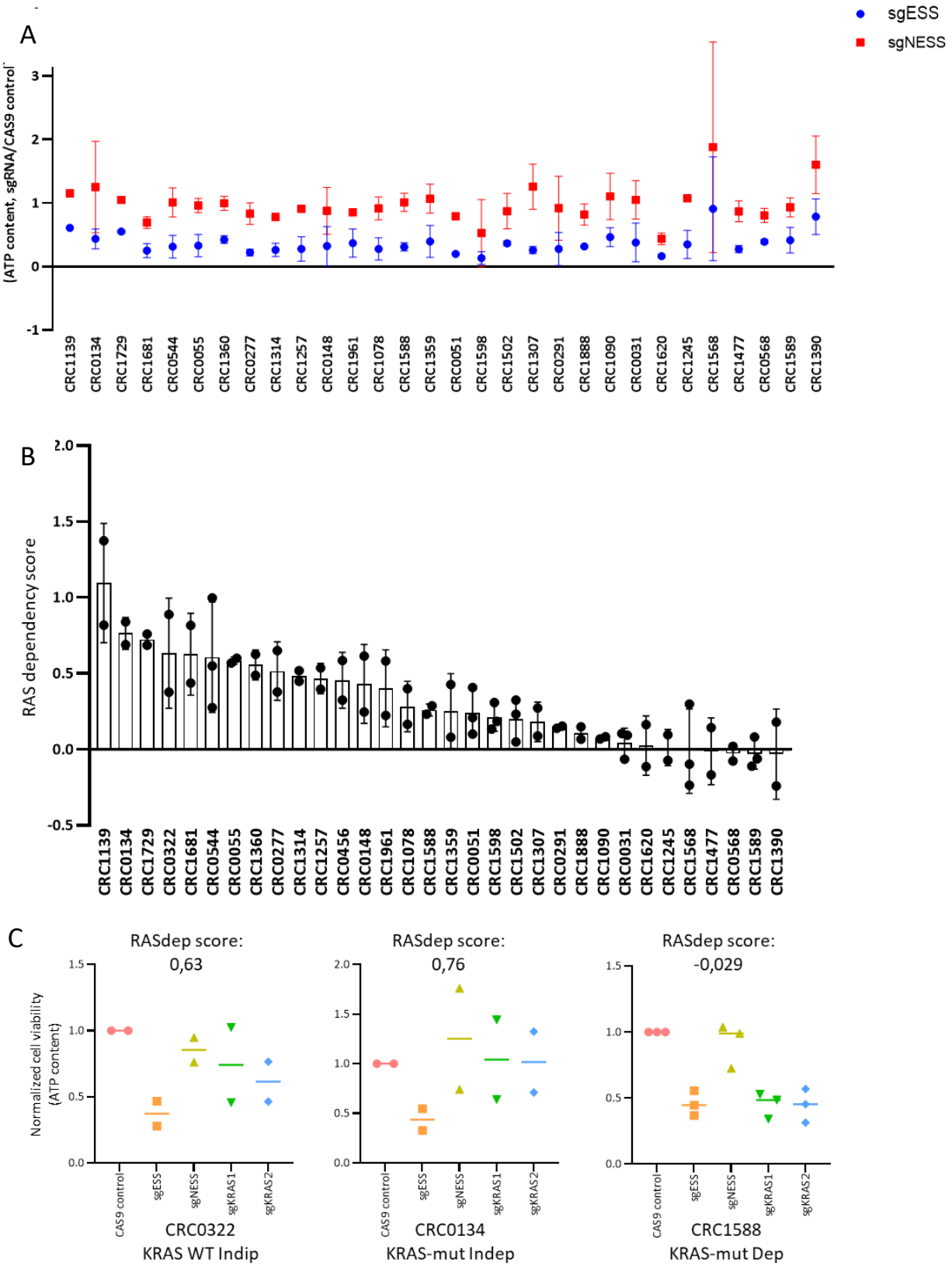

Figure 9. Ras dependency score in 30 KRAS-mutated PDXTs. A) Effect of essential and non-essential genes across full panel of organoid models shows that there is no difference in CRISPR/Cas9 editing and repair **B)** Each point represents the fraction of viable cells following

KRAS knock-out normalized against the number of viable cells surviving the knock-out of essential and non-essential control genes (sgKRAS - sgESS / sgNESS – sgESS). **C)** Dependency assay in three models, comprising a KRAS wild-type organoid, CRC0322. Results are the means of at least two independent experiments, each performed in three biological replicates.

KRAS-addicted CRC tumoroids are more sensitive than RAS-independent models to MEK inhibition

The RAS downstream signaling pathway *par excellence* is the MAPK cascade. On this ground, we assumed that, among KRAS mutant CRCs, those categorized as RAS-dependent could be more reliant on the MAPK pathway – therefore, more sensitive to MEK inhibition – than RAS-independent tumors. To corroborate this hypothesis, we conducted a dose-response screen in 36 KRAS-mutant tumoroids where we compared the response to two structurally different MEK inhibitors, selumetinib and trametinib, and related this response to the extent of KRAS dependency. We analyzed literature data in cancer cell lines to find optimal doses for MEK inhibitors and tailored available results into a distributed dose-response curve in tumoroids. Specifically, we used selumetinib at the maximum dose of 25 uM, with a five-fold dilution to the minimum dose of 0.04 uM; and trametinib at the maximum dose of 2.5 uM, with a five-fold dilution to the minimum dose of 4nM. The results of these screening showed that, as documented in other studies, the antiproliferative effect of trametinib was overall stronger than that of selumetinib at each dose used (Fig. 10). Moreover, the pharmacological blockade of MEK1/2 with both inhibitors in our KRAS-mutant models resulted in a distributed susceptibility, with some models that were clearly more sensitive than others to blockade of the MAPK pathway (Fig. 10). The response to selumetinib and trametinib, used at the intermediate concentration of 1uM and 100nM, respectively, was strongly correlated (Fig. 11), confirming that the biological activity of either compound was ascribable to on-target inhibition. In addition, when we compared the models that had been subject to both KRAS dependency assays and the MEKi screen, we observed that response to KRAS genetic depletion and response to MEK pharmacologic inhibition were highly correlated (Fig. 12). Collectively, these results indicate that KRAS mutant, RAS-dependent CRCs depend on MAPK pathway activity more than KRAS mutant, RAS independent CRCs.

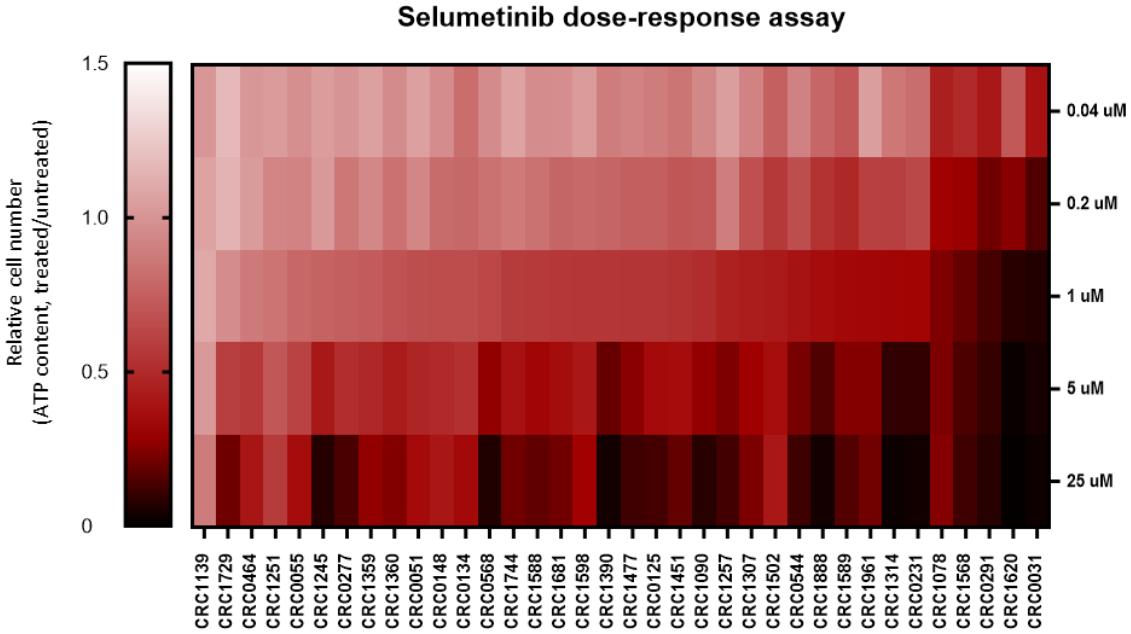
Selumetinib dose-response assay
Relative cell number
(ATP content, treated/untreated)
1.5
1.0
0.5
0
0.04 uM
0.2 uM
1 uM
5 uM
25 uM
CRC1139
CRC1729
CRC0464
CRC1251
CRC0055
CRC1245
CRC0277
CRC1359
CRC1360
CRC0051
CRC0148
CRC0134
CRC0568
CRC1744
CRC1588
CRC1681
CRC1598
CRC1390
CRC1477
CRC0125
CRC1451
CRC1090
CRC1257
CRC1307
CRC1502
CRC0544
CRC1888
CRC1589
CRC1961
CRC1314
CRC0231
CRC1078
CRC1568
CRC0291
CRC1620
CRC0031

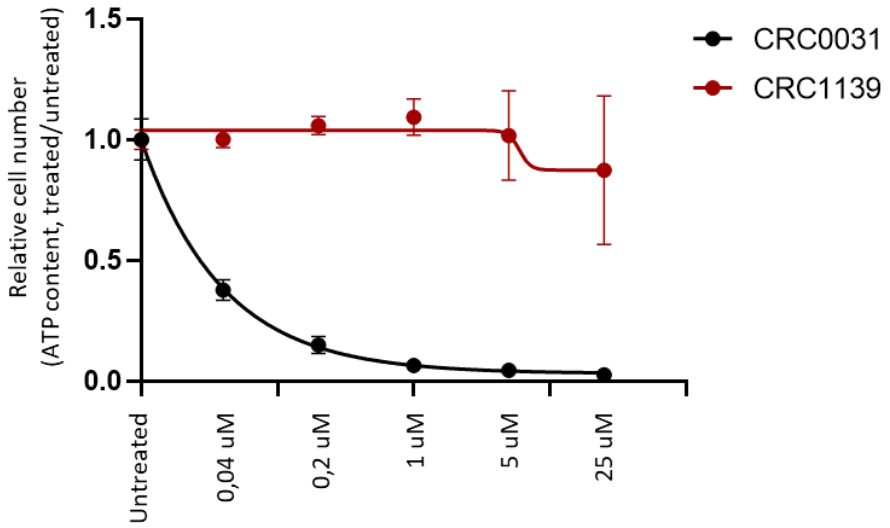
Relative cell number
(ATP content, treated/untreated)
1.5
1.0
0.5
0.0
CRC0031
CRC1139
Untreated
0,04 uM
0,2 uM
1 uM
5 uM
25 uM

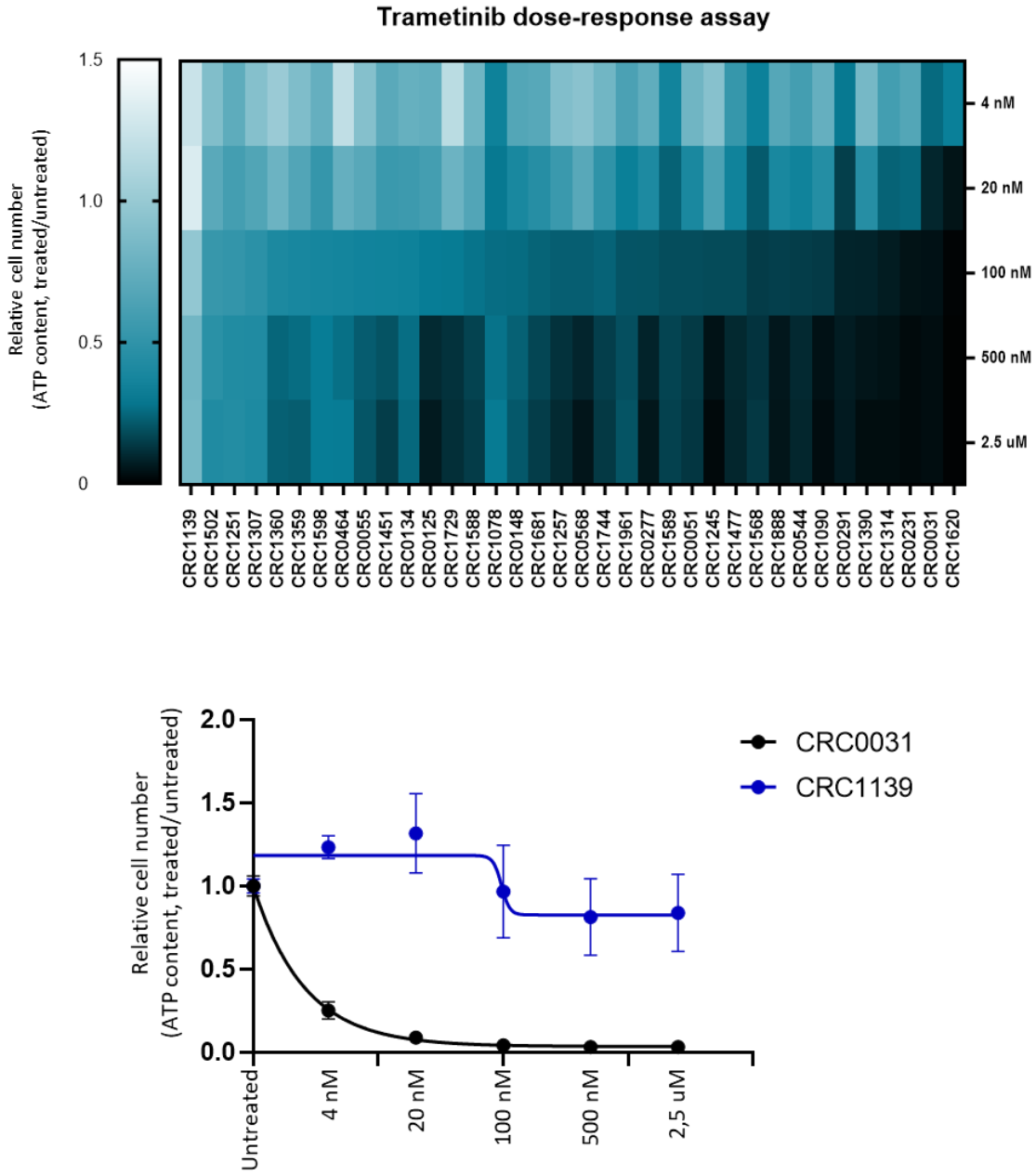

Figure 10. Heatmap representations of dose-response curves for selumetinib and trametinib. PDXT models are listed from least responsive to most responsive to an intermediate drug concentration along the dose-response curve for selumetinib **A**) and trametinib **B)**. The bottom panels depict dose-response curves for two representative cases, CRC0031 (sensitive) and CRC1139 (resistant), in response to selumetinib and trametinib. Viable cells were measured after seven days of treatment using ATP content as a proxy of cell numbers. Data were plotted relative to untreated controls. Results are the means of at least two independent experiments, each performed in five biological replicates.

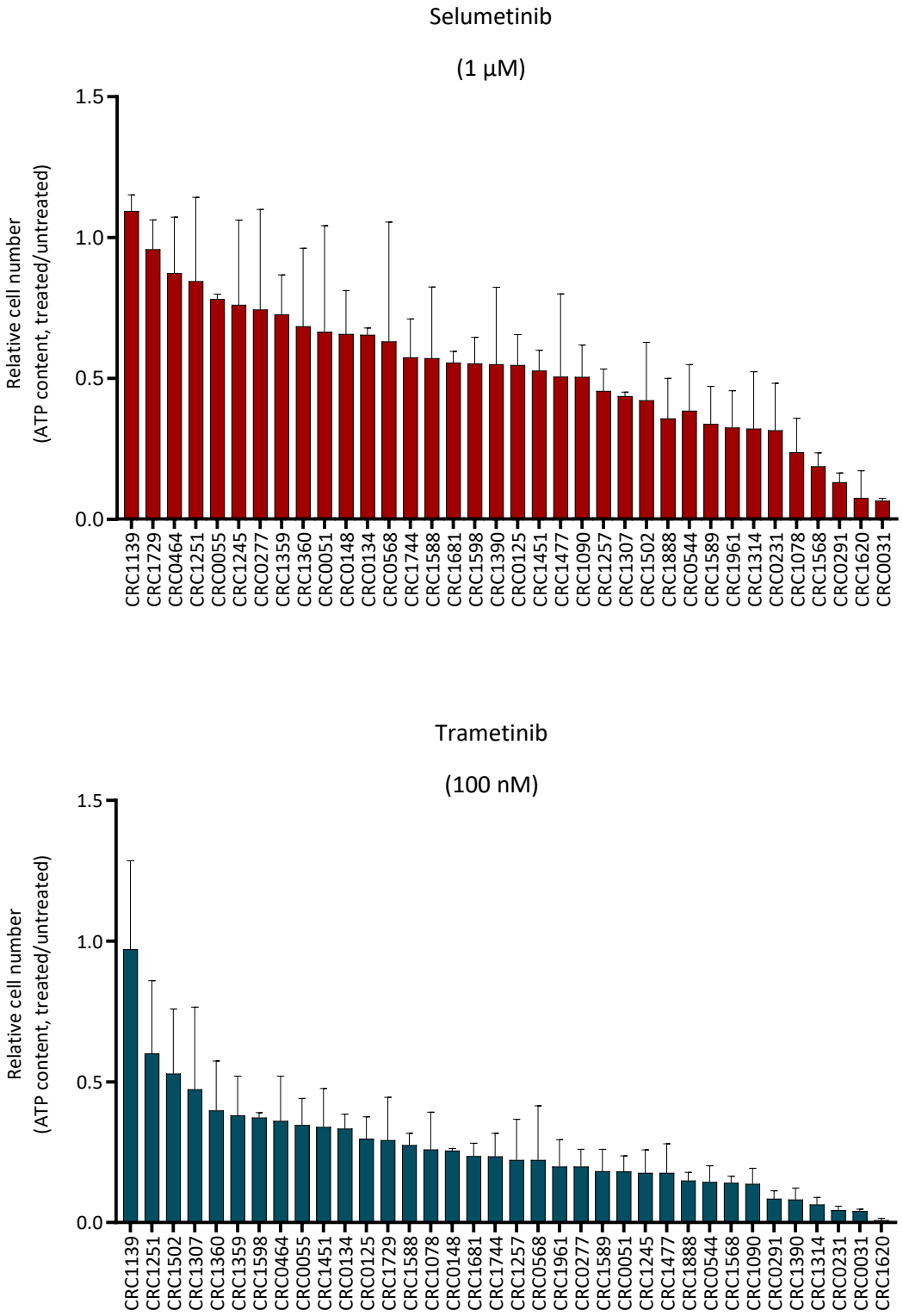

Figure 11. Waterfall plots showing the response to selumetinib (1 uM) and trametinib (100 nM). Viable cells were measured after seven days of treatment using ATP content as a proxy of cell numbers. Data were plotted relative to untreated controls. Results are the means ± SEM of at least two independent experiments, each performed in five biological replicates.

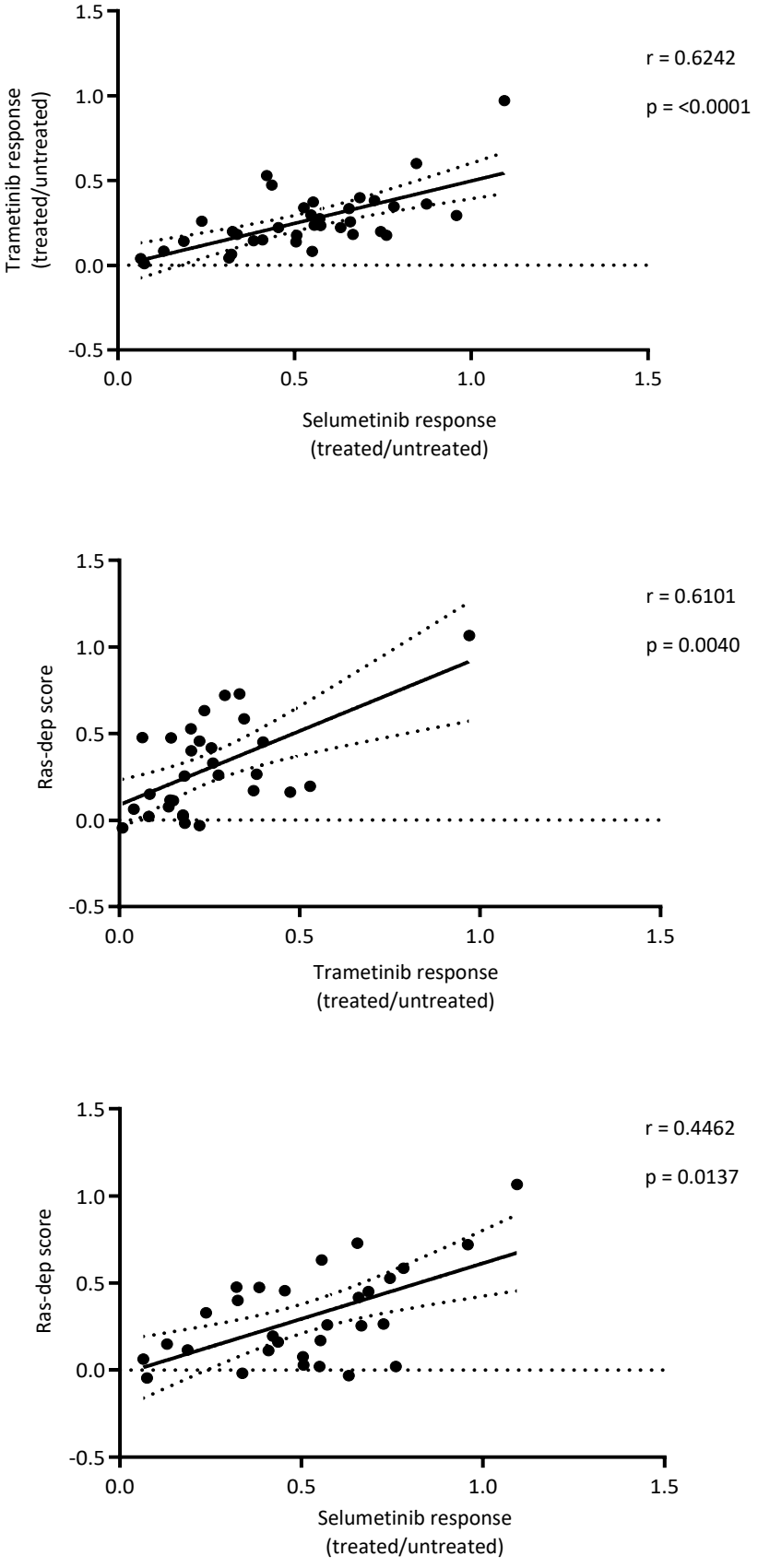

Figure 12. Scatter plots of trametinib response, selumetinib response and RAS-dependency score. Each dot represents the mean of at least two biological replicates, each performed in at least three technical replicates. Spearman correlation (r) results and associated p-value (p) are indicated.

KRAS-addicted tumoroids do not benefit from MEK inhibition *in vivo*

To explore whether the KRAS dependence (and MEKi sensitivity) observed *in vitro* could be reproduced *in vivo*, we decided to transplant KRAS-dependent models into NOD/SCID mice and test tumor responses to trametinib treatment. We selected two models, CRC0031 and CRC0291, which showed both a strong KRAS dependency and a clear response to MEK1/2 pharmacologic blockade *in vitro* (Fig. 13A). In accordance with previously published studies in both preclinical models and patients, we did not observe any evident therapeutic benefit of trametinib monotherapy in either model, after two (CRC0031) or four (CRC0291) weeks of treatment. Lack of effect could not be ascribed to poor pharmacodynamic activity of the compound; indeed, treated tumors showed consistent reduction of phospho-ERK levels, suggestive of efficient MEK inactivation by trametinib (Fig. 13B). We speculate that this therapeutic inefficacy is due to compensatory mechanisms or signal redundancies that become functional and blunt the effect of MEK inhibition only in the *in vivo* setting.

Gene expression analysis reveals differentially enriched pathways in RAS-dependent versus RAS-independent tumoroids

The distillation of functional enrichments in KRAS-dependent versus KRAS-independent PDXTs may prove useful for two purposes: i) to identify potentially lethal interactions in KRAS independent tumors; ii) to pinpoint co-dependencies able to unleash the therapeutic effect of MEK inhibition in KRAS-dependent tumors in the *in vivo* setting. Accordingly, we performed a mutational and transcriptional characterization of the entire KRAS-mutated tumoroid cohort for which KRAS dependency scores were available.

Based on targeted next-generation sequencing for 116 relevant cancer genes, all tumors with KRAS mutations at an allele frequency of close to 1 (7 tumoroid cases), either due to LOH events or homozygous mutations, were found to have a low dependency score,

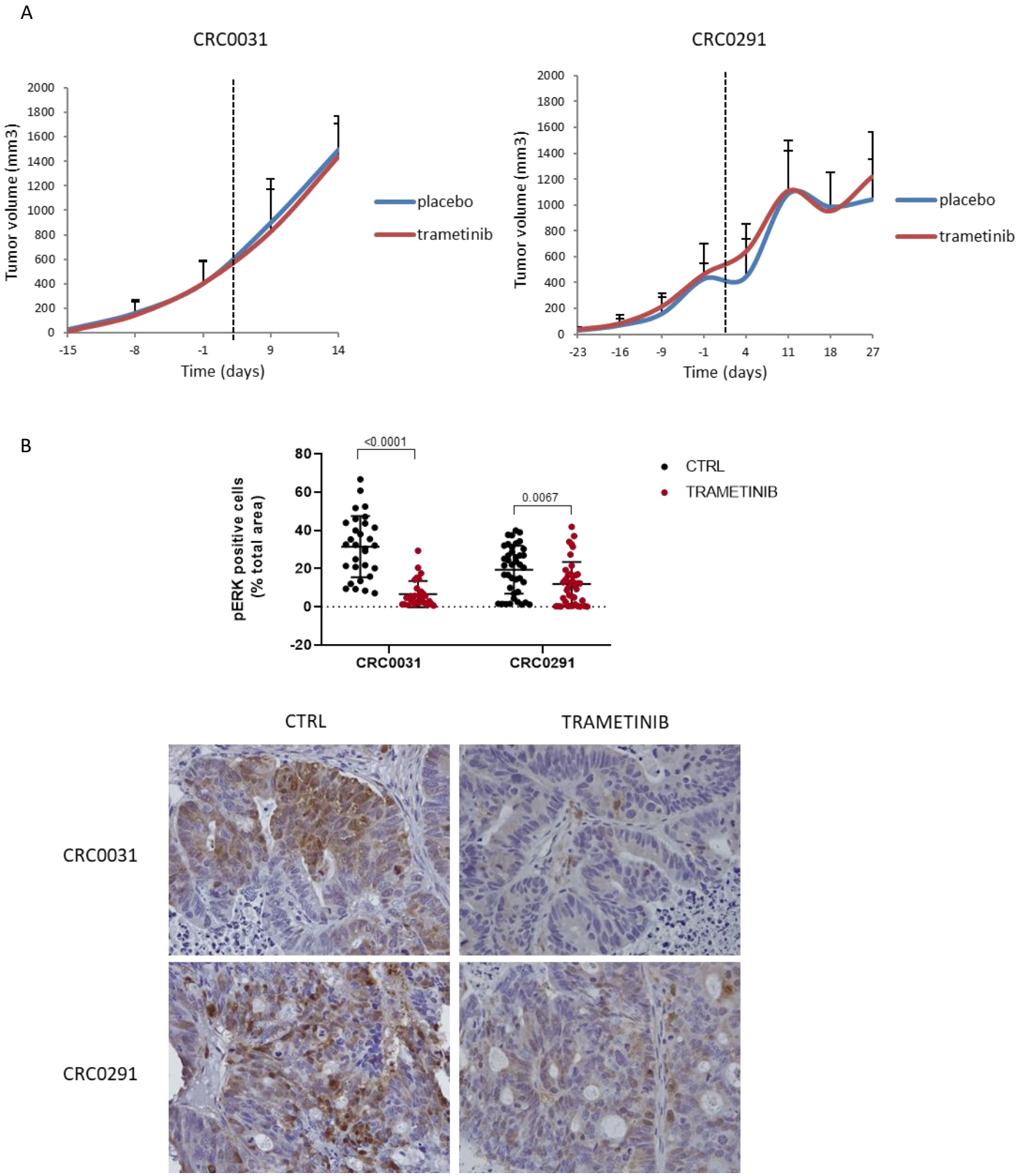

Figure 13. MEK inhibition monotherapy is ineffective in KRAS-addicted models *in vivo.* A) Tumor growth curves of two KRAS-dependent mCRC PDXs exposed to vehicle or trametinib (1 mg/kg daily, administered by gavage). Dotted lines indicate start of treatment. n = 5 to 10 animals for each treatment arm. Error bars indicate SD. **B)** Morphometric quantification of phospho-ERK immunoreactivity in two KRAS-dependent PDXs after treatment with vehicle (until tumors reached an average volume of 1500 mm3) or trametinib. Each dot represents the average of 10 optical fields (40×) in a section from randomly chosen tumors from vehicle- and trametinib-treated mice bearing a PDX from the same original patient (CRC0031 n= 30 optical fields, CRC0291 n=40 optical fields). The plots show means — SD. Statistical analysis by ratio paired *t* test. Scale bar, 50 µm.

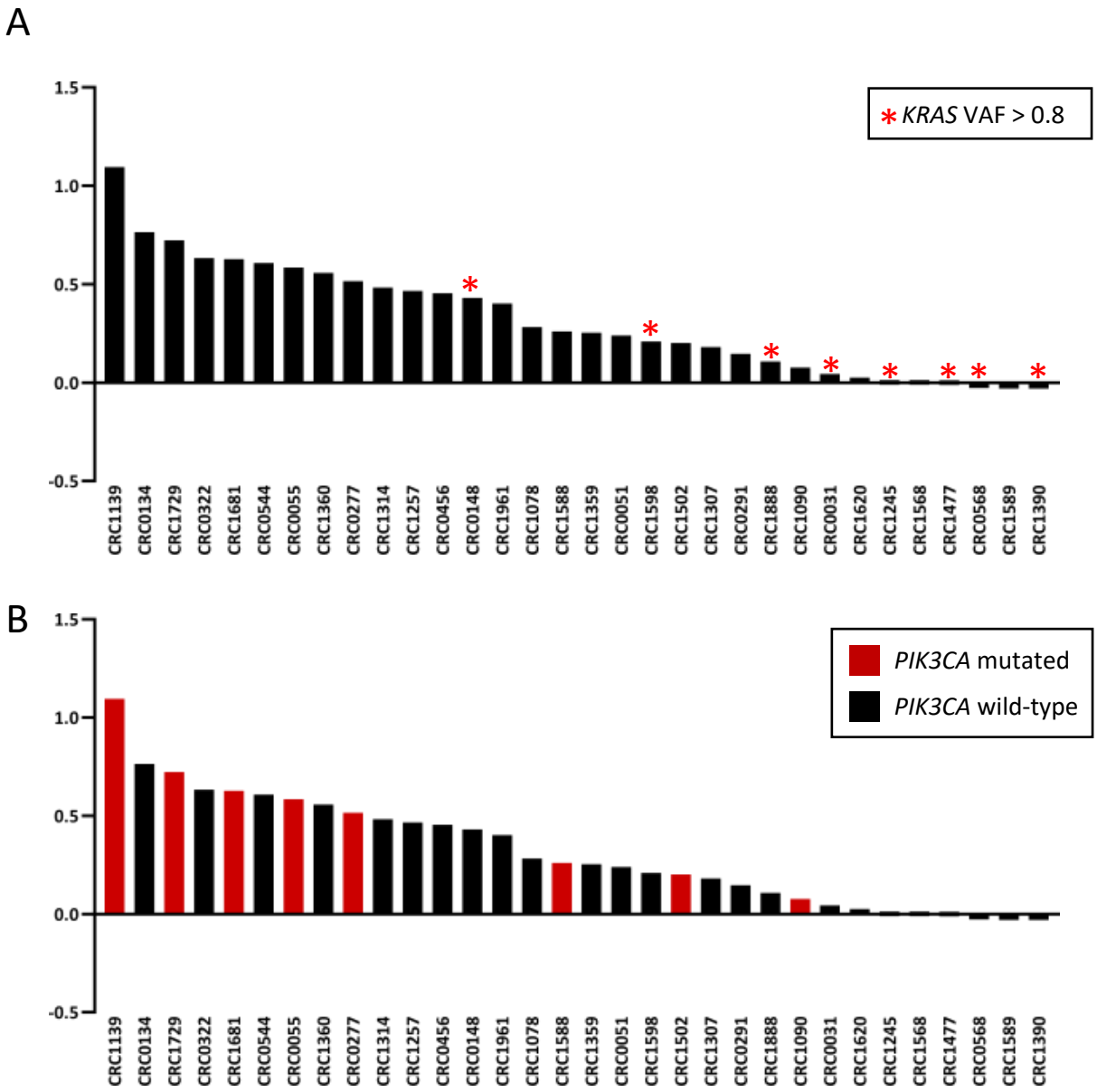

Figure 14. KRAS allelic frequency and PI3K mutations in KRAS dependent and independent CRC organoids. A) Cases exhibiting a KRAS variant allele frequency (VAF) greater than 0.8 are indicated with an asterisk above their respective bars, which indicate their level of dependency on RAS. Q1: quartile with lower KRAS dependency score; Q4: quartile with higher KRAS dependency score; Q2-Q3: quartiles with intermediate KRAS dependency score. Q1 versus (Q2+Q3+Q4) p = 0.01587 by fisher test. **B**) *PIK3CA* mutations are highlighted in the RAS-dependency waterfall plot. Q1 versus (Q2+Q3+Q4) nominal p=0.016 by fisher test.

thus, a higher dependency on oncogenic KRAS signaling activity (Fig. 14A). Analyzing mutations in other cancer genes, only mutations in the PIK3CA gene were significantly associated with KRAS independency (nominal p=0.016) (Fig. 14B). Moreover, the only PIK3CA mutated model that displayed a strong KRAS dependence (CRC1090) had a co-existing mutation in the CTNNB1 gene, encoding β-catenin. As mentioned above,

mutations in the CTNNB1 gene were significantly over-represented in PDXTs that failed validation, likely because CRC cells with mutant β-catenin are less fit in WNT-deprived culture medium than APC mutant cells. We speculate that this liability may render cancer cells more dependent on KRAS-driven ERK activation, blunting the compensatory effect of PI3K hyperactivation when KRAS is knocked out.

As an alternative means to identify KRAS co-dependencies, we explored the transcriptional profiles of our tumoroid collection with the aim to investigate the functional properties of KRAS-dependent and -independent PDXTs. We reanalyzed the expression data obtained from tumoroids in the biobank for 30 samples under basal (unperturbed) conditions. In order to identify the transcriptional traits that most differentiate KRAS-dependent from independent tumors, we conducted differential gene expression analysis between the upper and the lower quartiles of the ranking based on the KRAS dependency score (8 and 7 models respectively, some of which in biological replicates). Comparing the transcriptional profiles of the models populating the KRAS-independent quartile versus the models in the KRAS-dependent quartile, we identified 184 upregulated and 332 downregulated genes (Fig. 15) (Table 3 https://doi.org/10.6084/m9.figshare.23500188.v1). PDE4B and the polymeric immunoglobulin receptor (PIGR) resulted among the most upregulated genes in the KRAS-independent class. PDE4B, a member of the PDE family, breaks down cAMP, which is considered an inducer of anti-inflammatory responses. Indeed, PDE4B acts as important player in the development and clinical manifestation of inflammation, as well as inflammation-induced tumors [172]. PIGR resulted hypermethylated and downregulated in CRC patients and associated with reduced overall survival. Moreover, PIGR overexpression inhibited malignant phenotypes in *in vitro* studies and impaired CRC cells growth in animal models [173]. On the contrary, KRT6A and TSPAN18 emerged as significantly more expressed in the KRAS-dependent tumor group. KRT6A has been linked to the epithelial-mesenchymal transition in lung cancers and consequently it has been associated with a poor prognosis [174]. TSPAN18, which belongs to the tetraspanins family, is involved in cell adhesion, migration and invasion processes [175]. The observation that genes that appear to contrast tumor progression are more expressed in KRAS-independent tumors, whilst genes associated with poor prognosis are more expressed in KRAS-dependent suggests that KRAS dependent tumors display

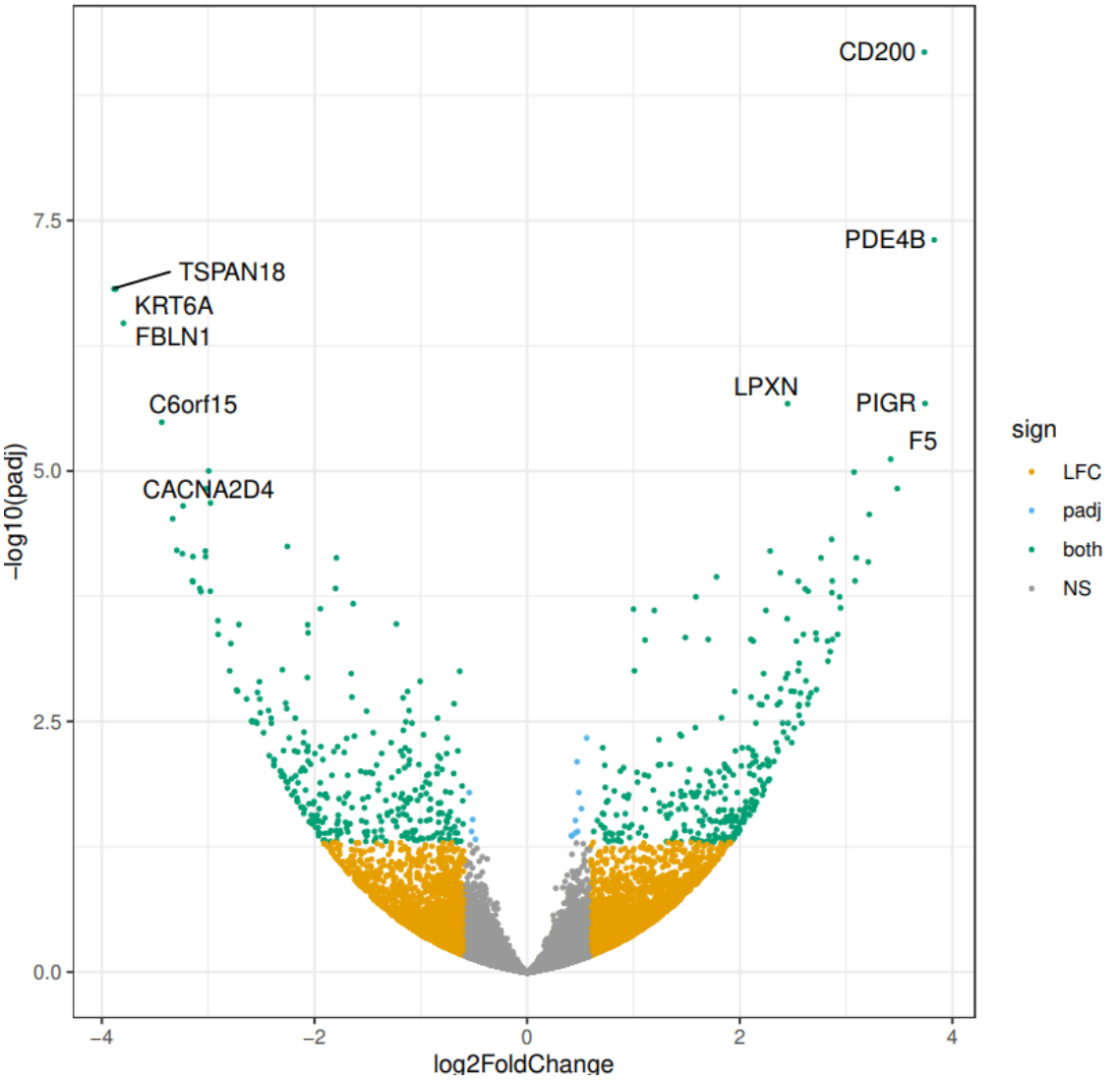

Figure 15. Differentially expressed genes in KRAS-dependent and KRAS-independent top quartiles. Volcano plot showing the magnitude of the differential gene expression between KRAS-dependent and KRAS-independent top quartiles. Each dot represents one gene with detectable expression in both conditions. The colour code is described in legendon the right.tumors,

more aggressive and pro-invasive traits compared to the KRAS-independent counterpart. After single gene analysis, we moved to GSEA enrichment analyses, with the final aim to catch a view of the whole phenotypic profiles of KRAS-dependent and -independent tumor groups. GSEA enrichment analyses highlighted 11 Hallmark and 306 Curated signatures (Molecular Signatures Database) as differential between the two groups (Fig.16) (Table 4 https://doi.org/10.6084/m9.figshare.23500200.v1). First of all, gene sets linked to KRAS signaling activity and KRAS dependency were enriched in the

KRAS-dependent subgroup. This observation reinforced the reliability of our CRISPR/Cas9-based dependency assay as a tool for stratifying KRAS mutated tumors according to their functional addiction to KRAS itself. In accordance with the literature [176, 177], a gene set referred to MYC targets was enriched in KRAS addicted tumors, consistent with a higher activity of the KRAS downstream pathway (Fig. 16A). Three different gene sets related to ribosome components were strongly enriched in KRAS dependent tumoroid cases (Fig. 16B). We ensured that the components of these gene sets were protein-coding genes to exclude results altered by the possible presence of rRNA attributable to technical issues. The upregulation of transcripts linked to protein translation suggests that tumors that mostly rely on oncogenic KRAS activity were also characterized by more intense protein synthesis activity, possibly also in part due to MYC-driven signaling. We hypothesized that this intense protein synthesis activity could result in higher growth rates in KRAS- dependent PDXTs. However, there was no correlation between the growth rate of our tumoroids under basal conditions and the level of dependence on KRAS (Fig. 16C). KRAS addicted tumors were also characterized by upregulation of TGFβ signaling and traits of epithelial-mesenchymal transition (EMT) (Fig.16A). This is consistent with the notion that TGFβ-dependent signals are usually pro-invasive in full-blown tumors harboring SMAD inactivation, such as our metastatic lesions [178]. On the opposite side, tumors in which KRAS deletion was not detrimental were characterized by increased expression of genes related to Interferon and STAT-JAK activity. This result is in line with previous observations, whereby interferon- and inflammatory-related genes proved to be upregulated in KRAS-mutant CRC *in vitro* models exhibiting resistance to MEK inhibition [179], and may indicate that pro-inflammatory cues convey compensatory signals that render tumors less reliant on KRAS signaling. These findings highlight the potential of developing targeted therapies for KRAS-mutant CRC based on their level of dependence on KRAS signaling. By identifying the level of KRAS dependence in individual tumors, targeted therapies could be developed to selectively inhibit KRAS signaling in KRAS-dependent or independent tumors. This personalized strategy could improve patient outcomes by increasing the likelihood of response to treatment and reducing unnecessary toxicity.

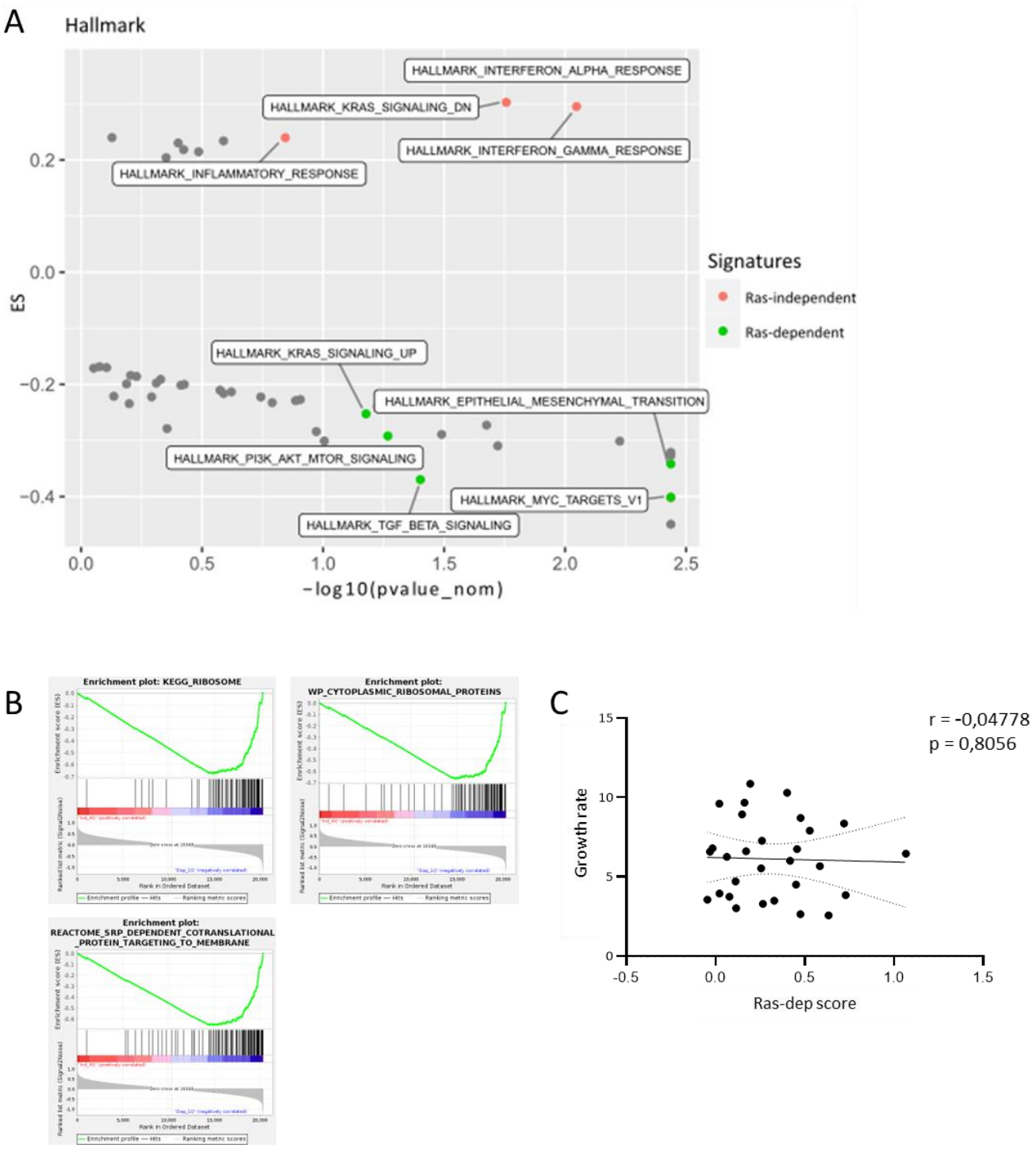

Figure 16. Differential gene expression in KRAS dependent and KRAS independent KRAS-mutant organoids. A) Scatter plot showing GSEA results of differential gene expression profiles obtained comparing KRAS-dependent versus KRAS-independent organoids. Enrichments are plotted on the y axes, and their significance is plotted on the x axis. ES, enrichment score. B) GSEA plots showing modulation of ribosome components enriched in KRAS-dependent models. C) Scatter plots of growth rate and RAS-dependency score. Growth rate was calculated from ATP levels (Cell Titer-Glo) of untreated cells 7 days after plating, normalised to day 1. Each dot represents the mean of at least two biological replicates, each performed in at least three technical replicates. Spearman correlation (r) results and associated p-value (p) are indicated.

DISCUSSION

The RAS oncogene is among the most commonly mutated genes in cancer. RAS mutations are identified in about half of patients diagnosed with metastatic colorectal cancer, conferring poor prognosis and lack of response to anti-epidermal growth factor receptor antibodies. Despite its biological pervasiveness, mutant KRAS has been recalcitrant to pharmacologic targeting owing to the complex regulation of its intrinsic catalytic activities and steric constraints. Therefore, therapeutic strategies initially revolved around the rationale of inhibiting 'classical' RAS downstream effectors, namely the MAPK kinase cascade and the PI3K-AKT axis. Monotherapy with MEK inhibitors - such as trametinib – proved to be ineffective in patients with KRAS mutant tumors (specifically, KRAS mutant lung cancer) [139], likely due to redundant signaling through upstream RTK activity and stimulation of parallel signal transduction cascades bypassing MEK inhibition and reactivating ERK signaling. On this ground, combinations exploiting vertical and/or horizontal blockade of the RAS pathway have been assessed to frustrate adaptive resistance mechanisms. In therapy refractory mCRC, several combinations of MEKi with PI3K inhibitors, AKT inhibitors, or mTOR inhibitors have been tested in clinical trials, but none of them provided a therapeutic advantage. Indeed, 0% ORR was observed with combinations of MEKi plus PI3K inhibitors (copanlisib, alpelisib, pictilisib, or buparlisib), PI3K/mTOR dual inhibitors (gedatolisib, voxtalisib, or omipalisib), and AKT inhibitors (MK-2206, ipatasertib, or afuresertib).

The failure of therapies against conventional RAS downstream transducers ignited the development of novel RAS-directed drugs. Extensive pharmacologic efforts materialized into the advent of several novel inhibitors targeting the KRASG12C variant, affording a traditionally undruggable protein with proof-of-concept clinical actionability. These agents have proved to be one of the most promising therapeutic discoveries in recent years, but their reach in the context of mCRC has been suboptimal. In particular, the clinical employment of KRASG12C inhibitors in mCRC is heavily limited by the low prevalence of this specific KRAS mutation, which hovers around 4%. Moreover, even in the few patients with tumors harboring the KRAS G12C mutation, the therapeutic efficacy of anti-KRAS G12C monotherapy is hampered by hyperactivation of EGFR [108]. This is not unexpected, given the impact of EGFR activity on resistance to BRAF inhibitors

in BRAF mutant mCRC. The observation that EGFR signaling compensates for KRAS G12C blockade in mCRC has recently led to the proposal of combining KRASG12C inhibitors with anti-EGFR antibodies. However, a recent study has shown that this combination can fuel the development of acquired resistance [180].

Based on the above considerations, it is fair to conclude that effective therapies for KRAS mutant mCRC are still a long way off. The scenario is complicated by additional pieces of evidence, which apply to all KRAS mutant tumors including CRC. First, preclinical work has suggested that not all KRAS-mutant tumors rely on aberrant RAS activity for their growth and survival; therefore, stratification based on the functional assessment of KRAS dependency rather than on the mere detection of KRAS mutations may improve the therapeutic response of patients with KRAS-mutant tumors. Second, the identification of co-extinction targets is crucial because even if direct inhibitors have been (and will be) developed for KRAS, they may not always be effective in treating all KRAS-mutant tumors. Therefore, finding other targets that can work synergistically with the direct inhibitors could enhance their effectiveness. Co-extinction targets are expected to act as adjuvants, enhancing the action of mutant KRAS-targeting drugs, and, when combined, can potentially substitute for direct inhibitors if these are not yet ready or effective.

Experimentally, the main approach used to identify KRAS dependencies has been the deployment of loss-of-function screens based on RNAi technology, applied to immortalized (commercial) human cancer cells. Settleman's group has used RNAi to knock-down KRAS in several immortalized cancer cell lines, identifying two categories of RAS dependency. In lung and pancreatic cancer cell lines, the authors identified a specific gene expression signature that was associated with KRAS addiction, which included genes involved in EMT [93], putting forward the concept that reliance on KRAS is closely associated with the differentiation status of epithelial cells. When epithelial cancer underwent EMT, their dependence on KRAS was reduced; conversely, when they underwent MET (mesenchymal-epithelial transition), their dependence on KRAS was increased. In a following study focused on CRC cell lines, a subset of KRAS-dependent cells was found to be sensitive to TGFβ-activated kinase 1 (TAK1) inhibition [94]. In this study, TAK1 appeared to act as a mediator that promotes cell survival in cancer cells with hyperactive KRAS-dependent Wnt signaling. Mechanistically, KRAS was reported to

activate the bone morphogenetic protein-7 (BMP-7) signaling pathway specifically in KRAS-dependent cells. This activation led to the activation of TAK1 and prompted nuclear localization of β-catenin, which promoted the transcriptional upregulation of Wnt target genes endowed with pro-mitogenic and anti-apoptotic functions. However, TAK1 inhibitors, such as 5Z-7-oxozeaenol, had a limited use in the clinic due their off-target effects, since they also block MEK and other kinases [181].

In an independent RNAi screen performed in human cancer cell lines of different tumor types (4 KRAS wild type and 4 KRAS mutant), Scholl and colleagues demonstrated that that the STK33 serine/threonine kinase was selectively essential in cancer cells with KRAS mutations [153]. They then evaluated STK33 dependency in 25 additional pan-cancer cell lines and found that this kinase was preferentially required in KRAS mutant cells that also depended on sustained KRAS expression for their proliferation. STK33 promoted cancer cell viability by regulating the suppression of BAD-mediated mitochondrial apoptosis, and this activity was seemingly confined to KRAS mutant, KRAS-dependent cancer cell lines. This led to investigating STK33 as a potential therapeutic target for KRAS-mutant cancers. While the kinase function of STK33 initially generated excitement for its therapeutic potential, subsequent research showed that STK33 kinase activity apparently is not required for KRAS-mutant cancers, although other strategies that result in loss (rather than enzymatic inactivation) of STK33 protein may still hold therapeutic potential [182].

Many other studies have been conducted to find a susceptibility in KRAS mutant cancers [63, 97, 183], but results have been generally inconsistent and hardly reproducible, possibly due to lack of standardization in the RNAi methodology used (including post-hoc analytical tools) and RNAi-related off target effects. To overcome these limitations, more recent studies have applied CRISPR/Cas9 technology for loss-of-function genetic screens, which allows for the complete knock-out of target genes. While CRISPR/Cas9 technology has improved genetic perturbation, it cannot on its own overcome the limitations associated with different cellular and genetic contexts. In fact, attempts to reproduce published KRAS synthetic lethal targets using CRISPR/Cas9 have also failed [184]. The differences observed between different studies can be attributed to the fact that cancer cell lines cannot fully replicate the complex biological characteristics of the original tumor. Organoids are three-dimensional structures, containing multiple cell

types that are organized in a spatially and functionally relevant manner. Cancer organoids (also known as tumoroids) more closely resemble the complexity and functionality of *in vivo* tissues compared to traditional two-dimensional cell culture. Moreover, organoids have been shown to exhibit gene expression profiles that are more similar to their *in vivo* counterparts than cell lines. This means that the genes targeted by a CRISPR/Cas9 screen in tumoroids are more likely to have similar effects in 'real' tumors in patients, increasing the translational and clinical relevance of the findings.

On these premises, our efforts focused on stratifying our tumoroid models and mapping their dependency on KRAS either by methodical gene knock-out or by pharmacologic inhibition of KRAS downstream pathways through the administration of the MEK inhibitors selumetinib or trametinib. Firstly, with both experimental approaches we observed a spectrum of effects, ranging from complete loss of viability to complete neutrality after KRAS knock-down or MEK neutralization; this reinforces the notion that not all KRAS mutant CRCs are created equal, and some but not others deeply rely on mutant KRAS for their continued growth. More importantly, we observed a substantial consistency between the degree of gene dependency and the degree of susceptibility to pharmacologic inhibition, highlighting the critical role of the MAPK pathway in funnelling most of KRAS-dependent biology.

Our results with MEK inhibitors in mCRC tumoroids are at odds with clinical experience, which has clearly shown lack of efficacy of MEK inhibitor monotherapy in patients with different types of KRAS mutant tumors. It is worth noting that we also found a disconnection between tumoroid-based findings and the outcome of *in vivo* experiments. Specifically, when we treated with trametinib two PDX models whose matched tumoroids had strong dependency on KRAS and strong sensitivity to MEK inactivation, no therapeutic effect was observed in spite of successful pharmacodynamic neutralization of MEK. This suggests that MEK inhibition is necessary but not sufficient to reduce the fitness of KRAS mutant, KRAS dependent mCRC tumors, and raises the need to identify co-vulnerabilities to be targeted together with the MAPK cascade. To pursue this goal, we first evaluated differentially active pathways from a functional point of view in tumoroids classified as KRAS-independent versus KRAS-dependent. In contrast to previous observation from Settleman and colleagues in commercial cell lines representative of tumor models other than colon cancer [92], we observed an

accentuation of EMT features in the subset of KRAS-dependent CRC tumoroids rather than in the subset of KRAS-independent models. In our interpretation, KRAS dependency is a reflection of KRAS oncogenic activity, which likely encourages the aggressive phenotypes associated with EMT. This reasoning is in line with clinical evidence, whereby the prognosis of KRAS mutant CRCs is typically less favorable than that of KRAS wild-type tumors.

TGFβ-related signatures were also enriched in KRAS-addicted PDXTs. It is well known that tumors with high TGFβ signaling, but with SMAD loss due to genetic or epigenetic inactivation, are refractory to the anti-proliferative effect of TGFβ, while retaining response to TGFβ pro-invasive activity. Since one of the effects of TGFβ is to induce EMT, both EMT and clinical aggressiveness are consistent with increased TGFβ expression in KRAS-dependent tumors. All in all, these considerations suggest that targeting the TGFβ pathway may be a potential therapeutic strategy in KRAS-dependent tumors.

In a complementary perspective, we observed that tumoroids that were not influenced by KRAS genetic deletion had intrinsically active signals linked to the interferon pathway and to the innate inflammatory response. This finding may explain, at least partly, why models that proved to be KRAS-dependent and MEKi sensitive as tumoroids were refractory to MEK blockade as PDXs. We surmise that cytokines released by macrophages and NK cells, which are known to be present in NOD-SCID mice, could stimulate a pro-inflammatory milieu and act on tumor cells to make them less susceptible to MEK inhibition. This hypothesis is in line with independent in vitro studies, whereby interferon- and inflammatory-related genes proved to be upregulated in KRAS-mutant CRC models exhibiting resistance to MEK inhibition [179]. One potential therapeutic approach to interfere with interferon downstream signaling is to target the JAK/STAT pathway. Ruxolitinib, a selective JAK1/2 inhibitor, demonstrated significant improvement in patients with polycythemia vera and myelofibrosis, leading to FDA approval of its use for these diseases [185-187]. Several clinical trials have evaluated the effect of ruxolitinib in solid tumors, but they have produced disappointing results, with several being terminated prematurely. This may be due to JAK inhibition interfering with immune cell functions, which could counteract some of the drug's anti-cancer effects [188]. It is evident that only a particular subset of solid tumors is likely to be susceptible to JAK inhibition.

We are currently conducting a global CRISPR/CAS9 screen in KRAS-dependent and KRAS-independent PDXTs in the presence of trametinib, with the final aim to identify specific genetic targets that can improve the sensitivity of trametinib treatment *in vitro* and potentiate its therapeutic effects *in vivo*. In addition, we aim to discover new vulnerabilities in independent tumors that may be targeted by novel cancer therapies. By leveraging the power of CRISPR/Cas9 technology and the breadth of our tumoroid collection, we hope to gain a deeper understanding of the complex genetic and molecular mechanisms that drive cancer progression and therapy resistance in KRAS mutant mCRC and identify new avenues for the development of more effective treatments.

MATERIALS AND METHODS

Specimen collection and annotation

Tumor and matched normal samples were obtained from patients treated by liver metastasectomy at the Candiolo Cancer Institute (Candiolo, Torino, Italy), Niguarda (Milan, Italy), Mauriziano Umberto I (Torino), and San Giovanni Battista (Torino). All patients provided informed consent. Samples were procured and the study was conducted under the approval of the Review Boards of the Institutions.

Overview of the sequenced samples

Targeted DNA sequencing was performed in 148 tumoroids; 148 PDXs; 4 human samples; and 1 control sample with known mutational status of the covered genes; 125 of the sequenced PDXTs ended the validation process successfully. Shallow sequencing was performed in 146 tumoroids; 149 PDXs; 4 human samples; and 3 control samples with known copy number profiles. 125 of the sequenced PDXTs ended the validation process successfully. RNA sequencing was performed in 220 tumoroids (all passed quality checks).

DNA and RNA extraction, sgRNA PCR amplification and Sanger sequencing

Total DNA and RNA were was extracted using the Maxwell® RSC Blood DNA Kit (Promega) automated extraction platform following the manufacturer's instructions. KRAS-amplified products were obtained by PCR using the following primers: sgKRAS1 5'-TGACAAAAGTTGTGGACAGGT-3' and 5'- AGAAACCAAAGCCAAAAGCA-3'; sgKRAS2 5'-CTTAAGCGTCGATGGAGGAG-3' and 5'- GGTGCTTAGTGGCCATTTGT-3'; sgPLK1 5'-AAGAGATCCCGGAGGTCCTA-3' and 5'- AGAGCCAAGAAGCCCTTACC-3'; sgCYP2A13 5'-ATCTCTCTCCCACCCCACTC-3' and 5'-CCCTGTTGAGCCGAATCC-3'. Sanger sequencing was performed using the following primer: sgKRAS1 5'-CACTGCTCTAATCCCCCAAG-3'; sgKRAS2 5'-AAGAAGCAATGCCCTCTCAA-3'; sgPLK1 5'-GCTGCGGTGAATGGATATTT-3'; sgCYP2A13 5'-TCTCCATCGCCACCCTAAG-3'. To obtain bulk RNA-seq data, RNA was extracted using miRNeasy Mini Kit (Qiagen), according to the manufacturer's protocol. The quantification and quality analysis of RNA was performed on a Bioanalyzer 2100 (Agilent), using RNA 6000 Nano Kit (Agilent).

Analysis of mutant variants

Targeted sequencing was performed on an Illumina NovaSeq 6000 instrument by IntegraGen SA. Paired-end 2x100bp reads were obtained, aiming at ~500x depth for each sample on the

targeted regions (402.4 kbp). The panel (Twist Bioscience) covered exons of 116 genes from a manually curated list of recurrently mutated drivers in CRC. Initial QC was performed with FastQC (v0.11.9) by IntegraGen; for PDX samples, murine reads were filtered using Xenome (v1.0.0) with default parameters, after building k-mer indexes for the human genome (GRCh38, downloaded from https://gdc.cancer.gov/about-data/gdc-data-processing/gdc-reference-files) and murine genome (mm10, obtained from iGenomes). The GATK Best Practices Workflow for somatic mutation calling was followed to perform mutation calling with Mutect2 (bwa v0.7.17-r1188 - parameters -K 100000000 -Y, GATK 4.1.4.0); alignment was performed versus GRCh38; alignment metrics were gathered with picard CollectHsMetrics. dbSNP (for quality recalibration, downloaded from NCBI, ftp://ftp.ncbi.nih.gov/snp/organisms/human_9606/VCF/All_20180418.vcf.gz) and Gnomad (release 2.1.1) were used as external references for common human polymorphisms. The resulting list of filtered mono-allelic mutations was annotated using PCGR (version 0.9.1); to avoid germline contamination, only coding mutations found in tiers ≤ 3 (https://pcgr.readthedocs.io/en/latest/tier_systems.html) were kept for further analyses. CGA and MSK mutational data was downloaded from (https://www.cbioportal.org/study/clinicalData?id=crc_msk_2017 and https://www.cbioportal.org/study/summary?id=coadread_tcga_pan_can_atlas_2018 - Mutated_Genes.txt). To compute frequencies of clonal events only mutations with AF > 0.2 were kept. To compare mutational landscapes between PDXs and PDXTs a more lenient filter (AF > 0.05) was applied.

Copy number profiles

Shallow-sequencing was performed on Illumina NovaSeq S4 instrument by Biodiversa SRL. Paired-end 2x150bp reads were obtained, aiming at 0.65x depth for each sample. Initial QC was performed with FastQC (v0.11.8); for PDX samples, murine reads were filtered using Xenome (v1.0.0) with the same procedure described for targeted sequencing. Total or human classified reads were when aligned versus GRCh38 with bwa (v0.7.17-r1188 - parameters -K 100000000 -Y) following GATK best practices; then, duplicates were marked using picard (2.18.25). Alignment metrics were gathered with samtools (v1.9) flagstat and picard CollectWgsMetrics. Segmented fold changes were obtained with QDNAseq (v1.22.0) with a bin size of 15kb (annotations obtained from QDNAseq.hg38), using default parameters and pairedEnds=TRUE. Before computing correlations a pseudocount of 1 was added to all fold changes to compute log2; a pseudocount of 0.01 was used for visualization. Log2 values with a pseudocount of 1 in .seg format were used as input for the GISTIC2.0 module in GenePattern

(https://cloud.genepattern.org, default parameters and TRHuman_Hg38.UCSC.add_miR.160920.refgene.mat, Gistic v2.0.23). TCGA Gistic output (specifically all_thresholded.by_genes.txt) was downloaded from the GDCl (https://gdc.cancer.gov/about-data/publications/coadread_2012); for MSK-IMPACT, the file with segmented signals was downloaded from cBioPortal (https://www.cbioportal.org/study/clinicalData?id=crc_msk_2017) and GISTIC was run as previously described.

Gene expression analyses

Quality control checkpoints

For RNA-seq experiments, on day 0, tumoroid models were plated on a thin layer of BME type II (Cultrex) in complete medium with EGF (300,000 cells/well in 12-well plate). On day 5, RNA was extracted using the Maxwell® RSC miRNA Tissue Kit (Promega) automated extraction platform following the manufacturer's instructions.Total RNA was processed for RNA-seq analysis with the TruSeq RNA Library Prep Kit v2 (Illumina) following manufacturer's instructions, and sequenced on a NextSeq 500 system (Illumina) by Biodiversa SRL. Single-end 151bp reads were obtained, aiming at 20M reads for each sample. Read counts were obtained using an automated pipeline (https://github.com/molinerisLab/StromaDistiller), that uses a hybrid genome composed of both human and mouse sequences to exploit the aligner ability to distinguish between human-derived reads, representing the tumor component, and mouse-derived reads, representing the murine host contaminating RNA material. Reads were aligned using STAR [189] (version 2.7.1a, parameters – m outSAMunmapped Within – outFilterMultimapNmax 10 – outFilterMultimapScoreRange 3 – outFilterMismatchNmax 999 – outFilterMismatchNoverLmax 0.04) versus this hybrid genome (GRCh38.p10 plus GRCm38.p5hg38 with Gencode version 27 and mouse GRCm38 with Gencode version 16, indexed with standard parameters and including annotation information from the GENCODE 27 plus m16 comprehensive annotation). Aligned reads were sorted using sambamba [190] (version 0.6.6) and only non-ribosomal reads were retained using split_bam.py [191] (version 2.6.4) and rRNA coordinates obtained from the Gencode annotation and repeatmasker track downloaded from UCSC genome browser hg38 and mm9. featureCounts [192] (version 1.6.3) was run with the appropriate strandness parameter (-s 2) to count the non multi-mapping reads falling on exons and reporting gene-level information (-t exon -g gene_name) using combined Gencode basic gene annotation (27 plus m16).

Quality check criteria included: i) number of total reads ≥ 15M; ii) reads assigned to genes by feature counts ≥ 60%; iii) reads assigned to human genes over the total of assigned reads ≥ 30%.

By applying these filters, only samples with at least 5M human reads were considered for analysis. To remove samples with lymphomatous characteristics [193], different sources of information were considered: i) Principal Component analysis of expression data (samples with PC2 ≥ 30 were discarded): ii) computation of a sample-level score for a leukocyte expression signature [194], averaging fpkm values for all the signature genes (samples with an average leukocyte signature ≥ were discarded); iii) PDX global methylation data [https://www.biorxiv.org/content/10.1101/2023.01.24.525314v1], when available; iv) for a subset of samples, xenografts were explanted and subjected to histopathological analysis by hematoxylin-and-eosin staining. Positivity for one of these filters flagged samples as lymphomatous and excluded them from analysis.

Variance stabilized expression and robust fpkm values were obtained using DESeq2 (version 1.26.0), tmm using edgeR (version 3.28.1) starting from the read counts assigned to human genes only.

D*ifferential expression analysis*

The described pipeline ran for a large RNAseq dataset comprising both basal conditions and treated tumoroids and xenografts, alongside some human tumor tissues, but the analyses shown in this work are focused only on xenografts and tumoroids in basal conditions, that were respectively 480 and 220 at the beginning, with 470 and 220 passing the quality filters. Only data coming from validated tumoroids has been kept for the comparative analysis.

Differentially expressed genes (DEGs) analyses were obtained with DESeq2 (v1.26.0 [195]) with design: batch+type. Here batch is used to correct for sequencing batch and type specifies if the sample is a KRAS independent or dependent tumoroid. We defined the dependency of the tumoroids based on their co-competition scores: KRAS independent PDOs belong in the upper quartile while dependent belong in the lower quartile. The analysis was performed with 11 samples for KRAS dependent group and 12 samples for KRAS independent group, derived respectively from 7 and 8 models, thanks to the availability of biological replicates for 8 models. This resulted in 184 upregulated and 332 downregulated genes in the independent tumors (p-adjusted < 0.05 and |log2FoldChange| > 0.58).

DEGs were used to perform Gene Set Enrichment Analysis (GSEA) with R libraries ClusterProfiler (v3.14.3 [196, 197]), DOSE (v3.12.0[198]), msigdbr (v7.4.1 [199]) and enrichplot (v1.6.1). GSEA highlighted 11 Hallmark and 306 Curated signatures (Molecular Signatures Database) as differential between the two groups.

WES mutational data was obtained for 30 models, where the 8 dependent and 8 independent ones at the extremes of the ras dependency spectrum were respectively used to detect gene level mutations enrichments, using a fisher test. A not thresholded approach was also tried with a GSEA like analysis, where samples were used instead of genes: mutation data defined sample sets (in parallel with gene sets) and the ranking was determined with the ras dependency score. This analysis did not yield additional results with respect to the fisher based one.
All the statistical analyses and plots were obtained using R (v3.6.3) and ggplot2 (v3.3.0).

Patient-derived tumoroid cultures

Tumoroids of CRC liver metastases were established from PDX explants. Tumor specimens (0,5cm x 0,5cm) were chopped with a scalpel and washed with PBS. After centrifugation, the final cell preparation was embedded in Matrigel® (Corning) or Cultrex Basement Membrane Extract (BME, R&D Systems) and dispensed onto 12-well or 24 well plates (Corning). After 10-20 minutes at 37°C, culture medium was added. Complete mCRC tumoroid medium composition is the following: Dulbecco's modified Eagle medium/F12 supplemented with penicillin-streptomycin, 2 mM L-glutamine, 1mM n-Acetyl Cysteine, B27 (Thermo-Fisher Scientific), N2 (Thermo-Fisher Scientific) and 20 ng/ml EGF (Sigma-Aldrich). Tumoroids were tested for Mycoplasma and maintained at 37°C in a humidified atmosphere of 5% CO2. Periodic checks of sample identity with the original human specimen (liver metastasis and, when available, normal liver) were performed using a 24 SNP custom genotyping panel (Diatech Pharmacogenetics), and results were analyzed using the MassARRAY Analyzer 4 (SEQUENOM® Inc, California). Culture expansion and biobanking were managed using the Laboratory Assistant Suite (145).

Cell cultures, gRNA design and CRISPR/Cas9 construction

HCT116 and GP5d cells were purchased from ATCC and were cultured in RPMI. The genetic identity of cell lines was validated by short tandem repeat profiling (Cell ID, Promega). The sequences of sgRNAs of the genes targeted for dependency assays were taken from the sgRNA list of The Human CRISPR Library v.1.0 (Addgene 67989) used in previous work [171]: sgESS *PLK1* 5' CGGACGCGGACACCAAGG 3'; sgNESS *CYP2A13* 5' TCACCGTGCGTGCCCCGG; sgKRAS1 *KRAS* exon 4 5' TTGTGTCTACTGTTCTAGA 3'; sgKRAS2 *KRAS* exon 3 5' AGATATTCACCATTATAGG 3'. For cell line transfection, oligonucleotides were synthesized and ligated into pSpCas9(BB)−2A-Puro (PX459, Addgene 62988) as previously reported [170]. For dependency assays, oligonucleotides were ligated into pKLV2-U6gRNA5(BbsI)-PGKpuro2AZsG-W (Addgene 67975).

Dependency assays

All plasmids have been previously described [200] and are available at Addgene (Cas9 vector, 68343; gRNA vector, 67975). Lentiviral vectors were produced by LipofectAMINE 2000 (Invitrogen)-mediated transfection of 293T cells (ATCC). PDXTs were transduced with Cas9 vector in Corning™ Falcon™ 15 mL conical tubes in the presence of polybrene (8 μg/ml). Tumoroids were incubated at 37°C in 5% CO2 overnight followed by replacement of the lentivirus-containing medium with fresh complete medium. Blasticidin (Thermo Fisher) selection commenced 48 hours after transduction at the concentration of 10 μg/ml, and was maintained throughout the assays. After blasticidin selection, PDXTs were expanded in 12-well plates. At day 0, PDXTs were transduced for 6 hours at 37°C in 5% CO_2 with viral particles containing sgRNAs targeting essential or non-essential genes, or KRAS sgRNA 1 and KRAS sgRNA2. After 6 hours, PDXTs were seeded in 2% BME culture medium at a confluence of 5000 cells/well in a 96-well plate, and parallel aliquots were seeded in adherent BME drops for subsequent protein and DNA analysis. The following day 2 μg/ml puromycin was added and tumoroids were cultured at 37 °C in 5% CO_2 for additional 7 days. Endpoint cell viability was measured using the Cell Titer-Glo luminescent assay kit (Promega). Ras-dependency score was calculated as indicated in the Results. PDXT parallel cultures for protein and DNA analysis were collected 4 days after infection.

Viability assays

Pharmacologic experiments were performed in 96-well plates with a thin layer of BME in each well. Tumoroids were washed with PBS, incubated with trypsin-EDTA solution for 5 minutes at 37°C and vigorously pipetted to obtain a single cell suspension. For experiments profiling PDXT response to cetuximab, cells were seeded in 2% BME culture medium at the confluence of 1,250, 5,000 or 20,000 cells/well in the absence of EGF. After 1-2 days from seeding, PDXTs were treated with the modalities indicated in the figure legends.

For experiments response to MEK1/2 inhibitors cells were seeded in 2% BME culture medium at the confluence of 5000 cells/well with EGF. After 2 days from seeding, PDXTs were treated with selumetinib or trametinib (Selleckchem) with the indicated modalities. On day 9, after 1 week of treatment, cell numbers were quantitated by ATP content (Cell Titer-Glo, Promega). Results were normalized against untreated cells.

Western blot analysis

Before biochemical analysis, tumoroids were grown in their respective media in the presence of puromycin (Sigma Aldrich) and/or blasticidin (Thermo Fisher Scientific). Four days after transduction, tumoroids were harvested and total cellular proteins were extracted by lysing cells

in boiling Laemmli buffer (1% SDS, 50 mM Tris-HCl [pH 7.5], 150 mM NaCl). Samples were boiled for 10 minutes and sonicated, and the amounts of proteins were normalized with the BCA Protein Assay Reagent Kit (Thermo Scientific). Total proteins were electrophoresed on precasted SDS-polyacrylamide gels (Invitrogen) and transferred onto nitrocellulose membranes (BioRad). Nitrocellulose-bound antibodies were detected by the enhanced chemiluminescence system (Promega). The following primary antibodies were used: rabbit anti-KRAS (Abcam); mouse anti-vinculin (Sigma-Aldrich).

PDX models and *in vivo* treatments

Tumor implantation and expansion were performed in 6-week-old male and female NOD/SCID mice as previously described [160]. Once tumors reached an average volume of ~400 mm^3, mice were randomized into treatment arms and treated with vehicle (0.5% carboxy methyl-cellulose, 0.1% Tween-80) or trametinib (1 mg/kg, daily gavage). Tumor size was evaluated once-weekly by caliper measurements, and the approximate volume of the mass was calculated using the formula 4/3π.(d/2)2. D/2, where d and D are the minor tumor axis and the major tumor axis, respectively. Operators were blinded during measurements. *In vivo* procedures and related biobanking data were managed using the Laboratory Assistant Suite [201]. Animal procedures were approved by the Italian Ministry of Health (authorization 806/2016-PR).

Immunohistochemistry and morphometric analyses

Tumors were formalin-fixed, paraffin-embedded, and subjected to phospho-ERK staining with the following antibodies: phosphor-p44/42 MAPK (Erk1/2) (Cell Signal). After incubation with secondary antibodies, immunoreactivities were revealed by incubation in DAB chromogen (Dako). Images were captured with the Leica LAS EZ software using a Leica DM LB microscope. Morphometric quantitation was performed by ImageJ software using spectral image segmentation.

Statistical and bioinformatics analyses

The number of biological (nontechnical) replicates for each experiment is reported in the figure legends, alongside the adopted statistical tests and metrics. For comparisons between two groups, statistical analyses were performed using two tailed t-tests, applying Welch's correction for unpaired tests. Similarity estimates between tumoroids and xenografts to compare matched and unmatched models were performed using two tailed Mann-Whitney tests. For experiments with more than two groups or when comparing dose-response curves in tumoroids, one-way ANOVA was used. When unequal SDs were assumed, Brown-Forsythe and Welch ANOVA tests

were applied. All graphs and statistical analyses were performed usingGraphPad Prism (v9.0) and R (v3.6.3), R base packages and the following libraries: precrec (0.12.9), ggplot2 (v3.3.0), pheatmap (v1.0.12), ComplexHeatmap (v2.2.0), sjPlot (2.8.10) and circlize (v0.4.15); with the exception of the CN heatmap (Fig 3B) that was made with python3/matplotlib (v3.7.3/3.4.3) and the sankeys plot (Fig 4B), made with the package networkD3 (v0.4) and its function sankeyNetwork. All the pipelines were developed and run with snakemake (v5.4.0), the code is available at the following repositories: i) https://github.com/vodkatad/snakegatk (Targeted sequencing and shallow-seq alignment and GATK best practices); ii) https://github.com/vodkatad/RNASeq_biod_metadata (RNAseq overall QC and metadata management); iii) https://github.com/vodkatad/biodiversa_DE (RNAseq differential analysis); iv) https://github.com/vodkatad/biobanca (overall comparative analyses).

REFERENCES

1. Hanahan, D. and R.A. Weinberg, *Hallmarks of cancer: the next generation.* Cell, 2011. **144**(5): p. 646-74.
2. Davies, R.J., R. Miller, and N. Coleman, *Colorectal cancer screening: prospects for molecular stool analysis.* Nat Rev Cancer, 2005. **5**(3): p. 199-209.
3. Fearon, E.R. and B. Vogelstein, *A genetic model for colorectal tumorigenesis.* Cell, 1990. **61**(5): p. 759-67.
4. Fearon, E.R., *Molecular genetics of colorectal cancer.* Annu Rev Pathol, 2011. **6**: p. 479-507.
5. Network, C.G.A., *Comprehensive molecular characterization of human colon and rectal cancer.* Nature, 2012. **487**(7407): p. 330-7.
6. Sung, H., et al., *Global Cancer Statistics 2020: GLOBOCAN Estimates of Incidence and Mortality Worldwide for 36 Cancers in 185 Countries.* CA Cancer J Clin, 2021. **71**(3): p. 209-249.
7. Advani, S. and S. Kopetz, *Ongoing and future directions in the management of metastatic colorectal cancer: Update on clinical trials.* J Surg Oncol, 2019. **119**(5): p. 642-652.
8. Siegel, R.L., K.D. Miller, and A. Jemal, *Cancer statistics, 2020.* CA Cancer J Clin, 2020. **70**(1): p. 7-30.
9. Kopetz, S., *New therapies and insights into the changing landscape of colorectal cancer.* Nat Rev Gastroenterol Hepatol, 2019. **16**(2): p. 79-80.
10. Van Cutsem, E., et al., *Metastatic colorectal cancer: ESMO Clinical Practice Guidelines for diagnosis, treatment and follow-up.* Ann Oncol, 2014. **25 Suppl 3**: p. iii1-9.
11. Sahin, I.H., et al., *Immune checkpoint inhibitors for the treatment of MSI-H/MMR-D colorectal cancer and a perspective on resistance mechanisms.* Br J Cancer, 2019. **121**(10): p. 809-818.
12. Hurwitz, H., et al., *Bevacizumab plus irinotecan, fluorouracil, and leucovorin for metastatic colorectal cancer.* N Engl J Med, 2004. **350**(23): p. 2335-42.
13. Jonker, D.J., et al., *Cetuximab for the treatment of colorectal cancer.* N Engl J Med, 2007. **357**(20): p. 2040-8.
14. Jain, R.K., *Normalizing tumor vasculature with anti-angiogenic therapy: a new paradigm for combination therapy.* Nat Med, 2001. **7**(9): p. 987-9.
15. Tong, R.T., et al., *Vascular normalization by vascular endothelial growth factor receptor 2 blockade induces a pressure gradient across the vasculature and improves drug penetration in tumors.* Cancer Res, 2004. **64**(11): p. 3731-6.
16. Lenz, H.J., *Cetuximab in the management of colorectal cancer.* Biologics, 2007. **1**(2): p. 77-91.
17. Strimpakos, A.S., K.N. Syrigos, and M.W. Saif, *Pharmacogenetics and biomarkers in colorectal cancer.* Pharmacogenomics J, 2009. **9**(3): p. 147-60.
18. Karapetis, C.S., et al., *K-ras mutations and benefit from cetuximab in advanced colorectal cancer.* N Engl J Med, 2008. **359**(17): p. 1757-65.
19. Douillard, J.Y., et al., *Panitumumab-FOLFOX4 treatment and RAS mutations in colorectal cancer.* N Engl J Med, 2013. **369**(11): p. 1023-34.
20. Amado, R.G., et al., *Wild-type KRAS is required for panitumumab efficacy in patients with metastatic colorectal cancer.* J Clin Oncol, 2008. **26**(10): p. 1626-34.
21. Mauri, G., et al., *The Evolutionary Landscape of Treatment for BRAF V600E Mutant Metastatic Colorectal Cancer.* Cancers (Basel), 2021. **13**(1).
22. Kopetz, S., et al., *Phase II Pilot Study of Vemurafenib in Patients With Metastatic BRAF-Mutated Colorectal Cancer.* J Clin Oncol, 2015. **33**(34): p. 4032-8.

23. Hyman, D.M., et al., *Vemurafenib in Multiple Nonmelanoma Cancers with BRAF V600 Mutations.* N Engl J Med, 2015. **373**(8): p. 726-36.
24. Corcoran, R.B., et al., *EGFR-mediated re-activation of MAPK signaling contributes to insensitivity of BRAF mutant colorectal cancers to RAF inhibition with vemurafenib.* Cancer Discov, 2012. **2**(3): p. 227-35.
25. Hong, D.S., et al., *Phase IB Study of Vemurafenib in Combination with Irinotecan and Cetuximab in Patients with Metastatic Colorectal Cancer with BRAFV600E Mutation.* Cancer Discov, 2016. **6**(12): p. 1352-1365.
26. Kopetz, S., et al., *Randomized Trial of Irinotecan and Cetuximab With or Without Vemurafenib in BRAF-Mutant Metastatic Colorectal Cancer (SWOG S1406).* J Clin Oncol, 2021. **39**(4): p. 285-294.
27. Kopetz, S., et al., *Encorafenib, Binimetinib, and Cetuximab in BRAF V600E-Mutated Colorectal Cancer.* N Engl J Med, 2019. **381**(17): p. 1632-1643.
28. Fell, J.B., et al., *Identification of the Clinical Development Candidate MRTX849 , a Covalent KRAS G12C Inhibitor for the Treatment of Cancer*. J Med Chem, 2020. **63**(13): p. 6679-6693.
29. Lanman, B.A., et al., *Discovery of a Covalent Inhibitor of KRAS G12C (AMG 510) for the Treatment of Solid Tumors.* J Med Chem, 2020. **63**(1): p. 52-65.
30. Wang, X., et al., *Identification of MRTX1133, a Noncovalent, Potent, and Selective KRAS G12D Inhibitor.* J Med Chem, 2022. **65**(4): p. 3123-3133.
31. Zhao, Y., et al., *Diverse alterations associated with resistance to KRAS(G12C) inhibition.* Nature, 2021. **599**(7886): p. 679-683.
32. Hallin, J., et al., *Anti-tumor efficacy of a potent and selective non-covalent KRAS G12D inhibitor.* Nat Med, 2022. **28**(10): p. 2171-2182.
33. HARVEY, J.J., *AN UNIDENTIFIED VIRUS WHICH CAUSES THE RAPID PRODUCTION OF TUMOURS IN MICE.* Nature, 1964. **204**: p. 1104-5.
34. Goldfarb, M., et al., *Isolation and preliminary characterization of a human transforming gene from T24 bladder carcinoma cells.* Nature, 1982. **296**(5856): p. 404-9.
35. Shih, C. and R.A. Weinberg, *Isolation of a transforming sequence from a human bladder carcinoma cell line.* Cell, 1982. **29**(1): p. 161-9.
36. Pulciani, S., et al., *Oncogenes in human tumor cell lines: molecular cloning of a transforming gene from human bladder carcinoma cells.* Proc Natl Acad Sci U S A, 1982. **79**(9): p. 2845-9.
37. Hall, A., et al., *Identification of transforming gene in two human sarcoma cell lines as a new member of the ras gene family located on chromosome 1.* Nature, 1983. **303**(5916): p. 396-400.
38. Shimizu, K., et al., *Isolation and preliminary characterization of the transforming gene of a human neuroblastoma cell line.* Proc Natl Acad Sci U S A, 1983. **80**(2): p. 383-7.
39. Plowman, S.J., et al., *K-ras 4A and 4B are co-expressed widely in human tissues, and their ratio is altered in sporadic colorectal cancer.* J Exp Clin Cancer Res, 2006. **25**(2): p. 259-67.
40. Castellano, E. and E. Santos, *Functional specificity of ras isoforms: so similar but so different.* Genes Cancer, 2011. **2**(3): p. 216-31.
41. Vetter, I.R. and A. Wittinghofer, *The guanine nucleotide-binding switch in three dimensions.* Science, 2001. **294**(5545): p. 1299-304.
42. Bourne, H.R., D.A. Sanders, and F. McCormick, *The GTPase superfamily: conserved structure and molecular mechanism.* Nature, 1991. **349**(6305): p. 117-27.
43. Simanshu, D.K., D.V. Nissley, and F. McCormick, *RAS Proteins and Their Regulators in Human Disease.* Cell, 2017. **170**(1): p. 17-33.
44. Baltanás, F.C., et al., *SOS GEFs in health and disease.* Biochim Biophys Acta Rev Cancer, 2020. **1874**(2): p. 188445.
45. Ballester, R., et al., *The NF1 locus encodes a protein functionally related to mammalian GAP and yeast IRA proteins.* Cell, 1990. **63**(4): p. 851-9.

46. Iversen, L., et al., *Molecular kinetics. Ras activation by SOS: allosteric regulation by altered fluctuation dynamics.* Science, 2014. **345**(6192): p. 50-4.
47. Karnoub, A.E. and R.A. Weinberg, *Ras oncogenes: split personalities.* Nat Rev Mol Cell Biol, 2008. **9**(7): p. 517-31.
48. Marcus, K. and C. Mattos, *Direct Attack on RAS: Intramolecular Communication and Mutation-Specific Effects.* Clin Cancer Res, 2015. **21**(8): p. 1810-8.
49. Cox, A.D., et al., *Drugging the undruggable RAS: Mission possible?* Nat Rev Drug Discov, 2014. **13**(11): p. 828-51.
50. Nimnual, A. and D. Bar-Sagi, *The two hats of SOS.* Sci STKE, 2002. **2002**(145): p. pe36.
51. Ruess, D.A., et al., *Mutant KRAS-driven cancers depend on PTPN11/SHP2 phosphatase.* Nat Med, 2018. **24**(7): p. 954-960.
52. Eulenfeld, R. and F. Schaper, *A new mechanism for the regulation of Gab1 recruitment to the plasma membrane.* J Cell Sci, 2009. **122**(Pt 1): p. 55-64.
53. Martinelli, E., et al., *Cancer resistance to therapies against the EGFR-RAS-RAF pathway: The role of MEK.* Cancer Treat Rev, 2017. **53**: p. 61-69.
54. Langfermann, D.S., O.G. Rössler, and G. Thiel, *Stimulation of B-Raf increases c-Jun and c-Fos expression and upregulates AP-1-regulated gene transcription in insulinoma cells.* Mol Cell Endocrinol, 2018. **472**: p. 126-139.
55. Lake, D., S.A. Corrêa, and J. Müller, *Negative feedback regulation of the ERK1/2 MAPK pathway.* Cell Mol Life Sci, 2016. **73**(23): p. 4397-4413.
56. Kawazoe, T. and K. Taniguchi, *The Sprouty/Spred family as tumor suppressors: Coming of age.* Cancer Sci, 2019. **110**(5): p. 1525-1535.
57. Ferrer, I., et al., *KRAS-Mutant non-small cell lung cancer: From biology to therapy.* Lung Cancer, 2018. **124**: p. 53-64.
58. Yaeger, R. and R.B. Corcoran, *Targeting Alterations in the RAF-MEK Pathway.* Cancer Discov, 2019. **9**(3): p. 329-341.
59. !!! INVALID CITATION !!! {}.
60. Moore, A.R., et al., *RAS-targeted therapies: is the undruggable drugged?* Nat Rev Drug Discov, 2020. **19**(8): p. 533-552.
61. Aguirre, A.J. and W.C. Hahn, *Synthetic Lethal Vulnerabilities in.* Cold Spring Harb Perspect Med, 2018. **8**(8).
62. Jullien-Flores, V., et al., *Bridging Ral GTPase to Rho pathways. RLIP76, a Ral effector with CDC42/Rac GTPase-activating protein activity.* J Biol Chem, 1995. **270**(38): p. 22473-7.
63. Barbie, D.A., et al., *Systematic RNA interference reveals that oncogenic KRAS-driven cancers require TBK1.* Nature, 2009. **462**(7269): p. 108-12.
64. Simicek, M., et al., *The deubiquitylase USP33 discriminates between RALB functions in autophagy and innate immune response.* Nat Cell Biol, 2013. **15**(10): p. 1220-30.
65. Apken, L.H. and A. Oeckinghaus, *The RAL signaling network: Cancer and beyond.* Int Rev Cell Mol Biol, 2021. **361**: p. 21-105.
66. Vigil, D., et al., *Ras superfamily GEFs and GAPs: validated and tractable targets for cancer therapy?* Nat Rev Cancer, 2010. **10**(12): p. 842-57.
67. Hobbs, G.A., C.J. Der, and K.L. Rossman, *RAS isoforms and mutations in cancer at a glance.* J Cell Sci, 2016. **129**(7): p. 1287-92.
68. Campbell, J.D., et al., *Distinct patterns of somatic genome alterations in lung adenocarcinomas and squamous cell carcinomas.* Nat Genet, 2016. **48**(6): p. 607-16.
69. Bailey, P., et al., *Genomic analyses identify molecular subtypes of pancreatic cancer.* Nature, 2016. **531**(7592): p. 47-52.
70. Yaeger, R., et al., *Clinical Sequencing Defines the Genomic Landscape of Metastatic Colorectal Cancer.* Cancer Cell, 2018. **33**(1): p. 125-136.e3.
71. Pylayeva-Gupta, Y., E. Grabocka, and D. Bar-Sagi, *RAS oncogenes: weaving a tumorigenic web.* Nat Rev Cancer, 2011. **11**(11): p. 761-74.

72. Prior, I.A., P.D. Lewis, and C. Mattos, *A comprehensive survey of Ras mutations in cancer.* Cancer Res, 2012. **72**(10): p. 2457-67.
73. Kandoth, C., et al., *Mutational landscape and significance across 12 major cancer types.* Nature, 2013. **502**(7471): p. 333-339.
74. Liu, P., et al., *Oncogenic PIK3CA-driven mammary tumors frequently recur via PI3K pathway-dependent and PI3K pathway-independent mechanisms.* Nat Med, 2011. **17**(9): p. 1116-20.
75. Hofmann, M.H., et al., *Expanding the Reach of Precision Oncology by Drugging All KRAS Mutants.* Cancer Discov, 2022. **12**(4): p. 924-937.
76. Hunter, J.C., et al., *Biochemical and Structural Analysis of Common Cancer-Associated KRAS Mutations.* Mol Cancer Res, 2015. **13**(9): p. 1325-35.
77. Rabara, D., et al., *KRAS G13D sensitivity to neurofibromin-mediated GTP hydrolysis.* Proc Natl Acad Sci U S A, 2019. **116**(44): p. 22122-22131.
78. Nadal, E., et al., *KRAS-G12C mutation is associated with poor outcome in surgically resected lung adenocarcinoma.* J Thorac Oncol, 2014. **9**(10): p. 1513-22.
79. Ihle, N.T., et al., *Effect of KRAS oncogene substitutions on protein behavior: implications for signaling and clinical outcome.* J Natl Cancer Inst, 2012. **104**(3): p. 228-39.
80. Hingorani, S.R., et al., *Trp53R172H and KrasG12D cooperate to promote chromosomal instability and widely metastatic pancreatic ductal adenocarcinoma in mice.* Cancer Cell, 2005. **7**(5): p. 469-83.
81. Ji, H., et al., *LKB1 modulates lung cancer differentiation and metastasis.* Nature, 2007. **448**(7155): p. 807-10.
82. Haigis, K.M., et al., *Differential effects of oncogenic K-Ras and N-Ras on proliferation, differentiation and tumor progression in the colon.* Nat Genet, 2008. **40**(5): p. 600-8.
83. Jackson, E.L., et al., *The differential effects of mutant p53 alleles on advanced murine lung cancer.* Cancer Res, 2005. **65**(22): p. 10280-8.
84. Jackson, E.L., et al., *Analysis of lung tumor initiation and progression using conditional expression of oncogenic K-ras.* Genes Dev, 2001. **15**(24): p. 3243-8.
85. di Magliano, M.P. and C.D. Logsdon, *Roles for KRAS in pancreatic tumor development and progression.* Gastroenterology, 2013. **144**(6): p. 1220-9.
86. Weinstein, I.B., *Cancer. Addiction to oncogenes--the Achilles heal of cancer.* Science, 2002. **297**(5578): p. 63-4.
87. Sharma, S.V. and J. Settleman, *Oncogene addiction: setting the stage for molecularly targeted cancer therapy.* Genes Dev, 2007. **21**(24): p. 3214-31.
88. Long, G.V., et al., *Overall Survival and Durable Responses in Patients With BRAF V600-Mutant Metastatic Melanoma Receiving Dabrafenib Combined With Trametinib.* J Clin Oncol, 2016. **34**(8): p. 871-8.
89. Soda, M., et al., *Identification of the transforming EML4-ALK fusion gene in non-small-cell lung cancer.* Nature, 2007. **448**(7153): p. 561-6.
90. Shaw, A.T., et al., *Crizotinib versus chemotherapy in advanced ALK-positive lung cancer.* N Engl J Med, 2013. **368**(25): p. 2385-94.
91. Lynch, T.J., et al., *Activating mutations in the epidermal growth factor receptor underlying responsiveness of non-small-cell lung cancer to gefitinib.* N Engl J Med, 2004. **350**(21): p. 2129-39.
92. Gerlinger, M., et al., *Intratumor heterogeneity and branched evolution revealed by multiregion sequencing.* N Engl J Med, 2012. **366**(10): p. 883-92.
93. Singh, A., et al., *A gene expression signature associated with "K-Ras addiction" reveals regulators of EMT and tumor cell survival.* Cancer Cell, 2009. **15**(6): p. 489-500.
94. Singh, A., et al., *TAK1 inhibition promotes apoptosis in KRAS-dependent colon cancers.* Cell, 2012. **148**(4): p. 639-50.

95. Hayes, T.K., et al., *Long-Term ERK Inhibition in KRAS-Mutant Pancreatic Cancer Is Associated with MYC Degradation and Senescence-like Growth Suppression.* Cancer Cell, 2016. **29**(1): p. 75-89.
96. Kapoor, A., et al., *Yap1 activation enables bypass of oncogenic Kras addiction in pancreatic cancer.* Cell, 2014. **158**(1): p. 185-197.
97. Lamba, S., et al., *RAF suppression synergizes with MEK inhibition in KRAS mutant cancer cells.* Cell Rep, 2014. **8**(5): p. 1475-83.
98. Patricelli, M.P., et al., *Selective Inhibition of Oncogenic KRAS Output with Small Molecules Targeting the Inactive State.* Cancer Discov, 2016. **6**(3): p. 316-29.
99. McDonald, E.R., et al., *Project DRIVE: A Compendium of Cancer Dependencies and Synthetic Lethal Relationships Uncovered by Large-Scale, Deep RNAi Screening.* Cell, 2017. **170**(3): p. 577-592.e10.
100. O'Bryan, J.P., *Pharmacological targeting of RAS: Recent success with direct inhibitors.* Pharmacol Res, 2019. **139**: p. 503-511.
101. Eser, S., et al., *Oncogenic KRAS signalling in pancreatic cancer.* Br J Cancer, 2014. **111**(5): p. 817-22.
102. Leung, E.L., et al., *Identification of a new inhibitor of KRAS-PDEδ interaction targeting KRAS mutant nonsmall cell lung cancer.* Int J Cancer, 2019. **145**(5): p. 1334-1345.
103. Marín-Ramos, N.I., et al., *A Potent Isoprenylcysteine Carboxylmethyltransferase (ICMT) Inhibitor Improves Survival in Ras-Driven Acute Myeloid Leukemia.* J Med Chem, 2019. **62**(13): p. 6035-6046.
104. Ostrem, J.M., et al., *K-Ras(G12C) inhibitors allosterically control GTP affinity and effector interactions.* Nature, 2013. **503**(7477): p. 548-51.
105. Statsyuk, A.V., *Let K-Ras activate its own inhibitor.* Nat Struct Mol Biol, 2018. **25**(6): p. 435-437.
106. Xue, J.Y., et al., *Rapid non-uniform adaptation to conformation-specific KRAS(G12C) inhibition.* Nature, 2020. **577**(7790): p. 421-425.
107. Canon, J., et al., *The clinical KRAS(G12C) inhibitor AMG 510 drives anti-tumour immunity.* Nature, 2019. **575**(7781): p. 217-223.
108. Amodio, V., et al., *EGFR Blockade Reverts Resistance to KRAS G12C Inhibition in Colorectal Cancer.* Cancer Discov, 2020. **10**(8): p. 1129-1139.
109. Amodio, V., et al., *EGFR Blockade Reverts Resistance to KRAS.* Cancer Discov, 2020. **10**(8): p. 1129-1139.
110. Mainardi, S., et al., *SHP2 is required for growth of KRAS-mutant non-small-cell lung cancer in vivo.* Nat Med, 2018. **24**(7): p. 961-967.
111. LoRusso, P.M. and J.S. Sebolt-Leopold, *One Step at a Time - Clinical Evidence That KRAS Is Indeed Druggable.* N Engl J Med, 2020. **383**(13): p. 1277-1278.
112. Ryan, M.B., et al., *Vertical Pathway Inhibition Overcomes Adaptive Feedback Resistance to KRAS.* Clin Cancer Res, 2020. **26**(7): p. 1633-1643.
113. Shao, D.D., et al., *KRAS and YAP1 converge to regulate EMT and tumor survival.* Cell, 2014. **158**(1): p. 171-84.
114. Li, S., et al., *Assessing Therapeutic Efficacy of MEK Inhibition in a KRAS.* Clin Cancer Res, 2018. **24**(19): p. 4854-4864.
115. Misale, S., et al., *KRAS G12C NSCLC Models Are Sensitive to Direct Targeting of KRAS in Combination with PI3K Inhibition.* Clin Cancer Res, 2019. **25**(2): p. 796-807.
116. Misale, S., et al., *Vertical suppression of the EGFR pathway prevents onset of resistance in colorectal cancers.* Nat Commun, 2015. **6**: p. 8305.
117. Yuan, T.L., et al., *Differential Effector Engagement by Oncogenic KRAS.* Cell Rep, 2018. **22**(7): p. 1889-1902.
118. Punekar, S.R., et al., *The current state of the art and future trends in RAS-targeted cancer therapies.* Nat Rev Clin Oncol, 2022. **19**(10): p. 637-655.

119. Guinney, J., et al., *The consensus molecular subtypes of colorectal cancer.* Nat Med, 2015. **21**(11): p. 1350-6.
120. Garnett, M.J., et al., *Systematic identification of genomic markers of drug sensitivity in cancer cells.* Nature, 2012. **483**(7391): p. 570-5.
121. Molina-Arcas, M., et al., *Coordinate direct input of both KRAS and IGF1 receptor to activation of PI3 kinase in KRAS-mutant lung cancer.* Cancer Discov, 2013. **3**(5): p. 548-63.
122. Basu, A., et al., *An interactive resource to identify cancer genetic and lineage dependencies targeted by small molecules.* Cell, 2013. **154**(5): p. 1151-1161.
123. Ebi, H., et al., *Receptor tyrosine kinases exert dominant control over PI3K signaling in human KRAS mutant colorectal cancers.* J Clin Invest, 2011. **121**(11): p. 4311-21.
124. Manchado, E., et al., *A combinatorial strategy for treating KRAS-mutant lung cancer.* Nature, 2016. **534**(7609): p. 647-51.
125. Normanno, N., et al., *The role of EGF-related peptides in tumor growth.* Front Biosci, 2001. **6**: p. D685-707.
126. Sibilia, M., et al., *The EGF receptor provides an essential survival signal for SOS-dependent skin tumor development.* Cell, 2000. **102**(2): p. 211-20.
127. Misale, S., et al., *Emergence of KRAS mutations and acquired resistance to anti-EGFR therapy in colorectal cancer.* Nature, 2012. **486**(7404): p. 532-6.
128. Allegra, C.J., R.B. Rumble, and R.L. Schilsky, *Extended RAS Gene Mutation Testing in Metastatic Colorectal Carcinoma to Predict Response to Anti-Epidermal Growth Factor Receptor Monoclonal Antibody Therapy: American Society of Clinical Oncology Provisional Clinical Opinion Update 2015 Summary.* J Oncol Pract, 2016. **12**(2): p. 180-1.
129. Pao, W., et al., *KRAS mutations and primary resistance of lung adenocarcinomas to gefitinib or erlotinib.* PLoS Med, 2005. **2**(1): p. e17.
130. Zhu, C.Q., et al., *Role of KRAS and EGFR as biomarkers of response to erlotinib in National Cancer Institute of Canada Clinical Trials Group Study BR.21.* J Clin Oncol, 2008. **26**(26): p. 4268-75.
131. Chapman, P.B., et al., *Improved survival with vemurafenib in melanoma with BRAF V600E mutation.* N Engl J Med, 2011. **364**(26): p. 2507-16.
132. Hauschild, A., et al., *Dabrafenib in BRAF-mutated metastatic melanoma: a multicentre, open-label, phase 3 randomised controlled trial.* Lancet, 2012. **380**(9839): p. 358-65.
133. Heidorn, S.J., et al., *Kinase-dead BRAF and oncogenic RAS cooperate to drive tumor progression through CRAF.* Cell, 2010. **140**(2): p. 209-21.
134. Hatzivassiliou, G., et al., *RAF inhibitors prime wild-type RAF to activate the MAPK pathway and enhance growth.* Nature, 2010. **464**(7287): p. 431-5.
135. Poulikakos, P.I., et al., *RAF inhibitors transactivate RAF dimers and ERK signalling in cells with wild-type BRAF.* Nature, 2010. **464**(7287): p. 427-30.
136. Hall-Jackson, C.A., et al., *Paradoxical activation of Raf by a novel Raf inhibitor.* Chem Biol, 1999. **6**(8): p. 559-68.
137. Vakana, E., et al., *LY3009120, a panRAF inhibitor, has significant anti-tumor activity in BRAF and KRAS mutant preclinical models of colorectal cancer.* Oncotarget, 2017. **8**(6): p. 9251-9266.
138. Henry, J.R., et al., *Discovery of 1-(3,3-dimethylbutyl)-3-(2-fluoro-4-methyl-5-(7-methyl-2-(methylamino)pyrido[2,3-d]pyrimidin-6-yl)phenyl)urea (LY3009120) as a pan-RAF inhibitor with minimal paradoxical activation and activity against BRAF or RAS mutant tumor cells.* J Med Chem, 2015. **58**(10): p. 4165-79.
139. Blumenschein, G.R., et al., *A randomized phase II study of the MEK1/MEK2 inhibitor trametinib (GSK1120212) compared with docetaxel in KRAS-mutant advanced non-small-cell lung cancer (NSCLC)†.* Ann Oncol, 2015. **26**(5): p. 894-901.
140. Caunt, C.J., et al., *MEK1 and MEK2 inhibitors and cancer therapy: the long and winding road.* Nat Rev Cancer, 2015. **15**(10): p. 577-92.

141. Yen, I., et al., *Pharmacological Induction of RAS-GTP Confers RAF Inhibitor Sensitivity in KRAS Mutant Tumors.* Cancer Cell, 2018. **34**(4): p. 611-625.e7.
142. Mallucci, L. and V. Wells, *The end of KRAS, and other, cancers? A new way forward.* Drug Discov Today, 2014. **19**(4): p. 383-7.
143. Alagesan, B., et al., *Combined MEK and PI3K inhibition in a mouse model of pancreatic cancer.* Clin Cancer Res, 2015. **21**(2): p. 396-404.
144. Do, K., et al., *Biomarker-driven phase 2 study of MK-2206 and selumetinib (AZD6244, ARRY-142886) in patients with colorectal cancer.* Invest New Drugs, 2015. **33**(3): p. 720-8.
145. Migliardi, G., et al., *Inhibition of MEK and PI3K/mTOR suppresses tumor growth but does not cause tumor regression in patient-derived xenografts of RAS-mutant colorectal carcinomas.* Clin Cancer Res, 2012. **18**(9): p. 2515-25.
146. Shimizu, T., et al., *The clinical effect of the dual-targeting strategy involving PI3K/AKT/mTOR and RAS/MEK/ERK pathways in patients with advanced cancer.* Clin Cancer Res, 2012. **18**(8): p. 2316-25.
147. Hartwell, L.H., et al., *Integrating genetic approaches into the discovery of anticancer drugs.* Science, 1997. **278**(5340): p. 1064-8.
148. Kaelin, W.G., *The concept of synthetic lethality in the context of anticancer therapy.* Nat Rev Cancer, 2005. **5**(9): p. 689-98.
149. O'Neil, N.J., M.L. Bailey, and P. Hieter, *Synthetic lethality and cancer.* Nat Rev Genet, 2017. **18**(10): p. 613-623.
150. Luo, J., et al., *A genome-wide RNAi screen identifies multiple synthetic lethal interactions with the Ras oncogene.* Cell, 2009. **137**(5): p. 835-48.
151. Lin, A. and J.M. Sheltzer, *Discovering and validating cancer genetic dependencies: approaches and pitfalls.* Nat Rev Genet, 2020. **21**(11): p. 671-682.
152. Driehuis, E. and H. Clevers, *CRISPR/Cas 9 genome editing and its applications in organoids.* Am J Physiol Gastrointest Liver Physiol, 2017. **312**(3): p. G257-G265.
153. Scholl, C., et al., *Synthetic lethal interaction between oncogenic KRAS dependency and STK33 suppression in human cancer cells.* Cell, 2009. **137**(5): p. 821-34.
154. Lin, L., et al., *The Hippo effector YAP promotes resistance to RAF- and MEK-targeted cancer therapies.* Nat Genet, 2015. **47**(3): p. 250-6.
155. Evers, B., et al., *CRISPR knockout screening outperforms shRNA and CRISPRi in identifying essential genes.* Nat Biotechnol, 2016. **34**(6): p. 631-3.
156. Dhanjal, J.K., N. Radhakrishnan, and D. Sundar, *Identifying synthetic lethal targets using CRISPR/Cas9 system.* Methods, 2017. **131**: p. 66-73.
157. Schuster, A., et al., *RNAi/CRISPR Screens: from a Pool to a Valid Hit.* Trends Biotechnol, 2019. **37**(1): p. 38-55.
158. Wang, T., et al., *Gene Essentiality Profiling Reveals Gene Networks and Synthetic Lethal Interactions with Oncogenic Ras.* Cell, 2017. **168**(5): p. 890-903.e15.
159. Drost, J. and H. Clevers, *Organoids in cancer research.* Nat Rev Cancer, 2018. **18**(7): p. 407-418.
160. Bertotti, A., et al., *A molecularly annotated platform of patient-derived xenografts ("xenopatients") identifies HER2 as an effective therapeutic target in cetuximab-resistant colorectal cancer.* Cancer Discov, 2011. **1**(6): p. 508-23.
161. Bertotti, A., et al., *The genomic landscape of response to EGFR blockade in colorectal cancer.* Nature, 2015. **526**(7572): p. 263-7.
162. Fujii, M., et al., *A Colorectal Tumor Organoid Library Demonstrates Progressive Loss of Niche Factor Requirements during Tumorigenesis.* Cell Stem Cell, 2016. **18**(6): p. 827-838.
163. Yin, J., et al., *Prognostic and Predictive Impact of Primary Tumor Sidedness for Previously Untreated Advanced Colorectal Cancer.* J Natl Cancer Inst, 2021. **113**(12): p. 1705-1713.

164. Jang, S., et al., *KRAS and PIK3CA mutations in colorectal adenocarcinomas correlate with aggressive histological features and behavior.* Hum Pathol, 2017. **65**: p. 21-30.
165. Rehman, A.H., R.P. Jones, and G. Poston, *Prognostic and predictive markers in liver limited stage IV colorectal cancer.* Eur J Surg Oncol, 2019. **45**(12): p. 2251-2256.
166. Matano, M., et al., *Modeling colorectal cancer using CRISPR-Cas9-mediated engineering of human intestinal organoids.* Nat Med, 2015. **21**(3): p. 256-62.
167. Van Cutsem, E., et al., *Cetuximab and chemotherapy as initial treatment for metastatic colorectal cancer.* N Engl J Med, 2009. **360**(14): p. 1408-17.
168. Sun, H., et al., *Comprehensive characterization of 536 patient-derived xenograft models prioritizes candidatesfor targeted treatment.* Nat Commun, 2021. **12**(1): p. 5086.
169. Parker, T.W., A.J. Rudeen, and K.L. Neufeld, *Oncogenic Serine 45-Deleted β-Catenin Remains Susceptible to Wnt Stimulation and APC Regulation in Human Colonocytes.* Cancers (Basel), 2020. **12**(8).
170. Ran, F.A., et al., *Genome engineering using the CRISPR-Cas9 system.* Nat Protoc, 2013. **8**(11): p. 2281-2308.
171. Behan, F.M., et al., *Prioritization of cancer therapeutic targets using CRISPR-Cas9 screens.* Nature, 2019. **568**(7753): p. 511-516.
172. Su, Y., et al., *The regulatory role of PDE4B in the progression of inflammatory function study.* Front Pharmacol, 2022. **13**: p. 982130.
173. Zhang, D., et al., *Polymeric immunoglobulin receptor suppresses colorectal cancer through the AKT-FOXO3/4 axis by downregulating LAMB3 expression.* Front Oncol, 2022. **12**: p. 924988.
174. Yang, B., et al., *KRT6A Promotes EMT and Cancer Stem Cell Transformation in Lung Adenocarcinoma.* Technol Cancer Res Treat, 2020. **19**: p. 1533033820921248.
175. Zhou, Z., et al., *The versatile roles of testrapanins in cancer from intracellular signaling to cell-cell communication: cell membrane proteins without ligands.* Cell Biosci, 2023. **13**(1): p. 59.
176. Yeh, E., et al., *A signalling pathway controlling c-Myc degradation that impacts oncogenic transformation of human cells.* Nat Cell Biol, 2004. **6**(4): p. 308-18.
177. Lee, T., et al., *Sensing and integration of Erk and PI3K signals by Myc.* PLoS Comput Biol, 2008. **4**(2): p. e1000013.
178. Onwuegbusi, B.A., et al., *Selective loss of TGFbeta Smad-dependent signalling prevents cell cycle arrest and promotes invasion in oesophageal adenocarcinoma cell lines.* PLoS One, 2007. **2**(1): p. e177.
179. Wagner, S., et al., *Suppression of interferon gene expression overcomes resistance to MEK inhibition in KRAS-mutant colorectal cancer.* Oncogene, 2019. **38**(10): p. 1717-1733.
180. Yaeger, R., et al., *Molecular Characterization of Acquired Resistance to KRASG12C-EGFR Inhibition in Colorectal Cancer.* Cancer Discov, 2023. **13**(1): p. 41-55.
181. McNew, K.L., et al., *MEK and TAK1 Regulate Apoptosis in Colon Cancer Cells with KRAS-Dependent Activation of Proinflammatory Signaling.* Mol Cancer Res, 2016. **14**(12): p. 1204-1216.
182. Babij, C., et al., *STK33 kinase activity is nonessential in KRAS-dependent cancer cells.* Cancer Res, 2011. **71**(17): p. 5818-26.
183. Corcoran, R.B., et al., *Synthetic lethal interaction of combined BCL-XL and MEK inhibition promotes tumor regressions in KRAS mutant cancer models.* Cancer Cell, 2013. **23**(1): p. 121-8.
184. Roman, M., E. Hwang, and E.A. Sweet-Cordero, *Synthetic Vulnerabilities in the KRAS Pathway.* Cancers (Basel), 2022. **14**(12).
185. Plosker, G.L., *Ruxolitinib: a review of its use in patients with myelofibrosis.* Drugs, 2015. **75**(3): p. 297-308.

186. Harrison, C.N., et al., *Long-term findings from COMFORT-II, a phase 3 study of ruxolitinib vs best available therapy for myelofibrosis.* Leukemia, 2016. **30**(8): p. 1701-7.
187. Verstovsek, S., et al., *Ruxolitinib versus best available therapy in patients with polycythemia vera: 80-week follow-up from the RESPONSE trial.* Haematologica, 2016. **101**(7): p. 821-9.
188. Schwartz, D.M., et al., *JAK inhibition as a therapeutic strategy for immune and inflammatory diseases.* Nat Rev Drug Discov, 2017. **17**(1): p. 78.
189. Dobin, A., et al., *STAR: ultrafast universal RNA-seq aligner.* Bioinformatics, 2013. **29**(1): p. 15-21.
190. Tarasov, A., et al., *Sambamba: fast processing of NGS alignment formats.* Bioinformatics, 2015. **31**(12): p. 2032-4.
191. Wang, L., S. Wang, and W. Li, *RSeQC: quality control of RNA-seq experiments.* Bioinformatics, 2012. **28**(16): p. 2184-5.
192. Liao, Y., G.K. Smyth, and W. Shi, *featureCounts: an efficient general purpose program for assigning sequence reads to genomic features.* Bioinformatics, 2014. **30**(7): p. 923-30.
193. Isella, C., et al., *Selective analysis of cancer-cell intrinsic transcriptional traits defines novel clinically relevant subtypes of colorectal cancer.* Nat Commun, 2017. **8**: p. 15107.
194. Isella, C., et al., *Stromal contribution to the colorectal cancer transcriptome.* Nat Genet, 2015. **47**(4): p. 312-9.
195. Love, M.I., W. Huber, and S. Anders, *Moderated estimation of fold change and dispersion for RNA-seq data with DESeq2.* Genome Biol, 2014. **15**(12): p. 550.
196. Wu, T., et al., *clusterProfiler 4.0: A universal enrichment tool for interpreting omics data.* Innovation (Camb), 2021. **2**(3): p. 100141.
197. Yu, G., et al., *clusterProfiler: an R package for comparing biological themes among gene clusters.* OMICS, 2012. **16**(5): p. 284-7.
198. Yu, G., et al., *DOSE: an R/Bioconductor package for disease ontology semantic and enrichment analysis.* Bioinformatics, 2015. **31**(4): p. 608-9.
199. Subramanian, A., et al., *Gene set enrichment analysis: a knowledge-based approach for interpreting genome-wide expression profiles.* Proc Natl Acad Sci U S A, 2005. **102**(43): p. 15545-50.
200. Tzelepis, K., et al., *A CRISPR Dropout Screen Identifies Genetic Vulnerabilities and Therapeutic Targets in Acute Myeloid Leukemia.* Cell Rep, 2016. **17**(4): p. 1193-1205.
201. Baralis, E., et al., *LAS: a software platform to support oncological data management.* J Med Syst, 2012. **36 Suppl 1**: p. S81-90.